A MODELING APPROACH TO ULTRASOUND EVALUATION OF MATERIAL PROPERTIES

A Dissertation presented to
the Faculty of the Graduate School
at the University of Missouri

In Partial Fulfillment of the Requirement for the Degree

Doctor of Philosophy

By

SRI WALUYO

Dr. Jinglu Tan, Dissertation Supervisor

DECEMBER 2010

The undersigned, appointed by the Dean of the Graduate School, have examined the dissertation entitled

A MODELING APPROACH TO ULTRASOUND EVALUATION OF MATERIAL PROPERTIES

presented by Sri Waluyo,

a candidate for the degree of Doctor of Philosophy,

and hereby that, in their opinion, it is worth of acceptance.

_____

Jinglu Tan, Ph.D.
Department of Biological Engineering

_____

Satish Nair, Ph.D.
Department of Electrical and Computer Engineering

_____

Fu-Hung Hsieh, Ph.D.
Department of Biological Engineering

_____

Gang Yao, Ph.D.
Department of Biological Engineering

ACKNOWLEDGEMENTS

The completion of this work would not be possible without the support of professors, colleagues, friends, and family. First of all I would like to express my deepest appreciation to my supervisor, Dr. Jinglu Tan, for his supervision, advice, support, great inspiration and keen interest throughout my four years working in his lab. I would also like to thank my committee members: Dr. Gang Yao, Dr. Fu-Hung Hsieh, and Dr. Satish Nair for their feedback and encouragement.

I must give special thanks to Dr. Guo Ya (David) for his support and help on programming and inspiring discussions during my study and research. I also thank my fellow students in the Department of Biological Engineering: Dr. Jinhua Yu (Grace), Maetee Patana-Anake (Mo), Xiaozhen Wang (Camille), Dr. Jong Lee, Ali Shuaib, and Xiaoguang Yang (Tom) that supported me in many ways during my study. My gratitude is also given to Mr. Gordon Ellison who helped make the experiment devices, Mr. Harold Huff who assisted on the mechanical measurements, and Ms. JoAnn Lewis and Ms. Deborah Ratliff for their administrative supports during my study. I must thank my friends: Maslina Mohd Ibrahim, Rilya Rumbayan, Yoon-Chee Pak, Yuritza Oliver, Roxana Martinez Campuzano that helped with the sensory tests. Further, I offer my regards and blessings to all of those who supported me in any respect during the project.

Finally, the greatest thanks go to my beloved wife Rahayu Kumalasari and son M. Hafizh Aryakumala for their patience and support from my initial preparation to the completion of my PhD program. Thank to my parents, brothers and sisters who have prayed for me throughout the years.

TABLE OF CONTENTS

LIST OF FIGURES

LIST OF TABLES

A MODELING APPROACH TO ULTRASOUND EVALUATION OF MATERIAL PROPERTIES

Sri Waluyo

Dr. Jinglu Tan, Dissertation Supervisor

ABSTRACT

A method for estimating the mechanical properties of a viscoelastic sample from ultrasound measurements was developed. The sample was represented as a mechanical network according to the Kelvin-Voigt model and linear state-space equations were derived to describe the system dynamics. Four parameters can be extracted by comparing the model with measured transmission waves. These parameters can be related to viscoelastic properties of the sample. Broadband pseudo-random binary sequences (PRBS) were designed and used to perturb the sample. The Levenberg-Marquardt method was employed to adjust the model parameters and the least-squares algorithm was used to obtain optimal model parameter estimates. Model verification showed that the algorithm developed could converge to known model parameters. Estimated model parameters showed consistency and reflected known facts about the materials tested. The model could capture the major dynamics of transmitted ultrasonic waves and allow repeatable estimation of model parameters. The model parameters could not only differentiate the materials tested but also follow expected trends of variation. A transfer function method was developed to compensate the transducer effects on measured material responses. The method provides a simple and practical way to extract the transducer dynamics from measurements. The

mechanical properties obtained from the model-based ultrasound (MBUS) method correlated positively with conventionally measured viscoelastic properties. As an application, the model parameters were used to predict sensory crispness of apples. The results indicated that the model parameters were useful for sensory crispness prediction and crispness was more correlated to the elastic modulus than to viscosity, which is consistent with existing research.

CHAPTER 1

INTRODUCTION

1.1 Background

Mechanical properties of biological materials have been a main concern for many researchers in biology-related areas over the past few decades. The studies are based on the fact that the behaviors of the mechanical properties are important to many biological functions and related to pathological phenomena. Aging of biological tissues and existence of diseases, for example, are traced to changes in mechanical properties of tissues. Thus, an understanding of the mechanical properties of tissues is of great importance particularly to assessing mechanical integrity, preventing injuries in tissues during and post surgery, and maintaining the normal physical motion of body (Kubo *et al*., 2003; Taha *et al*., 2009).

Mechanical properties also play an important role in the evaluation of many kinds of foods. Elasticity and viscosity are two of the most important mechanical properties for biological material evaluations. Characterization of the mechanical properties of food products is very important for determining a suitable handling method such as developing durable and superior thermal barrier coatings in food packaging. Very often mechanical property evaluations of foods correspond to crispness, a quality attribute that is important in determining the consumer acceptability of fruits and vegetables (McCracken, 1994; Mallikarjunan, 2004). Crispness of fruits and vegetables are related to the structural, physiological, and physiochemical characteristics of the products (Mizrach, 2008).

In food engineering, mechanical properties have been studied to reveal the structural properties of materials. The properties are primarily used to quantitatively define and interpret crispness, hardness, and other human sensory attributes of foods. According to Bourne (2002), crispness appears to be the most important characteristic of texture which is a mechanical behavior of foods obtained from sensory analysis. Some attempts have been made to correlate instrumental measurements of food mechanical properties with sensory quality such as crispness. Vickers (1988) and Seymour and Hamann (1988) used a combination of sound and mechanical properties to predict sensory crispness. Yamamoto *et al*., (1980) and Kilcast (2004) reported that the sensory firmness and crispness corresponded to Young's modulus and fracturability.

Mechanical tests to determine the texture attributes have mostly been depended on invasive methods. The load given to a sample is over the fracturability limit of the sample, hence it is destructive. The methods often lack the sensitivity to detect small changes of texture. Furthermore, invasive measurements are often limited to a set of sample, which may not reveal the variations in a food product. Development of noninvasive methods is needed.

1.2 Ultrasound Wave Propagation

It is commonly known that the ultrasound transducer works by converting electrical energy into mechanical waves and vice versa. The sound energy propagates through the medium as a series of compression and rarefaction waves, and generates a sound wave field. Particles surrounding the area of propagation vibrate back and forth as mechanical motion. Hence, it is common that sound wave is called a mechanical wave.

Mechanical waves require a medium for the transfer of energy from one point to another. When an external force is applied to the medium, waves propagate in the medium as a series of mechanical disturbances. The deformation, stress-strain behavior, and waveform usually relate to the material properties. Measuring the dynamics of ultrasound transmission through a medium is thus a way to study the medium material properties.

Most biological materials exhibit viscoelastic behavior, which is neither purely viscous nor elastic. Since metabolic activities change their properties over time, the behavior of biological materials differ from and more complex than, for example, metal materials. Assessing these properties is challenging because of nonlinear mechanical behaviors, irregular geometries, multi-constituent heterogeneities, natural damping, and complex boundary conditions (Fung, 1993). In the biomedical field, the mechanical behaviors of biological materials or biomaterials are essential to many biological functions and to pathological analysis. Understanding the mechanical behaviors of soft tissues is thus important for prosthesis design, diagnosis, and tissue engineering. In food applications, texture, which is usually evaluated in term of mechanical parameters, affects the quality of food products and consumer acceptance. Often quality attributes of food products such as blandness, crunchiness, and crispness, heavily depend on the product texture (Bourne, 2002). In addition, viscoelasticity is important for understanding physical processes such as molecular mobility in polymer phase transformations, motion of defects, and alloying atoms in crystalline solids (Lakes, 2004).

Many techniques, invasive or noninvasive, have been used to determine mechanical properties of biological materials. The viscoelastic behavior can be studied from the

relationship between excitation force and response by using a dynamic system model. Measurements can be performed by using stress-relaxation (Lakes, 2004; Zhang, 2005), quasi-static tests (Nitta and Shiina, 2002; Shiina, *et al*., 2007), and dynamic tests (Yamakoshi *et al.*, 1990). Furthermore, dynamic mechanical analysis techniques based on experimental data can be used to obtain the behavior of materials by modeling the dynamic system. In studying the dynamic responses, viscoelastic materials are often represented as mechanical systems consisting of masses, springs and dashpots. The dynamic method has the advantage of revealing the dynamic properties of viscoelastic materials such as elasticity and viscosity.

Ultrasound wave modeling based on first principles provides a physically meaningful way to relate material properties to wave characteristics. When a medium is excited by ultrasound, the vibration energy propagates through the medium (Cheeke, 2002). The sound wave depends on the medium properties and the excitation (Meirovitch, 1997). The material properties usually appear in the parameters of a model.

Even though numerous studies on ultrasound application in evaluation of biological materials have been reported, a complete understanding of the dynamic behavior of biological materials in response to ultrasound excitation is still lacking. Because biological materials vary, it is difficult to devise one method that can be applied in all cases. Most existing approaches are designed to evaluate individual mechanical properties, but viscoelastic properties are often coupled. Changes in one property may affect the measurement of another.

1.3 Research Objectives

This research was aimed at developing a mathematical model for ultrasound transmission in viscoelastic materials that allows for ultrasound-based evaluation and analysis of viscoelasticity of biological materials.

The specific objectives of this research were:

1) To develop a mathematical model for ultrasound transmission in viscoelastic materials,
2) To validate the model for its usefulness in revealing material properties from ultrasound measurements,
3) To apply the technique in differentiating and classifying biological materials based on property parameter estimates,
4) To develop a technique to compensate for the transducer effects on measured data,
5) To use estimated model parameters to predict the mechanical properties of certain biological materials, and
6) To predict the sensory quality of certain biological materials from mechanical properties measured with the model-based ultrasound technique.

CHAPTER 2

LITERATURE REVIEW

This chapter begins with a background of continuum mechanics from which the basic concept and definition of stress and strain are defined. The basic mechanical models used in studying the characteristics and behaviors of viscoelastic materials are presented and related literatures are given. Next, the wave equation is derived from the concepts of stress and displacement related by material properties. The wave equation is then applied and the ultrasound characteristics are discussed in the rest of this chapter.

2.1 Stress and Strain

In this section, the basic concepts of stress and strain and their relationship from continuum mechanics theory are presented with a brief review of their importance in studying the behaviors of viscoelastic materials.

2.1.1 Basic Concepts and Definitions

Basic concepts and definitions of stress and strain have been widely discussed in continuum mechanics. There are a variety of reference books describing the concepts and definitions of stress–strain for diverse applications (for example: Mase and Mase, 1999). Stress can be defined as a measure of force intensity exerted on a surface in a body. To understand the concept, we begin with a body diagram in Figure 2.1.

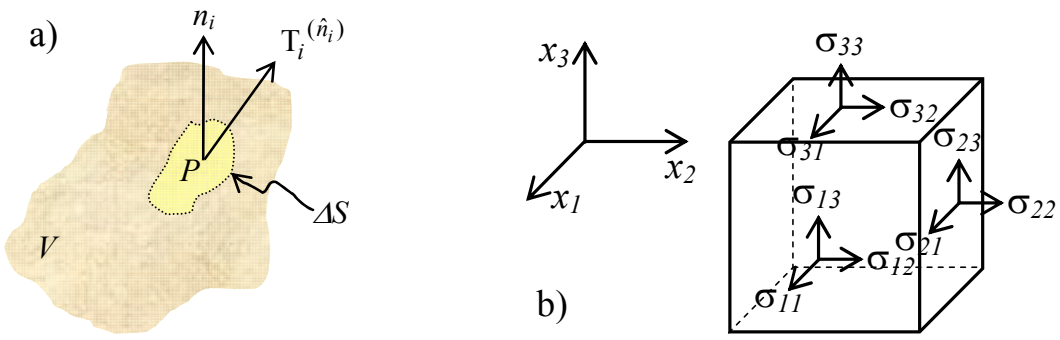

Figure 2.1. (a) A body with an infinitesimal surface element ΔS and a unit normal vector n_i, and (b) Stress tensor components on an infinitesimal volume element.

Let S be the surface area of an element in a body with volume V. $\hat{n}$ denotes a unit vector normal to the surface element. Point P is in the small element of area ΔS. The stress vector is defined as the resultant force ΔF acting on the surface element ΔS :

$$T_i^{(\hat{n}_i)} = \lim_{\Delta S \to 0} \frac{\Delta F}{\Delta S} \tag{2.1}$$

This stress vector depends on the orientation of the surface element and the amplitude and direction of force exerted. Stress tensor σ_{ij} relates to the stress vector at each orientation of the surface element. Employing the Cauchy's stress principle yields

$$T^{(\hat{n}_i)} = n_i . \sigma_{ij} \tag{2.2}$$

where i and j vary from 1 to 3 that represent the direction of the stress. The components of the stress tensor can be expressed in matrix form as

$$\sigma_{ij} = \begin{bmatrix} \sigma_{11} & \sigma_{12} & \sigma_{13} \\ \sigma_{21} & \sigma_{22} & \sigma_{23} \\ \sigma_{31} & \sigma_{32} & \sigma_{33} \end{bmatrix} \tag{2.3}$$

A stress symbolized with the same two subscripts (i.e. σ_{11}, σ_{22}, σ_{33}) is commonly called normal stress and can be a tensile or compressive stress. A stress with the two different subscripts (i.e. σ_{12}, σ_{13}, σ_{21}, σ_{23}, σ_{31}, σ_{32}) is a shear stress and usually symbolized by τ.

Stress acting on point P in an infinitesimal element as in Figure 2.1(a) may cause the element particle to deform. If $P(t_0, x_0)$ represents the position vector $\hat{p}$ at initial position x_0 at time $t = 0$ (un-deformed state) and $P(t, x)$ denotes the position vector $\hat{p}$ at corresponding position x at time t (deformed state), a measure of strain, ε can be expressed as

$$\varepsilon_{ij} = \tfrac{1}{2}\left(u_{i,j} + u_{j,i}\right) \tag{2.4}$$

where u is the displacement vector of a particle in the body. Equation (2.4) is derived based on the infinitesimal strain theory. In the large or finite strain theory, strain is commonly expressed as the ratio of total deformation (ΔL) to the initial dimension (L_0) of the material body or

$$\varepsilon = \frac{\Delta L}{L_0} \tag{2.5}$$

2.1.2 Stress and Strain in Viscoelastic Materials

In studying the behavior of biological materials, it is usually done by applying stresses to the material and recording the strain responses. It is well known that for most

biological materials the strain response to stress exhibits both solid- and fluid-like characteristics. Their behavior is often time-dependent and the stress-strain relationship changes as the strain rate changes. It is, thus, very often to express the behavior of a material in terms of stress, strain, and time effects.

Dynamic stress-strain compressive tests are usually used to evaluate the dynamic mechanical properties of biological materials. Masoudi *et al*. (2007) used mechanical tests to study the effect of storage duration of fruits on the mechanical parameters such as elastic modulus; failure energy, stress, and strain; and toughness, and they found that there were significant changes in the mechanical properties of the fruits over time. Taha *et al*. (2009) employed a linear viscoelastic model to identify the stiffness coefficient from creep and stress relaxation measurements of ligaments for medical surgery applications. They reported that the proposed method proved the need to consider collagen fiber recruitment to inter-relate creep and stress relaxation of ligaments. The results showed that a rheological model with variable stiffness was capable of predicting creep from experimentally measured stress relaxation with a reasonable accuracy.

Young's modulus is the proportionality constant between stress and strain and it can be estimated from the slope of the linear region of the stress-strain curve. The stress and strain relation for ideal elastic materials is expressed as $\sigma = E\,\varepsilon$, where σ is stress, ε is strain, and E is modulus of elasticity or Young's modulus. The viscosity coefficient is defined as the ratio of velocity gradient to the shear-stress by Newton's law of viscosity (Sung and Lee, 2003). For an ideal fluid, it can be written as $\sigma = \eta\,\dot{\varepsilon}$, where η represents the proportionality constant and is usually called viscosity.

2.2 Viscoelastic Models

According to Fung (1993), viscoelastic behavior of a biological material carrying mechanical waves can be modeled with its mechanical analogs of springs and dashpots. A spring represents the ideal elastic behavior of the material, while a dashpot is employed to describe the linear viscosity of it. Basic constitutive models from which more complex mechanical models are derived including Maxwell, Kelvin-Voigt, and the standard linear viscoelastic models (Özkaya *et al*., 1998). The Maxwell model consists of a spring and a dashpot connected consecutively, while the Kelvin-Voigt model comprises a spring and a dashpot connected in parallel. The standard linear solid model is a combination of Maxwell and Kelvin-Voigt models. It has a slightly more complex structure, involving elements in series and in parallel. The three basic mechanical models are shown in Figure 2.2.

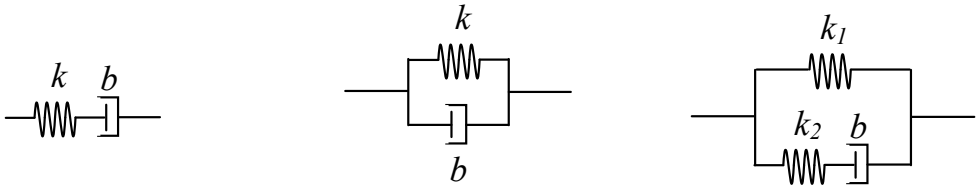

Figure 2.2. Basic mechanical models for viscoelastic materials: (a) Maxwell model; (b) Kelvin-Voigt model; and (c) The standard linear solid model. *k* represents the spring constant of the linear spring and *b* represents the damping coefficient of the dashpot.

Many other mechanical models have been derived and modified from the basic mechanical models. By modifying the connection of elements to the basic models, more complicated models can be obtained. Liu and Xu (2006; 2008), for example, employed two higher-order fractional viscoelastic material models consisting of a fractional Kelvin-Voigt model and a fractional Maxwell model to describe viscoelastic properties of biological materials. Liu and Bilston (2000) used the Maxwell model to examine ex vivo bovine liver; Farshad *et al*. (1999) utilized the Kelvin-Voigt model for ex vivo kidney; Chateline *et al*. (2004) observed viscoelastic properties of soft solid by using both the Maxwell and the Kelvin-Voigt models and found that the Kelvin-Voigt model better represented the viscoelastic properties of the medium. Fukashiro *et al*. (2001) employed the Kelvin-Voigt model to determine the characteristics of human muscle. They examined viscosity and elasticity of muscle fiber and tendon and found that the model could describe the viscoelastic characteristics of human tissues. By using the same model Kuchařová *et al*. (2007) quantified the viscous and elastic parameters for biomedical applications. Furthermore, Purkayastha *et al*. (1984) derived creep equations from the generalized Kelvin-Voigt model to characterize some biological materials by using the constants of the proposed model. The generalized linear solid model was employed to study the stress-strain behavior of ligament by using quasi-static tests (Thornton *et al*. 1997; Lakes and Vanderby, 1999; Hingorani *et al*., 2004). Even though there have been many mechanical models employed to extract mechanical property information of viscoelastic mediums, there is no obvious choice of model structure for a particular medium or application.

2.3 Viscoelastic Behaviors

According to the mechanical models depicted in Figure 2.2, the behavior of viscoelastic materials can be explained by using the constitutive equations that describe the dynamics relationship between stress and strain. Two kinds of test are usually performed, which are constant stress and constant strain. The analytical explanations of creep and stress relaxation behaviors for each model are exhibited in Figure 2.3 (Haddad, 1995). Creep occurs when stress is suddenly applied to a body and kept constant afterward, and the body continues to deform. Stress relaxation refers to the phenomenon that when a body is suddenly strained and the strain is maintained constant afterward, the corresponding stress induced in the body decreases with time (Fung, 1993).

The Maxwell model is particularly useful to describe stress relaxation by using the following equation:

$$\sigma(t) = \sigma_0 \exp\left(-\frac{t}{\tau_R}\right) \tag{2.6}$$

where t and τ_R are time and the stress time constant, respectively. The Kelvin Voigt model is often used to describe the creep function:

$$\varepsilon(t) = \varepsilon_0 \exp\left(1-\frac{t}{\tau_D}\right) \tag{2.7}$$

where τ_D is retardation time. Creep or stress relaxation functions are often used to determine parameters of models. Taha *et al.* (2009), for example, developed mechanical models and employed creep and stress relaxation tests to estimate stiffness parameters of

ligament. They showed that the mechanical models could capture the creep and stress relaxation behavior of ligament.

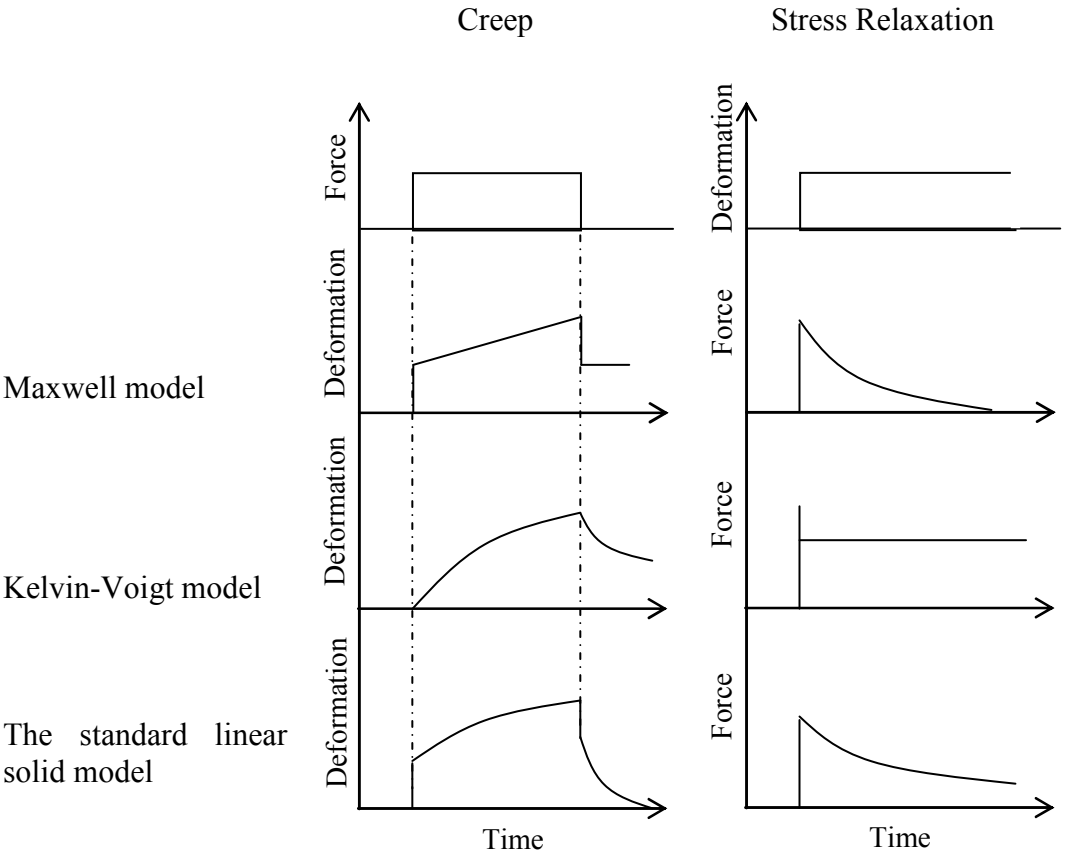

Figure 2.3. Creep and relaxation functions of the basic constitutive models

The dynamic responses of the viscoelastic models to a harmonic excitation are illustrated in Figure 2.4. When a purely elastic material is subjected to an external load, the energy is stored in the body and returned to the original position when the load is removed. In this case, the stress and strain curves have no phase difference, and the stress

is proportional to the strain (Figure 2.4a). For a purely viscous material, the excitation to the body is dissipated and the stress is proportional to the strain rate. The ratio between stress and strain rate is the viscosity of the material. The stress response of a Newtonian liquid is exactly 90^o out of phase with the strain input (Figure 2.4b). For viscoelastic materials, the stress and strain are not in phase. The strain lags behind the stress by angle φ (where $0 < \varphi < \pi/2$) as depicted in Figure 2.4c.

For a sinusoidal strain, $\varepsilon = \varepsilon_0 \cos \omega t$, the stress, load divided by area, can be represented in two components, one in phase with the strain, $\sigma_1 = \sigma_{10} \cos \omega t$, and the other out of phase, $\sigma_2 = \sigma_{20} \sin \omega t$. The complex modulus of elasticity is defined as the ratio of stress to strain, and expressed as

$$E' = \frac{\sigma_1}{\varepsilon} = \left|E^*\right| \cos \varphi \tag{2.8}$$

$$E'' = \frac{\sigma_2}{\varepsilon} = \left|E^*\right| \sin \varphi \tag{29}$$

The magnitude of the modulus is

$$\left|E^*\right| = \frac{\sigma_0}{\varepsilon_0} = \sqrt{E'^2 + E''^2} \tag{2.10}$$

The complex modulus, E^*, is

$$E^* = E' + iE'' \tag{2.11}$$

where E' refers as the real modulus or storage modulus which relates to the energy storage and E'' is the imaginary modulus or loss modulus and is associated with energy dissipation.

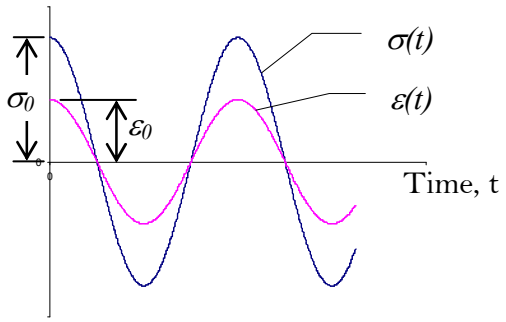

Stress, $\sigma(t) = \sigma_0 \cos(\omega t)$
Strain, $\varepsilon(t) = \varepsilon_0 \cos(\omega t)$

(a) Elastic material

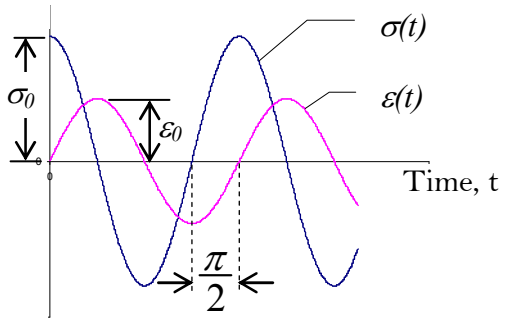

Stress, $\sigma(t) = \sigma_0 \cos(\omega t)$
Strain, $\varepsilon(t) = \varepsilon_0 \cos(\omega t - \pi/2)$

(b) Viscous material

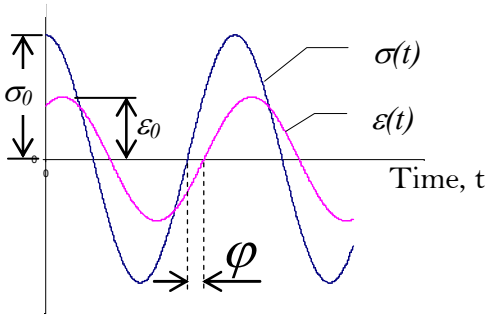

Stress, $\sigma(t) = \sigma_0 \cos(\omega t)$
Strain, $\varepsilon(t) = \varepsilon_0 \cos(\omega t - \varphi)$
Angle φ, where $0 < \varphi < \pi/2$

(c) Viscoelastic material

Figure 2.4. Typical stress-strain curves for harmonic excitation to elastic, viscous, and viscoelastic materials

The phase lag between the stress and strain is used to determine loss tangent $\tan(\varphi)$. The loss tangent is considered as a measure of damping, which is

$$\tan(\varphi) = \frac{E'}{E''} \tag{2.12}$$

Similarly, viscosity can also expressed in complex term as

$$|\eta^*| = \frac{\sigma_0}{\dot{\varepsilon}_0} = \sqrt{(\eta')^2 + (\eta'')^2} \tag{2.13}$$

where $\eta' = \frac{\sigma_0}{\dot{\varepsilon}} \sin(\varphi)$ is the real viscosity, and

$\eta'' = \frac{\sigma_0}{\dot{\varepsilon}} \cos(\varphi)$ is the imaginary viscosity.

2.4 Ultrasound for Nondestructive Evaluation

As described in the previous chapter, ultrasound is a mechanical wave that has frequency greater than 20 kHz. The energy of sound usually generated by a transducer is transferred from one point to another through a medium. The sound energy propagates through the medium as a series of mechanical motion: compression and rarefaction. If the medium is viscoelastic, the motion can be represented by a mechanical model. In this section, the basic theory of wave motion in one dimension is described. The characteristics of acoustic wave applied for evaluation of biological materials are then reviewed briefly.

2.4.1 Basic Theory of Wave Motion

If an external force is excited to a body, it may produce energy. The energy will propagate from one side at higher energy to another side at lower energy. The energy

propagation is typically expressed with the wave equation. Basically, wave motion can be described in a harmonic wave form as

$$u(x,t) = u_0 \cos(\omega t - kx) \tag{2.14}$$

where u is the amplitude of the wave at time t and position x, u_0 is half the peak-to-peak amplitude, k is the wave number (angular spatial frequency) and ω is the temporal frequency. Taking the second partial derivative of the equation with respect to space and time yields

$$\frac{\partial^2 u}{\partial x^2} = -k^2 u_0 \cos(\omega t - kx) \tag{2.15}$$

$$\frac{\partial^2 u}{\partial t^2} = -\omega^2 u_0 \cos(\omega t - kx) \tag{2.16}$$

Substituting equation (2.15) into (2.16) we get

$$\frac{\partial^2 u}{\partial x^2} = \frac{k^2}{\omega^2} \frac{\partial^2 u}{\partial t^2} \tag{2.17}$$

or,

$$\frac{\partial^2 u}{\partial x^2} = \frac{1}{\nu^2} \frac{\partial^2 u}{\partial t^2} \tag{2.18}$$

Equation (2.18) is the linear wave equation for one dimension (x direction), where $\nu = \frac{\omega}{k}$ is the phase velocity.

The wave equation above does not directly include the material properties. To express the wave equation incorporating the relevant material properties, it can be derived from the Newton's second law. Assume that a longitudinal ultrasonic wave is propagating along a body as shown in Figure 2.5 (Shull and Tittmann, 2002), the stress σ can be expressed as

$$\sigma = \frac{\partial \sigma}{\partial x} dx \quad \text{or,}$$

$$F = \left(\frac{\partial \sigma}{\partial x} dx \right) A \tag{2.19}$$

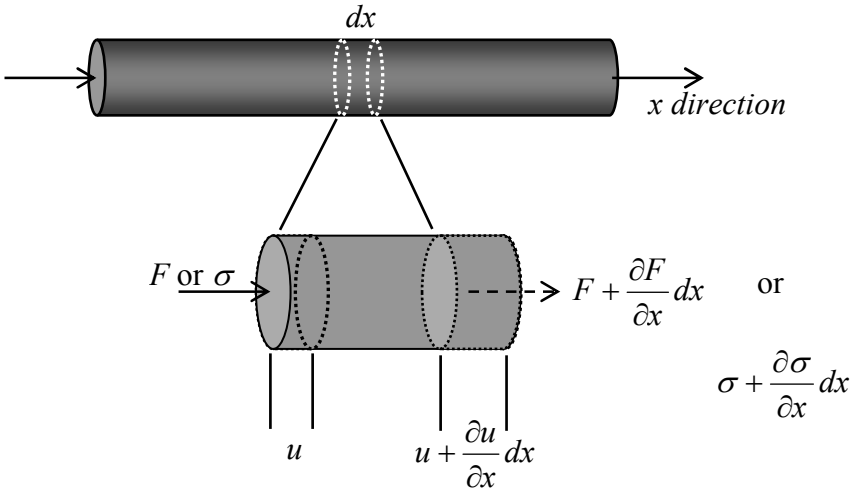

Figure 2.5. Ultrasound longitudinal wave propagating in a long thin rod

The Newton's second law states that

$$F = m\frac{\partial v}{\partial t} \tag{2.20}$$

$V = dx.A$ is the volume of the material. Equating with equations (2.19) and (2.20) yields

$$\left(\frac{\partial \sigma}{\partial x}dx\right)A = m\frac{\partial v}{\partial t} \tag{2.21}$$

$$\frac{\partial \sigma}{\partial x} = \rho\frac{\partial^2 u_x}{\partial t^2} \tag{2.22}$$

where ρ is the density of the material, u is the displacement vector, and subscript x denotes the displacement in x-direction. Assume that the displacement is infinitesimal, the Poisson's ratio effects can be neglected, and the material can be treated as linear elastic, the stress is proportional to strain, ε,

$$\sigma = E\,\varepsilon \tag{2.23}$$

where E is modulus elasticity of the material and commonly called the Young's modulus. Taking the first derivative of this equation with respect to the space (displacement) yields

$$\frac{\partial \sigma}{\partial x} = E\frac{\partial \varepsilon}{\partial x} \tag{2.24}$$

Substituting this equation into Eqn. (2.22), we get

$$E\frac{\partial^2 u_x}{\partial^2 x} = \rho\frac{\partial^2 u_x}{\partial t^2} \tag{2.25}$$

$$\frac{\partial^2 u_x}{\partial^2 x} = \frac{\rho}{E}\frac{\partial^2 u_x}{\partial t^2} \tag{2.26}$$

This equation is another expression of the wave equation that depends on material properties. Now we can derive the relationship between phase velocity and material properties, $v = \sqrt{\frac{E}{\rho}}$.

2.4.2 Ultrasound Characteristics

One of the important characteristics of ultrasound in characterizing material properties is sound velocity. Utilization of this property is based on the fact that when an ultrasonic wave passes through different materials, the sound velocities are different. The characteristic of the wave can then be related to material properties and expressed by

$$k^* = \frac{\omega}{c} + i\alpha \tag{2.27}$$

where k^* is a complex wave number, c is sound velocity, ω is the angular frequency (= $2\pi f$), α is the attenuation coefficient, f is frequency, and $i = \sqrt{-1}$. According to equations (2.17) and (2.26), the wave number in the equation can be related to the material properties: Young's modulus, E, and density of the material, ρ via the following equation:

$$\left(\frac{k^*}{\omega}\right)^2 = \frac{\rho}{E} \tag{2.28}$$

This equation obviously states that ultrasonic velocity is determined by the density and the elastic response of the material. The material properties can thus be expressed in terms of compressibility or a storage modulus (Coupland and McClements, 2001).

According to this fact, sound velocity has been utilized as a nondestructive ultrasound parameter in engineering and evaluation of biological materials.

Sound velocity in a medium is not only influenced by the current temperature but also the history of temperature. The effect of temperature on sound velocity in some liquids under thermal cycles was investigated by Koc and Vatandas (2006). They reported that the area encompassed by the hysteresis curve from heating and cooling measurements can be used to identify the medium. Because of the temperature dependence, ultrasound velocity is a useful variable in investigating the dynamic phase transition temperature of industrial materials as reported by Todo and Tatsuzaki (1974). Sound velocity has also been used in evaluation of fruits and vegetables. Setsuo and Jun'ichi (1999) reported that ultrasound velocity could be used to evaluate the freshness and processing degree of cucumbers and kiwifruits. The measured ultrasound velocity decreased with decreasing freshness and processing, and decreased with increasing ripeness. Ultrasound transmission velocity can also be used to estimate material firmness.

Another important property of ultrasound is attenuation. When sound waves propagate through a medium the amplitude of the sound waves decays exponentially with distance. The amplitude decrease is because of intra-molecular friction, absorption and scattering in the medium (Cheeke, 2002). The absorption is generally caused by a physical phenomenon that convert ultrasound into heat, while scattering occurs in inhomogeneous materials. The attenuation coefficient is often used to quantify the decrease in amplitude of ultrasonic wave. Attenuation increases with the frequency of the sound wave and decreases with the density of medium. The attenuation coefficient, α, is defined by the following expression:

$$u = u_o e^{-\alpha x} \tag{2.29}$$

where u_0 is the initial ultrasound signal amplitude and u is the amplitude of the signal after the signal travels distance x from the initial location. The attenuation can be expressed in unit of nepers per unit length. It is also often expressed in decibels (dB), which is defined as

$$\alpha\ (dB) = 20 \log_e \left(\frac{u}{u_o} \right) \tag{2.30}$$

A number of studies on the relationship between sound attenuation and material properties have been published. Quantitative characterization of the linkage between ultrasound attenuation and physiological parameters of fruits was reported by Mizrach *et al*. (1999) and Mizrach (2000; 2008). They found that ultrasound attenuation was a good indicator of changes in firmness, water content, acidity and oil in biological tissues during physiological processes. Sharma (1968) investigated the excess absorption of ultrasound in monatomic fluids using the thermodynamic theory of relaxation processes. Botros *et al*. (1987) and Nakajima *et al*. (1999) developed a mechanism for ultrasound measurement for biological tissue characterization based on parameter attenuation. All the studies concluded that ultrasound velocity and attenuation are useful indices for material characterization.

The propagation of ultrasound through inhomogeneous media is more complex. When transmission of ultrasound meets density mismatch in medium, part of the sound energy will be reflected. The acoustic impedance can be utilized to characterize the properties of the medium. If the acoustic impedances of two media at normal incidence

are known to be Z_1 and Z_2, respectively, the fractions of the incident wave intensity that are reflected and transmitted can be calculated as (Cheeke, 2002)

$$R = \left(\frac{Z_2 - Z_1}{Z_2 + Z_1} \right)^2 \tag{2.31}$$

$$T = 1 - R = \frac{4 Z_2 Z_1}{(Z_2 + Z_1)^2} \tag{2.32}$$

where R is the reflection coefficient and T is the transmission coefficient. The acoustic impedance (Z) of a medium depends on the density (ρ) and sound velocity (c). The greater the impedance difference is between two adjacent mediums the more reflective the boundary will be. Reflection of sound wave associated with acoustic impedance is one of the principal physical properties for ultrasound imaging. A number of research efforts in characterizing biological materials using acoustic impedance have been reported. Deblock *et al*. (1998) used an impedance to determine the mechanical dynamic shear properties of some solutions. They reported that the reflection coefficient could be used to estimate dynamic viscosity and stiffness of the solutions. Acoustic impedance has been applied in medical diagnosis. Wachinger *et al*. (2008) developed an ultrasound image reconstruction method using acoustic impedance. Mamou *et al*. (2003) used ultrasonic scatterer sizes to diagnose disease in a tissue and Hozumi *et al*. (2005) characterized biological tissues based on the contrast in the acoustic impedance.

CHAPTER 3

MODEL DEVELOPMENT AND VALIDATION

This chapter introduces the basic ideas employed to model pressure waves through a viscoelastic medium and the assumptions used in the developed model. A network of the Kelvin-Voigt model was employed to discretize the medium and dynamic equations were derived from the mechanical network. The model structure was tested against ultrasound experiments. An algorithm was developed for model parameter estimation and model verification results are presented. Finally, the relations between model parameters and material properties were obtained and experimental data are presented.

3.1 Introduction

Characteristics of ultrasound propagation have been used in a variety of technologies including medical ultrasound (Nitta and Shiina, 2002; Nitta and Homma, 2005; Shiina *et al*., 2007), food processing (Ay and Gunasekaran, 2003; Koc and Vatandas, 2006), and ultrasonic noninvasive evaluation (Mizrach, 2000; Zude *at al*., 2006; Kim *et al*., 2009). Even though many studies have been reported, the physical processes of ultrasound propagation in a medium and its relations with material physical and mechanical properties are not fully understood.

Biological materials have dynamic metabolic functions, complex geometry, and shape heterogeneity; and their ultrasound characteristics are not yet well understood, especially for transmission waves. In terms of system modeling, the unknown ultrasound

characteristics through a material may be represented by the block diagram in Figure 3.1. The characteristics of the system can be studied from the relationship between excitation (input) and response (output).

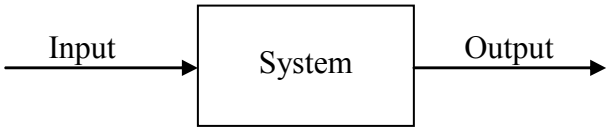

Figure 3.1. Input-output block diagram of a system

Ultrasound propagation has been extensively modeled and simulated in the literature based on inviscid or viscous wave equations. For example, Sushilov and Cobbold (2004) provides a time-domain solution to the wave equation for viscous media. Wismer (2006) proposes a modified viscous wave equation with power-law attenuation. Finite-element solution of the modified wave equation shows usefulness of the resulting algorithm in simulating scattering patterns for inhomogeneous media. These models have shown great promise for simulating ultrasound propagation (the forward problem), but the model structures, typically in the form of partial differential equations, may lead to difficulty in model parameter estimation from measured ultrasound signal (the inverse problem). Moreover, material mechanical properties such as stiffness and damping coefficients are not directly included in the wave equation. In this work, we would extract feature information from measured ultrasound transmission through a viscoelastic medium by using a simple mechanical model for the purpose of estimating mechanical

properties of biological materials. This study is based on the fact that ultrasound waves propagate through a medium as mechanical vibrations. The response of a medium depends on the behavior of the medium and on the excitation characteristics (Meirovitch, 1997).

In studying the behavior of viscoelastic materials the system in Figure 3.1 is often represented by a mechanical model consisting of masses, springs and dashpots. Spring is used to describe the elastic behavior of the medium, while dashpot is associated with the viscous resistance or dissipated energy. The basic mechanical models are the Maxwell model, Kelvin-Voigt model, and Standard Linear Solid model (Fung, 1993). The mechanical model representations have been extensively used to study the rheological behaviors of viscoelastic materials in the most engineering systems. Blanc (1993) studied the behavior of viscoelastic materials in the linear viscoelastic range by using mechanical wave propagation. The rheological properties of the samples were deduced from the phase velocity and the attenuation coefficient from Fourier transforms.

Mechanical property estimation by ultrasound has heavily relied on statistical correlations between measurable quantities, such as sound speed and intensity, and material properties of interest (Chen *et al*. 1994, 2004; Koc and Vatandas 2006), which give relationships of little physical meaning and limited generality. The aim of this work was to develop a mechanical model for ultrasound propagation in a viscoelastic medium that provides a physically meaningful basis for viscoelastic property evaluation. The medium was decomposed into a network of viscoelastic elements according to the Kelvin-Voigt model. The model parameters were optimized to predict ultrasound responses to designed perturbations.

3.2 Model Development

3.2.1 Basic Representation

When a medium is excited by an ultrasonic wave, the sound moves away from the source and generates a sound field in the region ahead of the generator. Because piston ultrasound generators are used in this study, the sound wave field can be treated as a column (cylinder) of pressure waves (ASTM, 2007) with a shear transition zone to the stationary medium. This zone would affect the movement of the cylinder by shear stress and strain at the cylinder surface. In fact, the detailed stress or strain zone may be much more complex. Figure 3.2 illustrates the pressure wave propagation used in this study. The transducers are positioned in a "pitch-and-catch" mode at distance L. Longitudinal ultrasound is transmitted from the excitation transducer to the medium and the response is sensed by the receiver transducer. In order to yield a parsimonious model structure that could capture the main dynamic effects, we assume that the pressure wave column is approximately a cylinder with diameter D, the diameter of the transducer element. An outer region of the surrounding medium is considered stationary since the samples are either much larger than the transducer diameter or are held in a chamber or between two plates as is the case in this work.

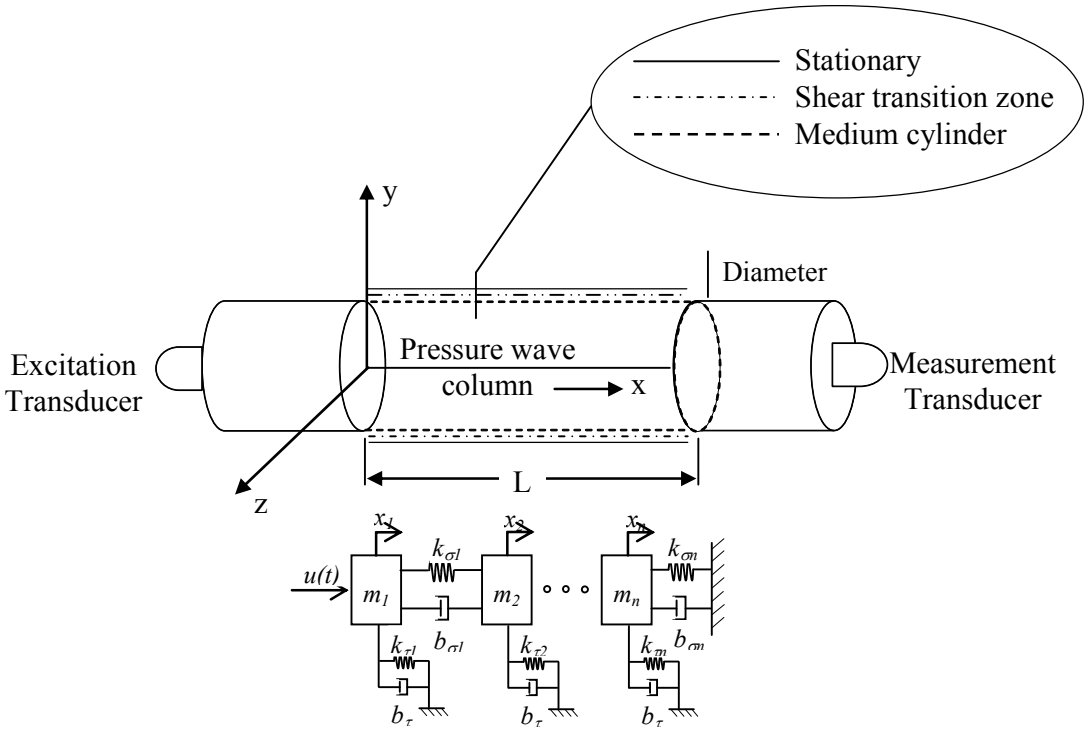

Figure 3.2. Illustration of pressure wave column with surrounding stationary medium in ultrasound transmission system

The medium in the pressure wave column may be discretized into a network of n elements. A discrete mechanical model based on the Kelvin-Voigt model can then be constructed to represent the medium. The Kelvin-Voigt model is used because it describes the dynamic behavior of soft solid tissues better than the Maxwell model (Chateline *et al*., 2004) and it is simpler than the standard linear solid model. Each element of the medium is characterized by five parameters: mass (m), normal stiffness coefficient (k_σ), shear stiffness coefficient (k_τ), normal damping coefficient (b_σ), and shear damping coefficient (b_τ). The normal stiffness and damping are used to represent the viscoelastic properties of the material under normal stress (pressure), whereas the

shear stiffness and damping are used to represent the shear properties and to account for the effects of the surrounding, stationary material on the vibrating pressure column. Since the measurement transducer in this work is mounted on a measurement chamber, the backing material in the transducer is represented as a fixed boundary to the right end in Figure 3.3. Thus, what the measurement transducer "feels" is the force (or pressure) exerted by the medium via the last spring ($k_{\sigma n}$) and dashpot ($b_{\sigma n}$).

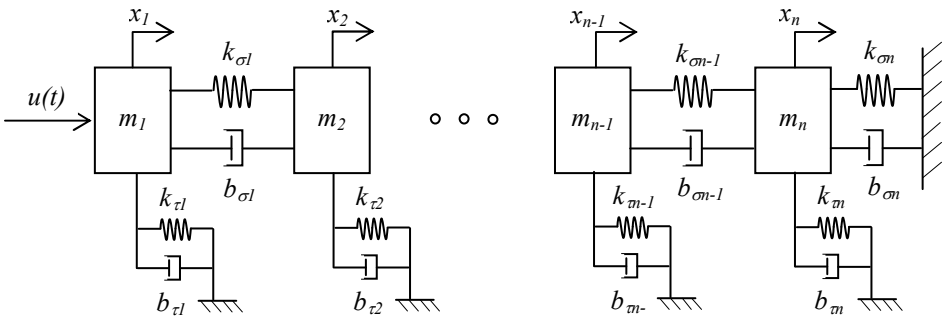

Figure 3.3. Finite-element mechanical model to represent one-dimensional ultrasound transmission in viscoelastic materials. u is input, x is displacement, m is mass, k is stiffness coefficient, and b is damping coefficient. Subscript σ and τ represent normal and shear direction, respectively. i (1, 2, 3,…, n) represents the i^{th} element in the network; and n is the number of elements.

3.2.2 Equations of Motion

For a system with n elements as shown in Figure 3.3, the behavior of a viscoelastic material can be described by using the second-order differential equation of motion. For the n masses, their motions are described by

$$m_1\ddot{x}_1 + (b_{\sigma 1} + b_{\tau 1})\dot{x}_1 - b_{\sigma 1}\dot{x}_2 + (k_{\sigma 1} + k_{\tau 1})x_1 - k_{\sigma 1}x_2 = u(t)$$

$$m_2\ddot{x}_2 - b_{\sigma 1}\dot{x}_1 + \left(b_{\sigma 1} + b_{\sigma 2} + b_{\tau 2}\right)\dot{x}_2 - b_{\sigma 2}\dot{x}_3 - k_{\sigma 1}x_1 + \left(k_{\sigma 1} + k_{\sigma 2} + k_{\tau 2}\right)x_2 - k_{\sigma 2}x_3 = 0$$

$$\vdots$$

$$m_n\ddot{x}_n - b_{\sigma n-1}\dot{x}_{n-1} + (b_{\sigma n-1} + b_{\sigma n} + b_{\tau n})\dot{x}_n - k_{\sigma n-1}x_{n-1} + (k_{\sigma n-1} + k_{\sigma n} + k_{\tau n})x_n = 0 \tag{3.1}$$

These equations can be written in a general matrix form as

$$\mathbf{M}\ \ddot{x}(t) + \mathbf{B}\ \dot{x}(t) + \mathbf{K}\ x(t) = \mathbf{B_o}\ u(t) \tag{3.2}$$

where t is time; $x(t)$ is the displacement vector and the dots denote differentiation of displacement with respect to time; $u(t)$ is the excitation vector; **M, B,** and **K** are the mass, damping coefficient, and stiffness coefficient matrices of the system, respectively; and $\mathbf{B_o}$ is the input matrix. **M**, **B**, **K**, and $\mathbf{B_o}$ are given by

$$\mathbf{M}_{(n\times n)} = \begin{pmatrix} m_1 & 0 & \ldots & 0 & 0 \\ 0 & m_2 & \ldots & 0 & 0 \\ \ldots & \ldots & \ldots & \ldots & \ldots \\ 0 & 0 & \ldots & m_{n-1} & 0 \\ 0 & 0 & \ldots & 0 & m_n \end{pmatrix} \tag{3.3}$$

$$\mathbf{B}_{(n\times n)} = \begin{pmatrix} \left(b_{\sigma 1} + b_{\tau 1}\right) & -b_{\sigma 1} & \ldots & 0 & 0 \\ -b_{\sigma 1} & \left(b_{\sigma 1} + b_{\sigma 2} + b_{\tau 2}\right) & \ldots & 0 & 0 \\ \ldots & \ldots & \ldots & \ldots & \ldots \\ 0 & 0 & \ldots & \left(b_{\sigma n-2} + b_{\sigma n-1} + b_{\tau n-1}\right) & -b_{\sigma n-1} \\ 0 & 0 & \ldots & -b_{\sigma n-1} & \left(b_{\sigma n-1} + b_{\sigma n} + b_{\tau n-1}\right) \end{pmatrix} \tag{3.4}$$

$$\mathbf{K} = \begin{pmatrix} (k_{\sigma 1} + k_{\tau 1}) & -k_{\sigma 1} & \dots & 0 & 0 \\ -k_{\sigma 1} & (k_{\sigma 1} + k_{\sigma 2} + k_{\tau 2}) & \dots & 0 & 0 \\ \dots & \dots & \dots & \dots & \dots \\ 0 & 0 & \dots & (k_{\sigma n-2} + k_{\sigma n-1} + k_{\tau n-1}) & -k_{\sigma n-1} \\ 0 & 0 & \dots & -k_{\sigma n-1} & (k_{\sigma n-1} + k_{\sigma n} + k_{\tau n-1}) \end{pmatrix} \tag{3.5}$$

$$\mathbf{B_o}_{(n\times 1)} = (1 \quad 0 \quad \dots \quad 0 \quad 0)^T \tag{3.6}$$

where *m, k*, and *b* are mass, stiffness coefficient, and damping coefficient, respectively. Subscripts σ and τ represent normal and shear directions, respectively, and *i* (1, 2, 3,…, *n*) represents the i^{th} elements in the network and *n* is the number of elements.

Since **M** in Eqn. (3.2) is invertible, the equation can be written into

$$\ddot{x}(t) = -\mathbf{M}^{-1}\mathbf{B}\dot{x}(t) - \mathbf{M}^{-1}\mathbf{K}x(t) + \mathbf{M}^{-1}\mathbf{B}_{\circ}u(t) \tag{3.7}$$

Eqn. (3.7) can be further expressed as

$$\frac{d}{dt}\begin{bmatrix} x(t) \\ \dot{x}(t) \end{bmatrix} = \begin{bmatrix} 0 & \mathbf{I} \\ -\mathbf{M}^{-1}\mathbf{K} & -\mathbf{M}^{-1}\mathbf{B} \end{bmatrix}\begin{bmatrix} x(t) \\ \dot{x}(t) \end{bmatrix} + \begin{bmatrix} 0 \\ \mathbf{M}^{-1}\mathbf{B}_{\circ} \end{bmatrix}u(t) \tag{3.8}$$

where **I** is the identity matrix. Equation (3.8) can be written in the state space form as

$$\dot{z}(t) = \overline{\mathbf{A}}z(t) + \overline{\mathbf{B}}u(t) \tag{3.9}$$

where

$$z(t) = [x(t) \quad \dot{x}(t)]^T \tag{3.10}$$

$$\overline{\mathbf{A}} = \begin{bmatrix} 0 & \mathbf{I} \\ -\mathbf{M}^{-1}\mathbf{K} & -\mathbf{M}^{-1}\mathbf{B} \end{bmatrix} \tag{3.11}$$

$$\overline{\mathbf{B}} = \begin{bmatrix} 0 \\ \mathbf{M}^{-1}\mathbf{B}_{\circ} \end{bmatrix} \tag{3.12}$$

$z(t)$, $\overline{\mathbf{A}}$ and $\overline{\mathbf{B}}$ are the state vector ($\in \Re^{2n\times 1}$), system matrix ($\in \Re^{2n\times 2n}$), and input matrix ($\in \Re^{2n\times 1}$), respectively. The formulation in state space form has $2n$ states equivalent to the displacements in the second-order system.

For a single medium that is discretized into equal-sized elements the model parameter values do not vary from element to element, and thus the masses, stiffness coefficients, and damping coefficients can be defined as

$$m_1 = m_n = \tfrac{1}{2}m; \quad m_2 = m_3 ... = m_{n-1} = m \tag{3.13}$$

$$k_{\sigma 1} = k_{\sigma 2} = ... = k_{\sigma i} = k_{\sigma} \tag{3.14}$$

$$k_{\tau 1} = k_{\tau 2} = ... = k_{\tau i} = k_{\tau} \tag{3.15}$$

$$b_{\sigma 1} = b_{\sigma 2} = \mathbf{...} = b_{\sigma i} = b_{\sigma} \tag{3.16}$$

$$b_{\tau 1} = b_{\tau 2} = \mathbf{...} = b_{\tau i} = b_{\tau} \tag{3.17}$$

By inserting Eqns. (3.13) – (3.17) into Eqns. (3.3) – (3.5), the matrix $\overline{\mathbf{A}}$ (Eqn. (3.11)) and vector $\overline{\mathbf{B}}$ (Eqn. (3.12)) can be written as Eqns. 3.18 and 3.19.

$$\mathbf{A}=\begin{bmatrix}
0 & 0 & 0 & \dots & 0 & 0 & 0 & 1 & 0 & 0 & \dots & 0 & 0 & 0 \\
0 & 0 & 0 & \dots & 0 & 0 & 0 & 0 & 1 & 0 & \dots & 0 & 0 & 0 \\
0 & 0 & 0 & \dots & 0 & 0 & 0 & 0 & 0 & 1 & \dots & 0 & 0 & 0 \\
\dots & \dots & \dots & \dots & \dots & \dots & \dots & \dots & \dots & \dots & \dots & \dots & \dots & \dots \\
0 & 0 & 0 & \dots & 0 & 0 & 0 & 0 & 0 & 0 & \dots & 1 & 0 & 0 \\
0 & 0 & 0 & \dots & 0 & 0 & 0 & 0 & 0 & 0 & \dots & 0 & 1 & 0 \\
0 & 0 & 0 & \dots & 0 & 0 & 0 & 0 & 0 & 0 & \dots & 0 & 0 & 1 \\
-\frac{2(k_\sigma+k_\tau)}{m} & \frac{2k_\sigma}{m} & 0 & \dots & 0 & 0 & 0 & -\frac{2(b_\sigma+b_\tau)}{m} & \frac{2b_\sigma}{m} & 0 & \dots & 0 & 0 & 0 \\
\frac{k_\sigma}{m} & -\frac{(2k_\sigma+k_\tau)}{m} & \frac{k_\sigma}{m} & \dots & 0 & 0 & 0 & \frac{b_\sigma}{m} & -\frac{(2b_\sigma+b_\tau)}{m} & \frac{b_\sigma}{m} & \dots & 0 & 0 & 0 \\
0 & \frac{k_\sigma}{m} & -\frac{(2k_\sigma+k_\tau)}{m} & \dots & 0 & 0 & 0 & 0 & \frac{b_\sigma}{m} & -\frac{(2b_\sigma+b_\tau)}{m} & \dots & 0 & 0 & 0 \\
\dots & \dots & \dots & \dots & \dots & \dots & \dots & \dots & \dots & \dots & \dots & \dots & \dots & \dots \\
0 & 0 & 0 & \dots & -\frac{(2k_\sigma+k_\tau)}{m} & \frac{k_\sigma}{m} & 0 & 0 & 0 & 0 & \dots & -\frac{(2b_\sigma+b_\tau)}{m} & \frac{b_\sigma}{m} & 0 \\
0 & 0 & 0 & \dots & \frac{k_\sigma}{m} & -\frac{(2k_\sigma+k_\tau)}{m} & \frac{k_\sigma}{m} & 0 & 0 & 0 & \dots & \frac{b_\sigma}{m} & -\frac{(2b_\sigma+b_\tau)}{m} & \frac{b_\sigma}{m} \\
0 & 0 & 0 & \dots & 0 & \frac{2k_\sigma}{m} & -\frac{2(2k_\sigma+k_\tau)}{m} & 0 & 0 & 0 & \dots & 0 & \frac{2b_\sigma}{m} & -\frac{2(2b_\sigma+b_\tau)}{m}
\end{bmatrix} \tag{3.18}$$

$$\mathbf{B}=\begin{bmatrix} 0 & 0 & 0 & \dots & 0 & 0 & 0 & \frac{2}{m} & 0 & 0 & \dots & 0 & 0 & 0 \end{bmatrix}^T \tag{3.19}$$

For transmitted waves, the measured output of the system is the total force exerted by the spring ($k_{\sigma n}$) and dashpots ($b_{\sigma n}$) on the measurement transducer and can be expressed as

$$y(t) = \mathbf{C}\, z(t) \tag{3.20}$$

where

$$\mathbf{C} = \begin{bmatrix} 0 & 0 & .. & ... & k_{\sigma n} & b_{\sigma n} \end{bmatrix}_{2n}^{T} \tag{3.21}$$

is the output matrix ($\in \Re^{2n\times 1}$).

3.2.3 Model Parameter Estimation

The aim of model parameter estimation is to find suitable model parameter values to make model predictions match experimental measurements. Since material density (ρ) is often known or measurable by other methods, m is assumed to be known. For equal-sized homogenous elements, there are only four model parameters to be estimated from the measured input and output signals: normal stiffness coefficient (k_σ), shear stiffness coefficient (k_τ), normal damping coefficient (b_σ), and shear damping coefficient (b_τ). The model prediction by Eqn. (3.20) can be obtained numerically by using the fourth-order Runge-Kutta method (Brown, 2007) defined as

$$k_1 = f\left(t, z, u(t)\right)$$

$$k_2 = f\left(t + \frac{h}{2}, z + \frac{k_1}{2}, u(t + \frac{h}{2})\right)$$

$$k_3 = f\left(t + \frac{h}{2}, z + \frac{k_2}{2}, u(t + \frac{h}{2})\right)$$

$$k_4 = f\left(t + h, z + k_3, u(t + h)\right)$$

$$z_{j+1} = z_j + \frac{\left(k_1 + 2k_2 + 2k_3 + k_4\right)}{6} h \tag{3.22}$$

where t is time, h is time step or sampling period, and subscript j is the index of data point.

A least-squares based algorithm is employed to evaluate the parameters of the state-space model. The errors between measurement $\left(y(t)\right)$ and model prediction $\left(\hat{y}(t)\right)$ are calculated as

$$e(t) = y(t) - \hat{y}(t) \tag{3.23}$$

The errors are to be minimized by adjusting the model parameters through iterations based on the Jacobian matrix. Each model parameter is evaluated for each data point by the following procedures:

$$\theta^{i+1} = \theta^i + \Delta\theta \tag{3.24}$$

$$\Delta\theta = (J'J + \lambda I)^{-1} J'\left(y(t) - \hat{y}(t)\right) \tag{3.25}$$

where θ is the vector of model parameters ($\theta = [k_\sigma, k_\tau, b_\sigma, b_\tau]^T$); λI is a diagonal identity matrix, and J is the Jacobian matrix of partial derivatives of $y(t)$ with respect to each

model parameter (Constantinides and Mostoufi, 1999). The Jacobian matrix J is expressed as

$$J = \begin{bmatrix} \frac{\partial y_1}{\partial \theta_1} & \cdots & \frac{\partial y_1}{\partial \theta_l} \\ \cdots & \cdots & \cdots \\ \frac{\partial y_j}{\partial \theta_1} & \cdots & \frac{\partial y_j}{\partial \theta_l} \end{bmatrix} = \begin{bmatrix} \frac{\partial y_1}{\partial k_\sigma} & \frac{\partial y_1}{\partial k_\tau} & \frac{\partial y_1}{\partial b_\sigma} & \frac{\partial y_1}{\partial b_\tau} \\ \cdots & \cdots & \cdots & \cdots \\ \frac{\partial y_j}{\partial k_\sigma} & \frac{\partial y_j}{\partial k_\tau} & \frac{\partial y_j}{\partial b_\sigma} & \frac{\partial y_j}{\partial b_\tau} \end{bmatrix} \tag{3.26}$$

where subscript j and l are the index of data point and the number of model parameters, respectively. With the Jacobian matrix, the Levenberg-Marquardt algorithm is used to minimize the prediction error. The model prediction is compared to the measurement to compute the mean squared error (Castello *et al.*, 2008) as

$$\text{MSE} = \frac{1}{N} \sum_{j=1}^{N} \left(y_j - \hat{y}_j \right)^2 \tag{3.27}$$

where N is number of data, (j = 1, 2, 3, …, N). The iteration stops when an objective minimum error is reached (e.g. 10^{-12}). The flowchart of the algorithm is shown in Figure 3.4 and was implemented in Matlab (version 7.1, MathWorks).

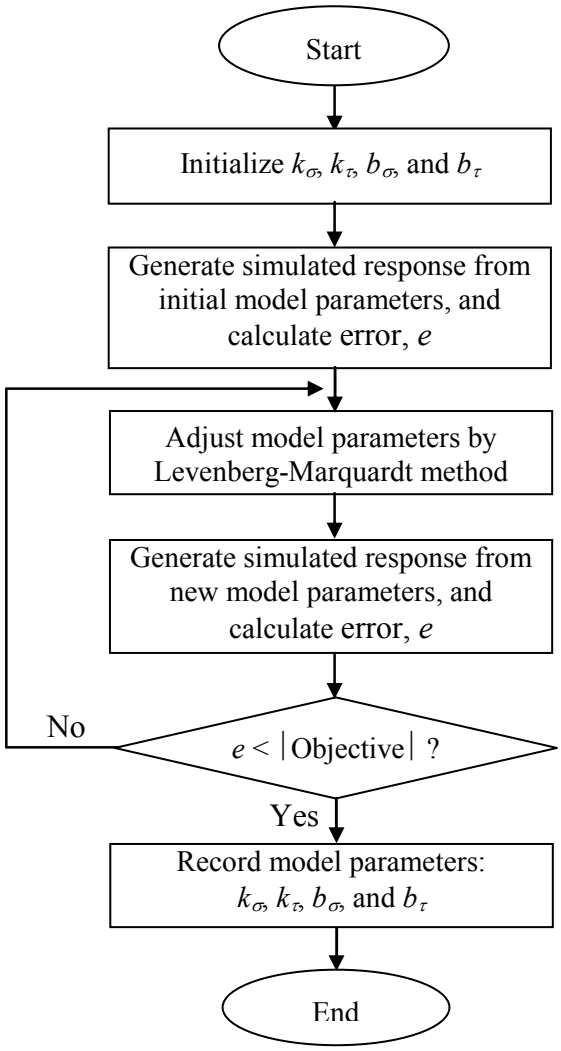

Figure 3.4. Flow diagram of parameter estimation procedure

3.3 Model Validation

All model parameters in the state space equation are geometry-dependent. In order to validate the developed model, the parameters should first be converted into non-geometry-dependent variables or material properties. The model parameters are mass (m), normal stiffness constant (k_σ), normal damping coefficient (b_σ), shear stiffness constant

(k_τ), and shear damping coefficient (b_τ). The material properties are ρ, E_σ, η_σ, E_τ, and η_τ representing density, normal elastic modulus, normal viscosity, shear elastic modulus, and shear viscosity, respectively. For constant element size (Figure 3.5) and homogeneous material, the mathematical expressions to relate the modal parameters to the material properties are as follows.

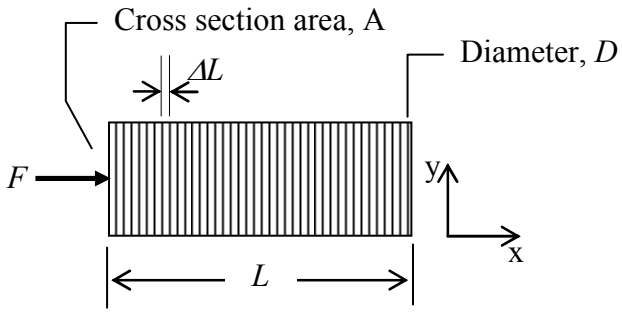

Figure 3.5. Diagram of medium cylinder used to determine relationships between the material properties and the model parameters

Mass is related to the density of sample and the volume of the cylinder medium by

$$\rho = \frac{m}{\frac{1}{4}\pi D^2 L} \tag{3.28}$$

The elastic modulus for normal stress, E_σ, is calculated by dividing the stress by the strain in the normal direction as

$$E_\sigma = \frac{F/\mathrm{A}}{\Delta \mathrm{x}/\mathrm{x}} \quad \text{or} \quad F = \frac{E_\sigma \mathrm{A}}{\mathrm{x}} \Delta \mathrm{x} \tag{3.29}$$

where F is external force applied to the medium, A is the cross sectional area of the medium cylinder, Δx is the displacement of medium from its initial length, x. According to Hooke's law:

$$F = k_\sigma . \Delta \mathrm{x} \tag{3.30}$$

where k_σ is spring constant in the normal direction. Equating Eqns. (3.29) and (3.30) we get

$$k_\sigma = \frac{E_\sigma \mathrm{A}}{\mathrm{x}} \tag{3.31}$$

If the length of medium cylinder is L, the medium is discretized into n equal-sized elements, and the diameter of pressure wave column is D, the elastic modulus in the normal direction, E_σ, is

$$E_\sigma = \frac{\left(L/n\right)}{\frac{1}{4}\pi D^2} k_\sigma \tag{3.32}$$

The conversion of damping coefficient b into viscosity η is based on the definition of friction

$$F = b_\sigma \frac{dx}{dt} \tag{3.33}$$

According to Newton's law of viscosity

$$\sigma = \eta_\sigma \frac{d\varepsilon}{dt} \tag{3.34}$$

where σ is stress and ε is strain. By replacing stress with force divided by the area we get

$$F = \eta_\sigma \tfrac{1}{4}\pi D^2 \frac{1}{x}\frac{dx}{dt} \tag{3.35}$$

Inserting Eqn. (3.33) into Eqn. (3.35), we get the normal viscosity as

$$\eta_\sigma = \frac{\left(L/n\right)}{\tfrac{1}{4}\pi D^2} b_\sigma \tag{3.36}$$

By using the same procedure, the elastic modulus in shear direction E_τ can be written as

$$E_\tau = \frac{k_\tau}{\pi D} \tag{3.37}$$

and the shear damping coefficient b_τ relates to the shear viscosity η_τ by the following expression.

$$\eta_\tau = \frac{b_\tau}{\pi D} \tag{3.38}$$

3.4 Model Verification and Experimental Set-up

3.4.1 Verification by Simulation

The developed model and the developed algorithm were first tested by simulation. With given model parameter values, the model was solved numerically to produce simulated output responses. In order to make the simulation more realistic, random noises were added to the simulated responses. The program then was run with a set of initial parameters different from the true values. The model parameter values estimated were

expected to converge to the true values. The mean squared error was used as the objective function.

3.4.2 Verification with Experimental Data

Experimental data for several different materials were used to test the developed model and algorithm. It was expected that the model parameter estimates have consistent relations with the physical properties of the medium.

Water was used as a test medium to validate the developed model and determine the optimal number of elements to be used to discretize the medium. Four concentrations of carboxymethylcellulose (CMC from Sigma-Aldrich, St. Louis-MO, USA) solutions were used to test the consistency of the parameter estimates. During the experiment the samples were kept at constant room temperature of 20^{o}C.

CMC solutions were made by mixing CMC powder with water and agitating the mixture with a mixer for about 30 minutes. After mixing and agitating, the solution was spun at 3500 rpm for 30 minutes with a centrifuge (Beckman J2-21M/E, USA) to remove air bubbles prior to ultrasound measurement. Four different CMC concentrations were prepared. The procedures for preparing the solutions were the same to avoid the effect of mechanical treatment history on the mechanical properties of the solutions.

3.4.3 Instruments

The experimental set-up for ultrasound measurement is shown in Figure 3.6. A pair of broadband ultrasound transducers (Panametrics, model A301S) with a center frequency of 0.5 MHz, diameter of 25.4 mm was used and positioned in pitch-catch

mode, one for excitation and the other for measurement. One transducer was mounted statically on a chamber (25 cm × 15 cm × 15 cm of length, width, and height, respectively) and the other one was an adjustable mount. The sample was put in between and had light contact with the two transducers. In this position the moveable transducer was then locked. In order to keep the sample stationary during the experiment a plate (8-cm square with thickness of 0.6 cm) made from acrylic was installed on each transducer casing. A personal computer (PC) was used to control the measurement system. The excitation signal was delivered from the PC to the function generator (Stanford Research Systems, Model DS340, frequency 15 MHz) by using the Arbitrary Waveform Composer (AWC) software. The PC and the function generator were connected via an RS-232 interface. A digital oscilloscope (GW Instek, Model GDS-2062) was used to record both the excitation and the response. When the response signal was very weak, it was amplified with a power amplifier (ValueTronic, model 310L, 50 dB, 250 kHz-110 MHz).

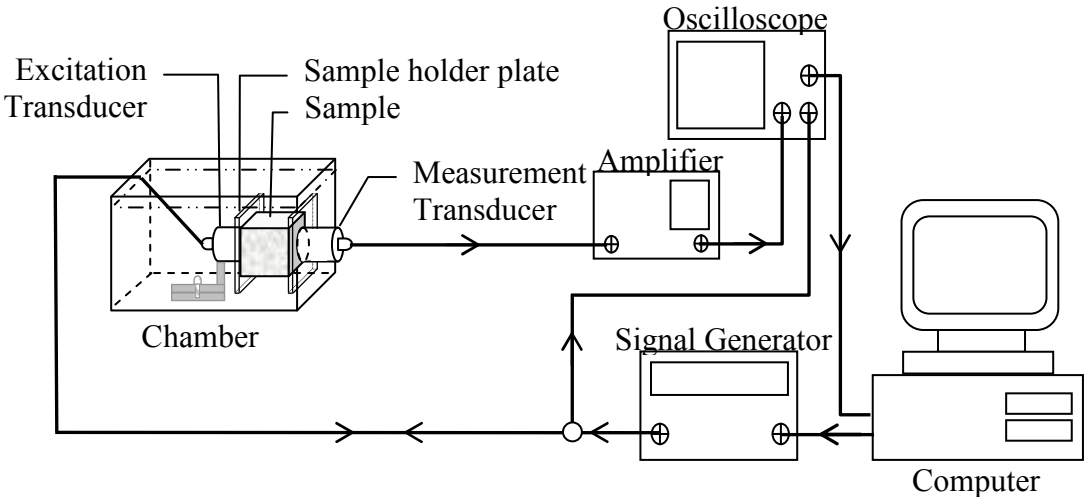

Figure 3.6. Experimental set-up

3.4.4 Perturbation Signal

A viscoelastic material system represented by Figure 3.3 is typically a low-pass filter with a certain bandwidth. Exciting the system with a sound wave at a given frequency only probes the system at that particular frequency. It does not reveal the material behavior in general. To reveal the material properties in a broadband of frequencies, pseudo-random binary sequences (PRBS) were used as excitation signals. This type of signal enables reliable estimation of model parameters and thus is very often used in model parameter estimation or solution of the inverse problem (Sung and Lee, 2003; Wilson, 2005; Mohanty, 2009). The advantages of PRBS signals include easy adjustment of the frequency composition and range, and easy implementation (Godfrey, 1993).

The ultrasound transducers used have a frequency band from about 0.3 MHz to 0.7 MHz with a center frequency of 0.5 MHz. Based on the frequency band, the spectrum of the desired PRBS signal must include the band. An example of the designed PRBS signal and its spectrum are given in Figure 3.7. As shown by the spectrum, a PRBS signal concentrates its power at multiple low frequencies. The bandwidth, as conventionally indicated by the -3 dB point, can be varied by changing the design parameters. The desired bandwidth for a given test material was experimentally determined by analyzing the power spectrum of the measured transmission waves. In our implementation, the measurement system has limited transducer bandwidth. The bit width of the designed PRBS was chosen based on the bandwidth of the transducers. The figure shows that the designed PRBS signal has a wide range of frequency components and the bandwidth was

around 2.62 M rad/s (0.42 MHz, dashed line, Figure 3.7b), matching the bandwidth of the transducers.

Spectrums of measured outputs are shown in Figure 3.7c. The spectrums basically resemble the broadband excitation spectrum in Figure 3.7b and are also affected by the band-pass nature of the transducers used. Figure 3.7c also shows that the output spectrums were a bit broader than the transducer band especially in low frequencies. The measurement is influenced not only by the dynamic characteristics of the transducer pair but also by the acoustic and mechanical behavior of the medium. The desired excitation bandwidth for a given test material was experimentally determined by broadening the bandwidth of the excitation (Figure 3.7b) in reference to the bandwidth of the transducer.

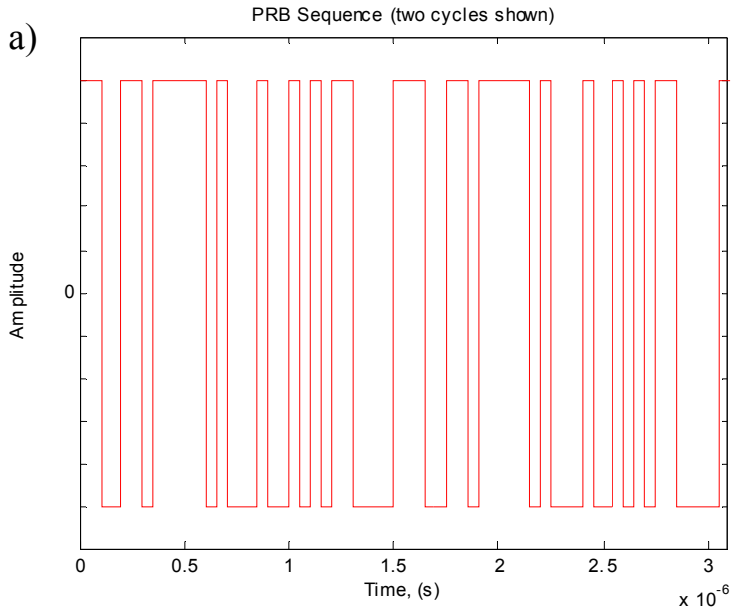

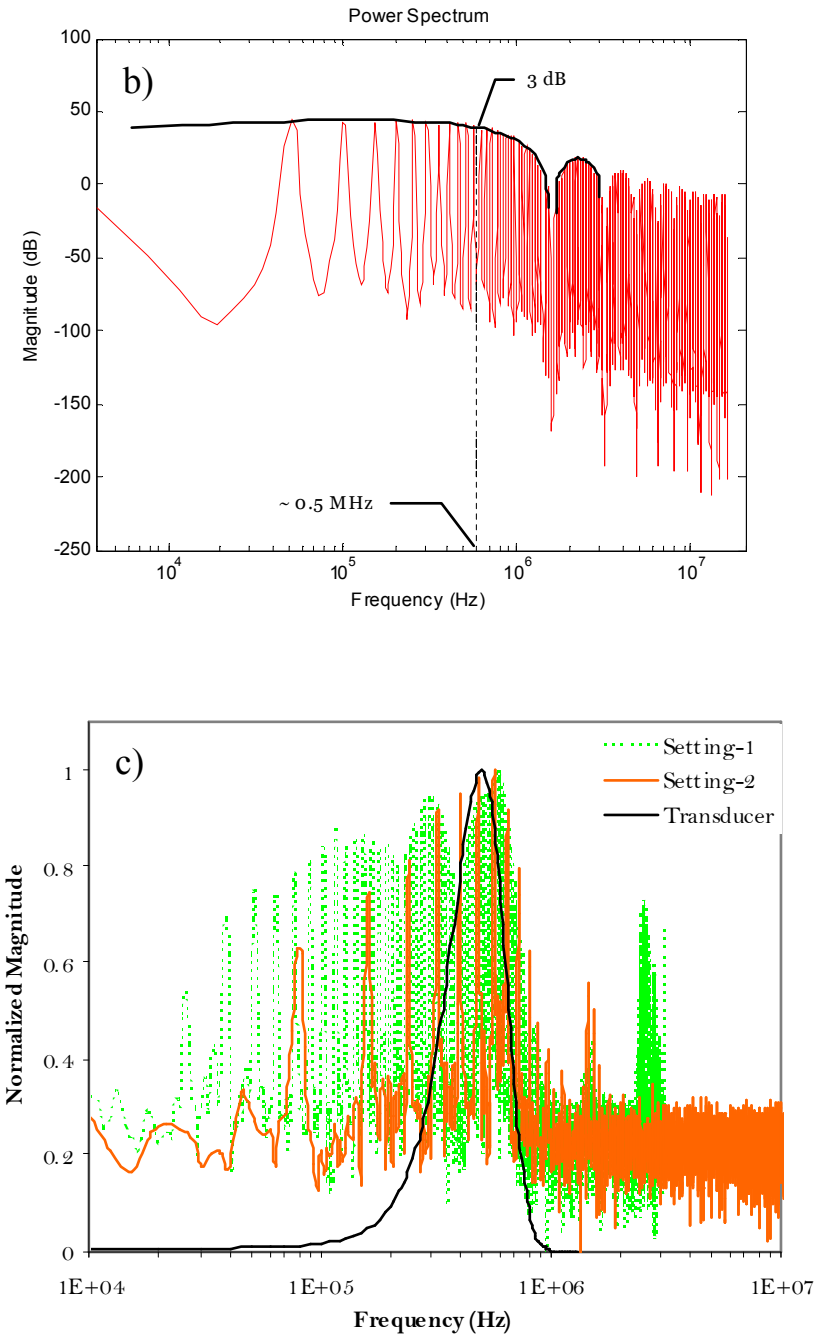

Figure 3.7. (a) PRBS excitation waveform, (b) PRBS spectrum, and (c) Spectrums of measured transmission wave through water with the transducer bandwidth. Setting-1: The PRBS bitwidth = 2.5 μs and acquired at 6.25 MS/s; Setting-2: The PRBS bitwidth = 0.4 μs and acquired at 25 MS/s.

3.5 Results and Discussion

3.5.1 Algorithm Convergence

In this test, the procedure for model parameter estimation would be verified according to the identification process described in Section 3.2.3 and Figure 3.4. A PRBS signal was used to perturb a medium and a set of 'true' parameter values was specified. The 'measured' response was generated by using the developed model from a set of 'true' parameter values with random noise added to the data (in this case, the noise was 10%). Noise is assumed to be of zero mean and independent of the true signal.

A set of initial values for the model parameters (derived from the initial material properties) and an objective function must be defined in the model parameter estimation. A good set initial value can reduce the number of iteration cycles needed and thus save computation time in the model parameter identification process. They also help avoid numerical instability and undesired local minimums.

Table 3.1 shows the estimated model parameters with initial values over and under the 'true' parameter values. As shown in Figure 3.8, four model parameters could be adjusted to minimize the model error. The results show that the errors in the estimated model parameters are very low (< 1%). Figure 3.8 shows the performance of the algorithm developed during iterations. From the results, it can be observed that the developed algorithm for model parameter identification worked very well. It can also be seen that by using the initial guess for the model parameters about 175% to 250% different from the 'true' values, the model parameter estimates could converge to the 'true' values. With both sets of initial values, the model was optimized to fit the "measured" output as shown Figure 3.9.

Table 3.1. Data used to test convergence of model parameter estimates

Density	= 1000 kg/m^3
Length of sample	= 0.05 m
Diameter of transducer	= 0.0254 m
Increment step for J-matrix	= 1%
Number of elements	= 10
Length of data	= 6200
Noise	= 10%

	k_σ	b_σ	k_τ	b_τ
'True' values	3.0000e+08	15.00	5.0000e+07	12.00
1. Initial values	6.0000e+08	37.5	1.0000e+08	30.00
(Over true values by)	(+100%)	(+150%)	(+100%)	(+150%)
Estimated Parameters	3.0006e+08	15.01	4.9959e+07	12.04
	(0.02%)	(0.09%)	(0.08%)	(0.30%)
2. Initial values	1.9500e+08	7.50	3.2500e+07	6.00
(Under true values by)	(-35%)	(-50%)	(-35%)	(-50%)
Estimated Parameters	2.9997e+08	15.01	4.9962e+07	12.03
	(0.01%)	(0.05%)	(0.08%)	(0.24%)

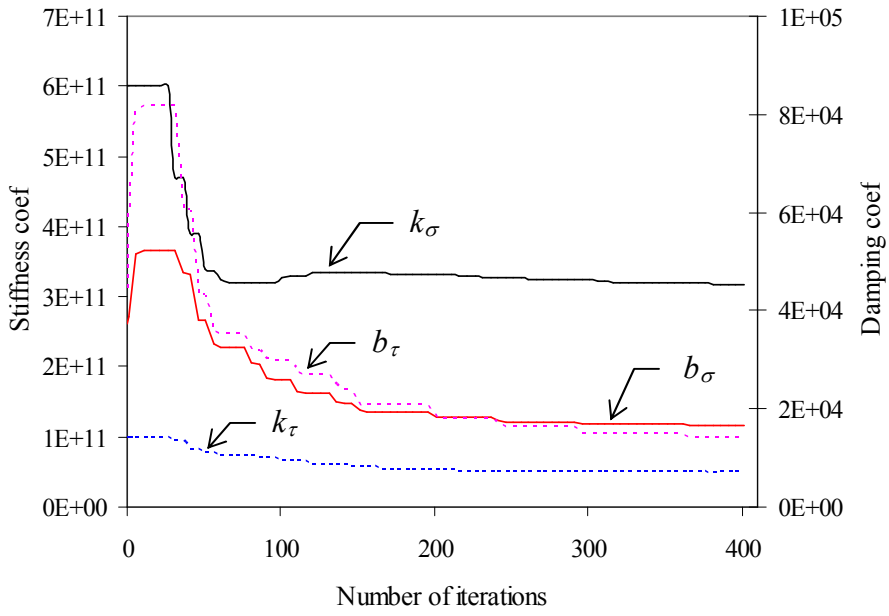

(a)

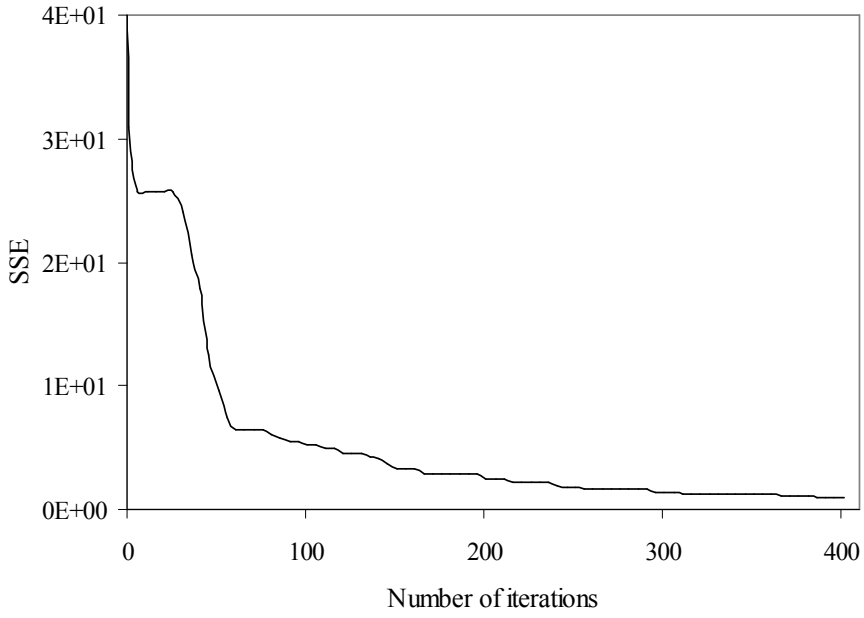

(b)

Figure 3.8. (a) Variation of parameters during identification processes, and (b) Error convergence.

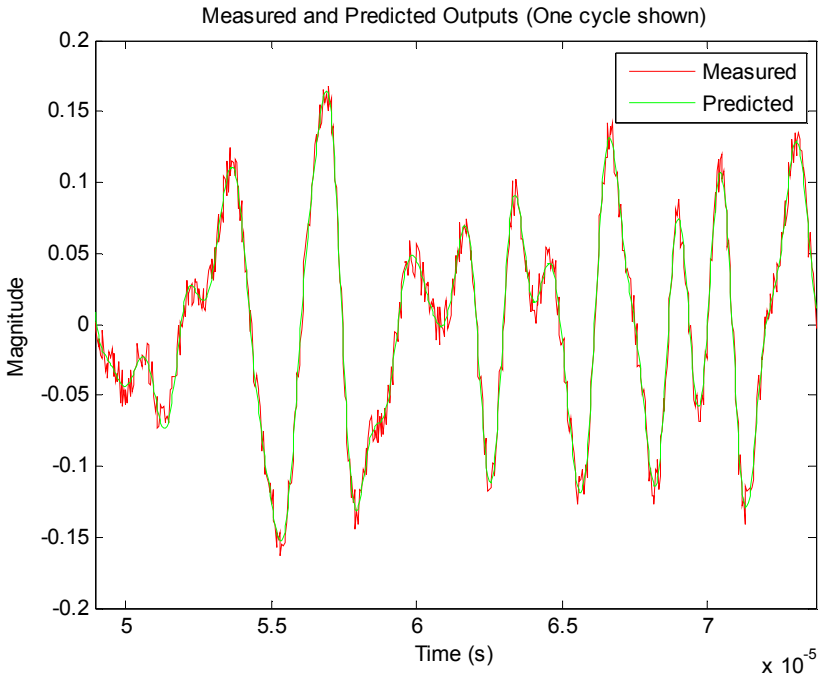

Figure 3.9. Comparison between "measured" and predicted output by the model

In adjusting the model parameters, each data point was evaluated with respect to all the model parameters based on the Jacobian method. Each data point may contain measurement errors because of noise and thus may affect the accuracy of model parameter estimation. Measurements for multiple cycles of the PRBS signal were used to reduce the effect of noise on estimation accuracy. The simulation results show that the errors in estimated damping coefficients were slightly higher than those in estimated stiffness coefficients.

For real viscoelastic materials, the exact model structure may not be known. Thus, the estimation of the model parameters from ultrasound measurements is strongly influenced by the model validity and the estimation technique used. Since most biological

materials contain a high percentage of water, a good medium for testing model validity would be water. Another reason for using water as a sample is its mechanical properties such as density, Young's modulus, and viscosity are well known. Since the dimension of the cylinder column in the measurement setup can be determined, the mass of medium for model parameter estimation can be calculated. The ultrasound arrival time can be estimated from the initial response. Since the length of the sample is measurable, the sound speed can be calculated. The initial value of stiffness coefficient (k) can be estimated from the relationship between density of the sample (ρ) and sound speed through the medium as, $v = \sqrt{\frac{k}{\rho}}$.

3.5.2 Determining Optimal Number of Elements

For a continuous medium, the number of elements as depicted in Figure 3.3 should be infinite, but an infinite system is not necessary for practical applications. An accurate numerical solution for a continuous system can often be obtained by using a finite number of elements. The number of elements affects the computation speed, algorithm convergence, and parameter estimate accuracy. In order to determine the optimum number of elements, we estimated the model parameters for different numbers of elements. While the model parameters in the state space equations (Eqns. (3.9) and (3.20)) are dependent on the element size, the material properties given by Eqns. (3.32), (3.36), (3.37), and (3.38) should converge when the number of elements increases.

Figures 3.10 and 3.11 show the material properties derived from the estimated model parameters for different numbers of elements. As expected, the material properties

stabilize with increasing number of elements. The normal elastic modulus and normal viscosity increased exponentially with the number of elements while the shear elastic modulus and shear viscosity decreased exponentially with the number of elements. For the sample size and experimental setup used, the estimated property values changed slowly when the number of elements is greater than 10. In other words, an *n* value of 10 could adequately represent the major system dynamics. Even though a greater number of elements would lead to higher estimation accuracy, it appeared to bring minimal additional benefits to use a number of elements greater that 10. The larger the number of elements, the more complex the model parameter estimation process is. For simplicity, *n* = 10 was selected and used.

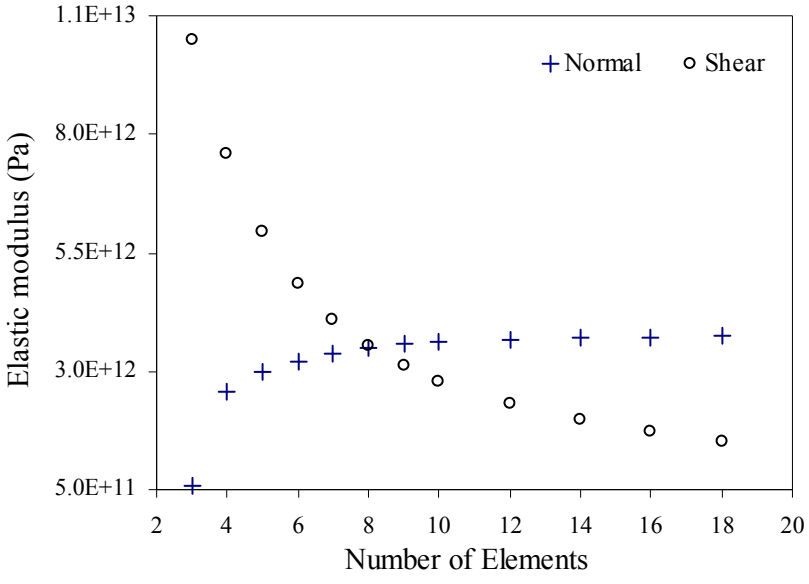

Figure 3.10. Estimated normal elasticity and shear elasticity using different numbers of elements

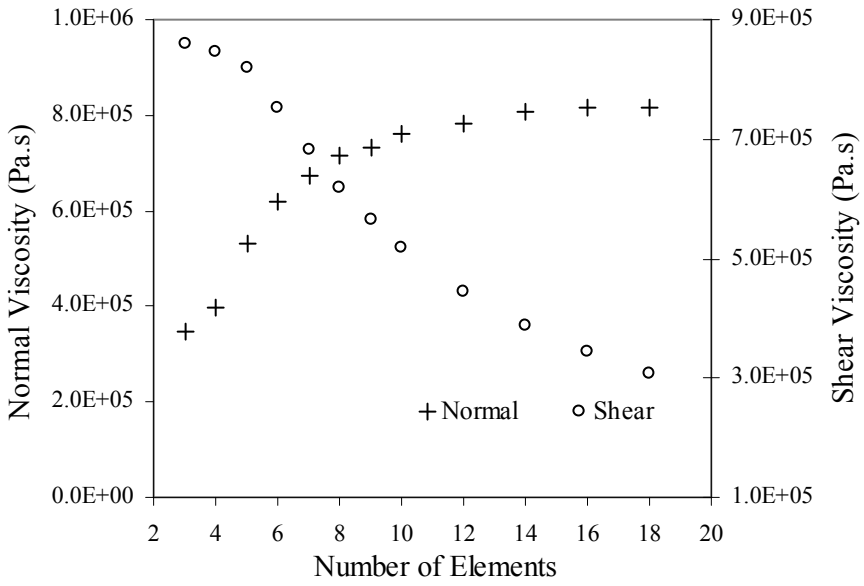

Figure 3.11. Estimated normal viscosity and shear viscosity using different numbers of elements

The number of elements used to discretize the medium would allow efficient model parameter estimation, though the estimated mechanical properties may differ from the conventional measurements. The dynamic mechanical properties of a viscoelastic medium are known to be frequency-dependent. Mahomed *et al*. (2008) reported that the storage modulus and loss modulus of viscoelastic materials increased with frequency.

3.5.3 Repeatability of Parameter Estimates

The repeatability of the parameter estimates was first tested by applying five different excitation signals to the system being investigated. The signals used had the same bandwidth but completely different waveforms. Repeatability was measured with the standard deviation of the estimated model parameters of the five measurements. Table

3.2 shows the effective material property estimates for water obtained by using different excitation signals. While the excitation waveforms are quite different, the effective material properties converged to very similar values with relatively small standard deviations (much less than 10% of mean of the effective parameters). This indicates that the experimental system and the parameter estimation algorithm gave repeatable parameter estimates from which the effective material properties are derived.

Table 3.2. Estimated mechanical properties of water for different excitation signals.

Excitation	**Effective Mechanical Properties**			
	E_σ ($\times 10^{12}$)	η_σ ($\times 10^{6}$)	E_τ ($\times 10^{12}$)	η_τ ($\times 10^{7}$)
PRBS-1	3.92	1.15	2.68	9.71
PRBS-2	3.91	1.10	2.63	9.53
PRBS-3	3.81	1.11	2.64	9.54
PRBS-4	3.67	1.15	2.63	9.63
PRBS-5	3.36	1.19	2.64	9.62
Mean	3.73	1.14	2.64	9.61
Std. Dev/Mean	6.19%	3.14%	0.69%	0.76%

3.5.4 Model Validation

A least-squares algorithm was employed for model parameter optimization. After parameter optimization, the model was able to predict the measured responses to an excellent level of accuracy for all the materials tested based on the mean squared error value. The chosen target for the mean squared error could produce a high level of goodness of fit between measurement and prediction. Figure 3.12 shows an example plot comparing the model prediction with measurement for a CMC solution (concentration

0.25%). Results for other concentrations are similar. This indicates that the proposed model structure could capture the major dynamics of wave transmission through the sample.

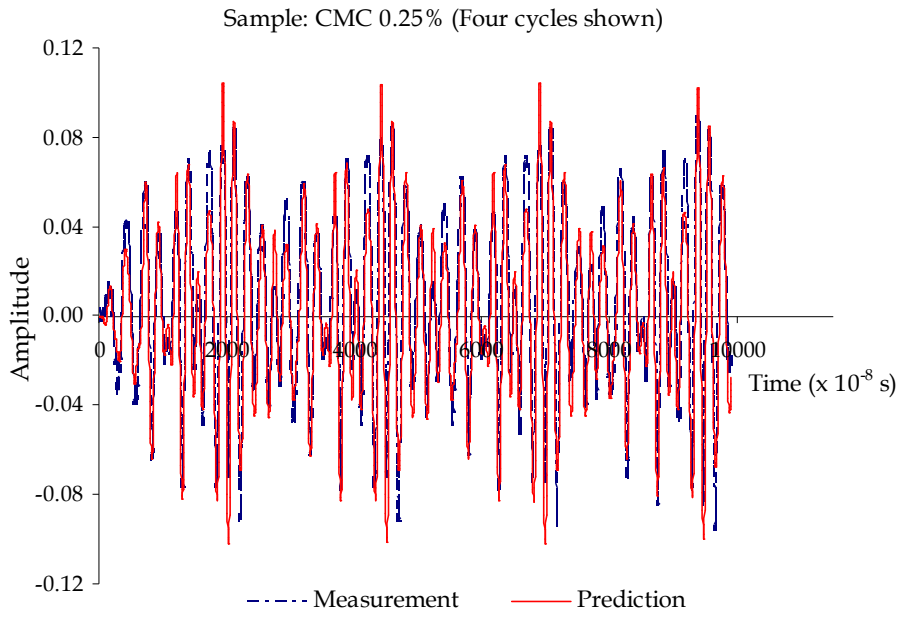

Figure 3.12. Comparison between measured and predicted responses for carboxymethylcellulose (CMC)

The consistency of the estimated model parameters was checked by measuring carboxymethylcellulose (CMC, from Sigma-Aldrich, St. Louis-MO, USA) solution for different concentrations. The viscosity of the CMC solutions should generally increase with increasing concentration as described by Yang and Zhu (2007). They reported that concentration of CMC solution correlates with its viscosity. Results from this work showed the same trend. The viscosity values had a nearly linear positive correlation with CMC concentration (Figure 3.14).

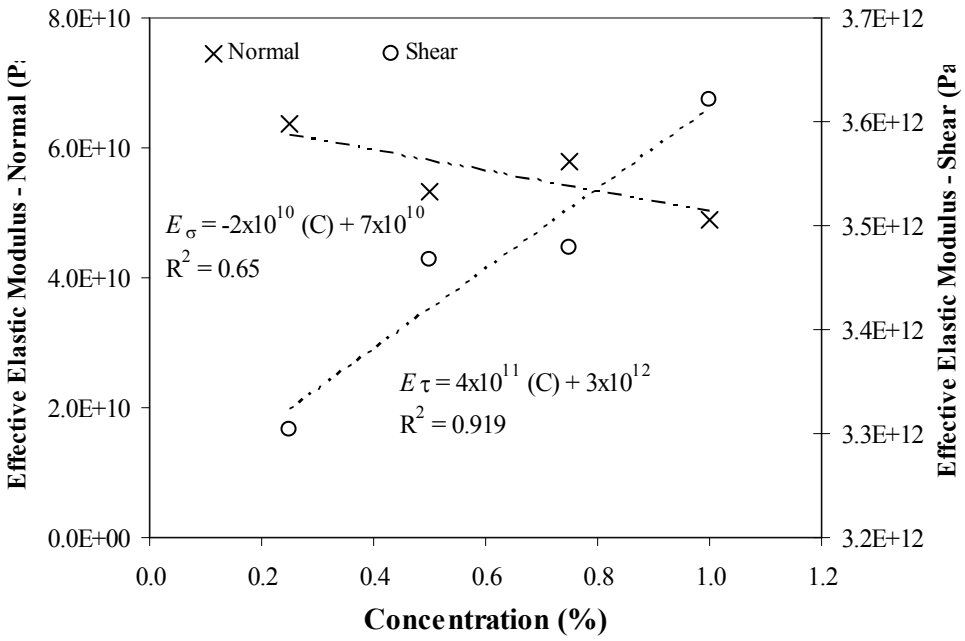

Figure 3.13. Effective elastic modulus of CMC at different concentrations

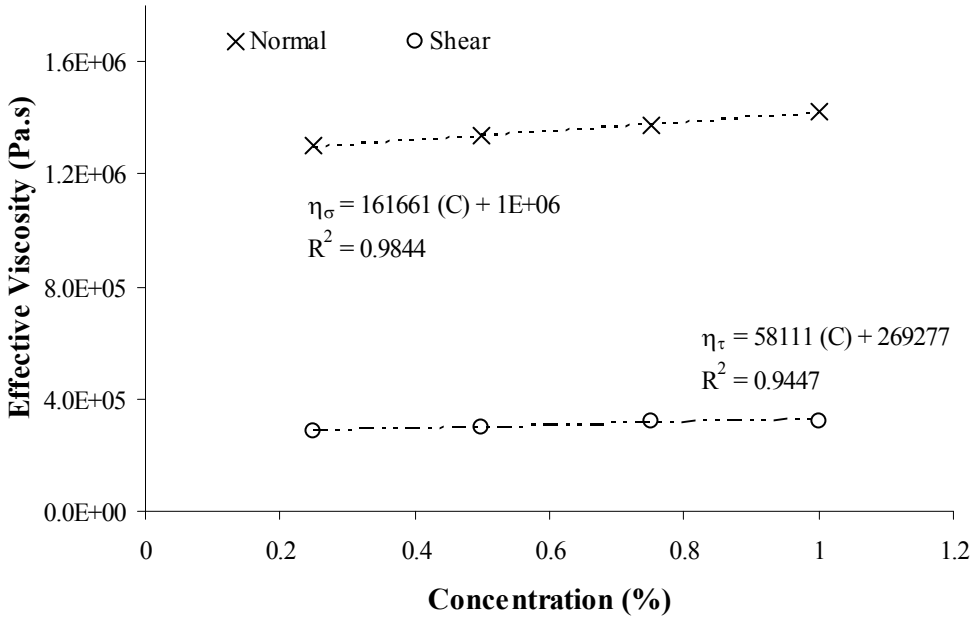

Figure 3.14. Dependence of damping coefficients on concentration (*C*) of CMC solutions

Many more experiments are needed to establish the relationships between the conventionally measured material property values and those obtained by the model-based ultrasound method. The preliminary experiments, nonetheless, showed that estimated parameters reflected some known facts in the materials tested, indicating good potential for further research.

3.6 Conclusion

A mechanical network based on the Kelvin-Voigt model was developed to represent ultrasound transmission wave through viscoelastic materials. The equations of motion were derived and expressed in the form of state space equations to describe the system kinetics. Pseudo random binary sequences (PRBS) signals were used to perturb the system and ultrasonic transmission was measured. The least-squares method was used to determine the optimum model parameters from a set of input-output data. Model verification showed that the algorithm developed could converge to the assigned material properties. The estimated model parameters were also consistent with the material properties. For a higher-viscosity medium, the model parameter estimates show higher damping coefficient values as expected. The model structure developed could predict the major behavior of the measured waves. That is evidence that the developed model could capture the major dynamics of the viscoelastic materials being investigated. The repeatability test showed that the parameter estimates were very close with relatively small standard deviations for different excitation signals. A ten-element system network could be used to estimate the material properties. The experiments showed that the

estimated parameters reflected some known facts about the materials tested, indicating good potential for future research.

CHAPTER 4

BIOLOGICAL TISSUE DIFFERENTIATION BASED ON MODEL PARAMETERS

This chapter presents an application of the proposed model as described in Chapter 3 for biological tissue differentiation and classification according to the viscoelasticity of the materials. Viscoelastic properties of several viscous liquids and soft tissues were determined. The chapter ends with a discussion about the potential of the developed model as a technique for quality evaluation of biological materials.

4.1 Introduction

Mechanical properties such as elasticity and viscosity of biological materials play an important role in medicine (Nitta and Homma, 2005; Girnyk *et al*., 2006; Kuchařová *et al*., 2007; Tanaka *et al*., 2008) and food quality evaluations (Singh *et al*., 2006; Mittal *et al*., 2007). Elasticity changes have been used to differentiate normal from diseased soft tissues (Forgacs *et al*., 1998; Zhang *et al*., 2008) and have been found useful for early detection of cancer and other tissue pathologies (Ophir *et al*., 1991). Blood diseases have been found to affect the viscosity characteristics of blood (Nitta and Homma, 2005). For food quality evaluation, elasticity and viscosity influence the sensory properties of foods (Echeverría *et al*., 2008). Assessing the dynamic elasticity and viscosity of biological materials is thus very important for clinical diagnosis, food quality evaluation, and other applications.

Classification and viscoelasticity evaluation of biological materials usually use ultrasound characteristics, such as velocity and attenuation to predict the concerned parameters (Botros *et al*., 1987; Chen *et al.,* 1994; Chen *et al*., 2004; Littrup *et al*., 2002; Khadeer *et al*., 2005; Nitta and Homma, 2005; Koc and Vatandas, 2006). Those parameters have demonstrated the usefulness of ultrasound as a measurement technique. The existing studies, however, have primarily relied on statistically correlating material characteristics of interest with sound velocity or attenuation. Sound velocity depends on multiple properties including density, elasticity, and attenuation; and statistical correlations usually do not represent the underlying physical relationships. As a result, the research findings can not be generalized easily. Since the studies estimate viscoelastic materials by characteristics of ultrasound, the found empirical correlations are usually a lack of physical quantification. Since ultrasound is a wave of mechanical vibration, modeling ultrasound transmission based on mechanics will allow quantitative determination of material properties in a physically meaningful manner. The basic mechanical models commonly used for studying the behaviors of solid and liquid are the Maxwell and Kelvin-Voigt models, respectively (Fung, 1993; Özkaya *et al*., 1998). Liu and Bilston (2000) used the Maxwell model to examine ex vivo bovine liver. Farshad *et al*. (1999) utilized the Kelvin-Voigt model for ex vivo kidney. Chateline *et al*. (2004) studied soft solid by using the Maxwell and Kelvin-Voigt models and found that the Kelvin-Voigt model provided a better estimation for viscoelastic properties. Many other mechanical models for ultrasound propagation are derived and modified from the two basic models. By adding more elements to the basic models, more complicated models can be obtained. Liu and Xu (2006, 2008) described viscoelastic properties of biological

materials by employing two higher-order fractional viscoelastic materials models (the fractional Voigt model and the fractional Maxwell model).

In this chapter, the mechanical model as described in Chapter 3 would be applied to describe the acoustic behaviors of real viscoelastic materials. Mechanical properties derived from the model parameters were then used for classification and differentiation analysis of the materials.

4.2 Materials and Methods

4.2.1 Samples

Two groups of viscoelastic materials, liquids and beef tissues, were used to test the capability of the model parameters for material differentiation. Five different liquids different viscoelastic properties were selected for the testing. The milk and syrups were purchased from a local store. As indicated in Table 4.1, the density and viscosity of these liquids are known to be different. For each liquid the measurement was performed five times as replication with 5-cm distance between the two transducers. During the experiment, the temperature of the sample was kept at constant room temperature (~20 ^{o}C).

Four fresh beef tissues: muscle, liver, kidney, and fat were obtained from a USDA select grade animal from the Meat Laboratory at the University of Missouri. The tissue samples were kept in an insulated container for the experiment within 4 hours after slaughter. The muscle and liver samples were cut into 5-cm cubes. Each tissue was measured at three different positions as replications. Muscle, especially, was measured in two different orientations: parallel and perpendicular to the direction of fibers.

Table 4.1. Density and viscosity of liquid samples

Sample	Density (kg/m^3)	Viscosity (Pa.s)
Water	998	0.0010
Milk	1006	0.0021
Syrup-1	1093	0.0938
Syrup-2	1197	0.3513
Syrup-3	1307	1.0396

4.2.2 Instrumentation

An ultrasound transducer pair (Panametrics, series A301S) with center frequency of 0.5 MHz were used as ultrasound generation and measurement and positioned in transmission mode. One transducer was mounted statically on a chamber, and the other one was hung in a holder and adjustable at the same center. The measurement chamber and its components are shown in Figure 4.1 and the diagram of the experimental setup is depicted in Figure 3.5 in Chapter 3. A function generator (Stanford Research Systems, Model DS340) was used to implement the excitation signals controlled via the Arbitrary Waveform Composer (AWC) software in a personal computer (PC). The PC and function generator were connected by using RS-232 interface. Both excitation signal and response signal in time domain from the transducers were acquired and recorded by digital oscilloscope (GW Instek, Model GDS-2062).

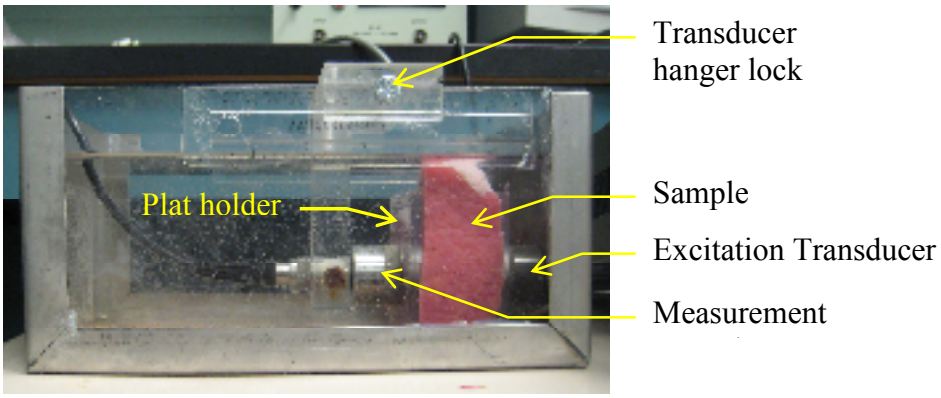

Figure 4.1. Measurement chamber and its components

4.2.3 Model Parameter Estimation

The procedures of model parameter estimation followed the description in Section 3.2.3. The model parameters were optimized to predict ultrasound responses to designed perturbations. Base on the results as explained in Section 3.5.2, ten elements were used to discretize the medium in the model parameter estimation. Pseudo-random binary sequence (PRBS) signal was designed and used to perturb the samples. A least-squares based algorithm was employed to evaluate the parameters of the developed state-space equations and the fourth-order Runge-Kutta method was used to compute model response. The errors between the model predictions and the measured responses were used to justify model parameters based on the Jacobian matrix. The Marquardt algorithm was performed until the residue of the model was minimized. The algorithm for model parameter estimation was coded in Matlab (version 7.1, MathWorks).

4.2.4 Statistical Analysis

The statistical software SPSS version 14.0 (SPSS Inc., Chicago, IL, USA) was used to perform data analysis and statistical computations for classification and clustering analysis. Two methods were used to analyze the test samples. Classification analysis was performed by using *k*-means method based on the mechanical properties derived from the model parameters. After classification analysis, each measurement data was discriminated linearly by the leave-one-out method to predict its group membership from the classification result. The percentage correctly classified was calculated from the number of measurement missed on a group.

4.3 Results and Discussion

4.3.1 Validation of the Estimated Mechanical Properties

Figures 4.2-4.6 show the fitting plots comparing the model predictions with measurements for liquids (only water presented) and beef soft tissues, respectively. As shown, the least-squares algorithm employed in the model parameter optimization could predict the measured responses to an excellent level of accuracy for all the materials tested. The mean squares error chosen could produce the optimum goodness of fitting between measurement and prediction. This indicates that the model structure proposed could capture the major dynamics of wave transmission through the viscoelastic materials tested.

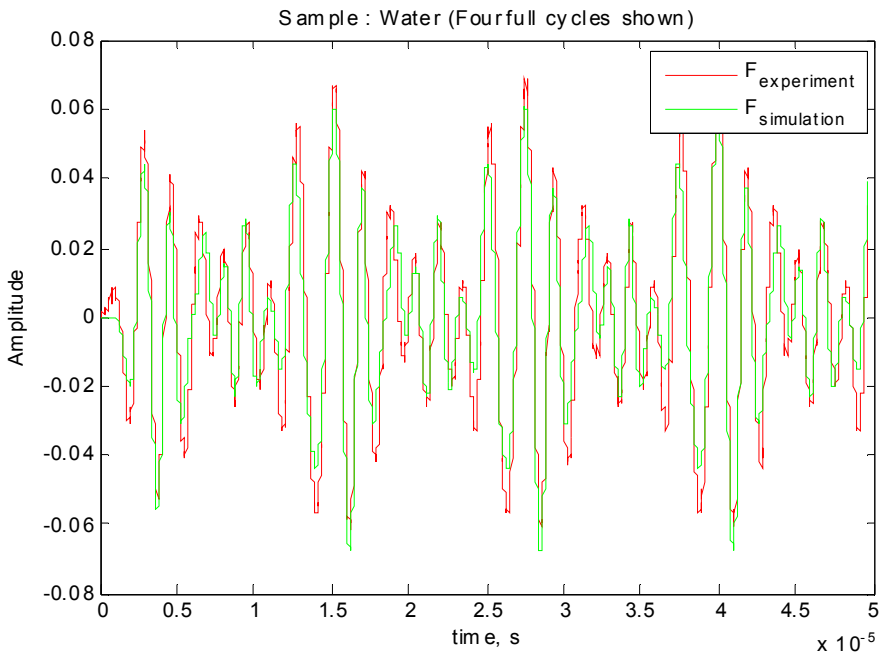

Figure 4.2. Comparison between model prediction and measured responses of water

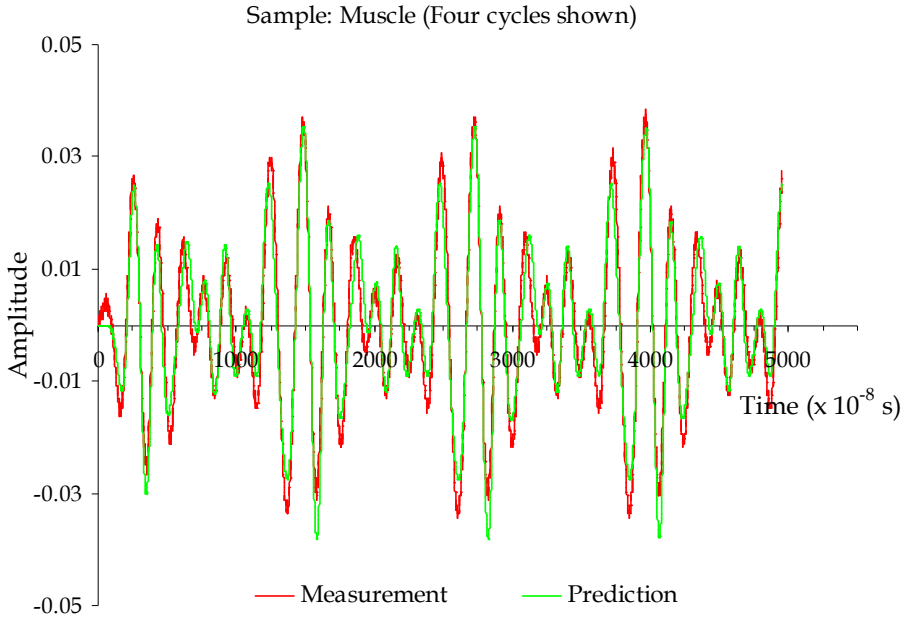

Figure 4.3. Comparison between model prediction and measured responses of muscle

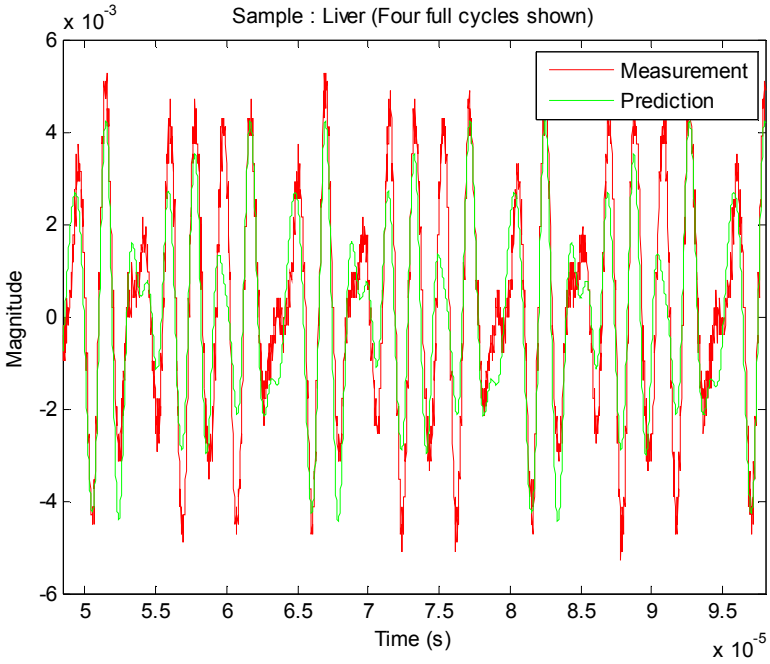

Figure 4.4. Comparison between model prediction and measured responses of liver

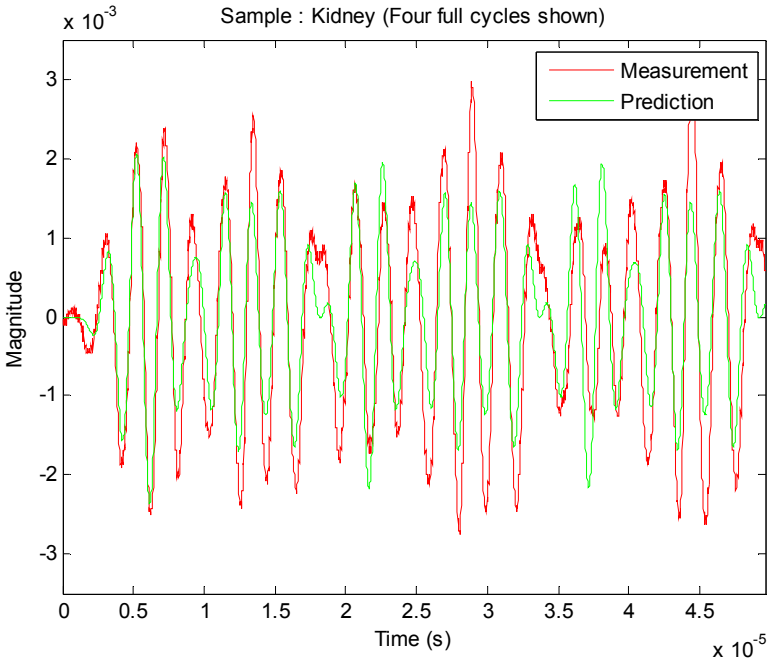

Figure 4.5. Comparison between model prediction and measured responses of kidney

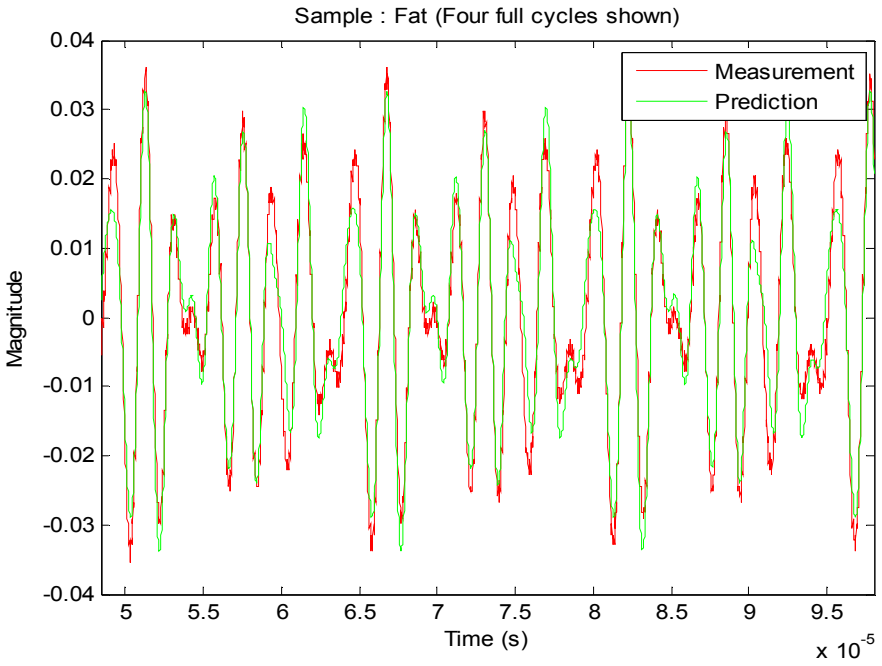

Figure 4.6. Comparison between model prediction and measured responses of fat

Tables 4.2 and 4.3 are the effective mechanical properties for the tested liquids and beef tissues, respectively. The standard deviations (shown as percent of mean) of the estimated model parameters among the replications are less that 2%. It is a relatively very small number. This verified the good repeatability of the parameter estimates. The standard deviations on the material property estimation of liver and kidney were slightly higher. It may be caused by the lack of homogeneity in their physical structure. Non homogeneity of kidney and liver structures may contribute to the measurement and thus affect the model parameter estimates. This does not show in the liquid medium which is more homogeny. In the biological tissue measurements, more over, it is hard to ensure that the contact between transducers and samples among the measurements is the same.

Table 4.2. Model validation of some liquids

Medium	Density (kg/m^3)	Effective Material Properties*			
		E_σ, $\times 10^{12}$	η_σ, $\times 10^5$	E_τ, $\times 10^{12}$	η_τ, $\times 10^5$
Water	998	3.22 (0.59%)	3.07 (1.82%)	2.11 (0.82%)	5.18 (0.05%)
Milk	1,006	3.39 (0.07%)	3.96 (0.12%)	2.31 (0.02%)	5.55 (0.05%)
Syrup-1 (Light)	1,093	3.97 (0.04%)	4.88 (0.12%)	2.59 (0.06%)	6.18 (0.06%)
Syrup-2 (Medium)	1,197	4.60 (0.15%)	7.24 (0.39%)	3.11 (0.19%)	6.83 (0.04%)
Syrup-3 (Heavy)	1,307	4.53 (0.31%)	4.99 (1.69%)	3.11 (0.76%)	7.21 (0.76%)

* Within each column, values of parameter estimates are means and standard deviation (in the bracket, as percent of mean) of five replications.

The viscosity of the liquids listed in Table 4.2 should generally increase from top to bottom (water, milk, to syrups). The effective viscosities derived from corresponding estimated damping coefficients followed the same general trend. The elastic properties also seem to slightly increase by increasing the medium density. Changing the concentration of dissolved material in solvent medium causes changes in the mechanical properties of the medium in term of density and bulk modulus. This affects the ultrasound waveform transmitted through the medium sensed by the transducer receiver and thus the estimated model parameters.

Table 4.3. Effective mechanical properties for fresh beef tissues

Medium	Density (kg/m^3)	Effective Mechanical Properties*			
		$E_\sigma(\times 10^{12})$	$\eta_\sigma(\times 10^5)$	$E_\tau(\times 10^{12})$	$\eta_\tau(\times 10^5)$
Muscle 0^o	1070	2.82 (0.55%)	4.94 (1.60%)	2.62 (1.16%)	6.14 (0.95%)
Muscle 90^o	1070	2.92 (2.92%)	5.26 (4.77%)	2.69 (0.91%)	5.84 (0.67%)
Liver	1060	1.37 (16.20%)	3.96 (12.17%)	3.05 (3.83%)	4.56 (4.75%)
Kidney	1040	1.97 (5.54%)	1.92 (77.20%)	2.78 (13.75%)	5.36 (17.57%)
Fat	919.6	2.80 (1.05%)	2.75 (10.14%)	2.03 (6.64%)	5.41 (1.70%)

*Within each column, values are mean and standard deviation (as percentage of mean) of three replications. Muscles are divided into two groups based on fiber orientation: 0^o means that excitation is in the fiber direction, and 90^o means that the excitation is perpendicular to the fibers.

The parameter estimates for muscles showed that the stiffness constant along the fiber was less than that in the perpendicular direction (statistically significant at p=0.05). This indicates that muscles are more elastic along the muscle fiber than in the perpendicular direction, which is consistent with Khadeer *et al*. (2005). They reported that when stress is applied perpendicular to the fiber orientation, both muscle fibers and connective tissue contribute to resistance, while when stress is applied along the fiber orientation, only muscle fibers contribute to resistance. Furthermore, the elastic modulus in the normal direction (E_σ) for muscle was greater than those for the other tissues, which is expected. In addition, Dukhin and Goetz (2002) reported that the fat content influences

the attenuation. The attenuation increased with increasing fat content. The effective material properties show shear viscosity for fat was relatively higher compared with kidney and liver. This result was also consistent with Akar *et al.* (2006) that muscle had higher damping coefficient than that of fat.

4.3.2 Multivariable Classification of the Medium

Differentiation of biological materials and especially soft tissues by ultrasound is an important and desirable capability for many applications. For that reason, the material properties obtained by the model-based ultrasound feature extraction method were tested for their ability to differentiate or classify the materials.

For a given geometry of measurement setup, the material properties have linear relationships with the model parameters as shown at equations (3.27), (3.31), (3.35), (3.36), and (3.37) in Chapter 3. Material classification can thus be based on either the estimated model parameters or the resulting material property values. The test samples were classified by two methods based on the effective material properties: *K*-mean clustering analysis and linear discriminant analysis. The leave-one-out scheme was used for testing in the linear discriminant analysis. Tables 4.4 and 4.5 show the classification results.

As shown in Table 4.4, the four properties all exhibited significant usefulness in differentiating the liquid samples. In particular, the mechanical properties in normal direction could each be used to classify the liquid samples to 100% accuracy. This is consistent with the fact that the samples are expected to differ the most in compressibility

and viscosity. As a result, classifications based on combinations of multiple parameters resulted in nearly perfect results by either method.

Table 4.4. Classification of liquid samples by estimated mechanical properties

Material	**Effective Mechanical Properties as Classifier***						
	E_σ	η_σ	E_τ	η_τ	E_σ, η_σ	E_τ, η_τ	E_σ, η_σ, E_τ, η_τ
Leave-one-out test results by linear discriminant analysis							
Water	a	ab	a	a	a	a	a
Milk	b	c	b	b	b	b	b
Syrup-1	c	d	c	c	c	c	c
Syrup-2	d	e	de	d	d	de	d
Syrup-3	e	d	de	e	e	de	e
% correctly classified	100	72.0	84.0	100	100	80.0	100
Leave-one-out test results by linear discriminant analysis							
Water	a	a	a	a	a	a	a
Milk	b	b	b	b	b	b	b
Syrup-1	c	c	c	c	c	c	c
Syrup-2	d	d	de	d	d	d	d
Syrup-3	e	ce	de	e	e	e	e
% correctly classified	100	92.0	80.0	100	100	100	100

*Within each column, different letters indicate different groupings at p = 0.05.

Table 4.5. Classification of soft tissues by model parameters (3 samples in each category)

Material	**Effective Mechanical Properties as Classifier***						
	E_σ	η_σ	E_τ	η_τ	E_σ, η_σ	E_τ, η_τ	E_σ, η_σ, E_τ, η_τ
K-mean clustering							
Muscle 0^o	a	a	a	a	a	a	a
Muscle 90^o	a	a	a	b	a	a	a
Liver	bc	b	b	cd	bc	b	b
Kidney	d	bc	ab	ac	d	ab	c
Fat	a	d	cd	b	a	cd	d
% correctly classified	73.3	93.3	73.3	66.7	73.3	73.3	100
Leave-one-out test results by linear discriminant analysis							
Muscle 0^o	a	a	a	a	a	a	a
Muscle 90^o	b	a	ac	a	a	a	a
Liver	c	bd	b	b	b	b	b
Kidney	d	bc	ab	ab	bc	ac	ac
Fat	ab	d	d	cd	d	d	d
% correctly classified	73.3	86.7	73.3	73.3	93.3	93.3	93.3

*Within each column, different letters indicate different groupings at $p = 0.05$.

The four material properties all showed excellent individual classification power for the soft tissue samples (Table 4.5). Although none of the individual properties completely differentiated all the samples or showed more usefulness than the others, a perfect or nearly perfect classification could be achieved by using a combination of

properties. This means that the tissue types differed by varying degrees in all the properties. As a consequence, multi-dimensional classification improved the results.

If the two muscle orientations were not treated as different tissues, all the classification results would improve and 100% correct classification rate could be achieved in a multi-parameter space. When the muscle samples were analyzed separately, however, multi-parameter classification could differentiate the muscle fiber orientations without errors. This shows that the model-based ultrasound method yields useful viscoelastic properties for soft tissue classification.

Since the model parameter estimates of kidney were less consistent (as shown that the standard deviations vary from 5% to 78% of mean), kidney could not perfectly differentiate from liver and muscle. The total percentage of correctly classified using multi-parameter, however, is still high (> 90%).

4.4 Conclusion

Model based ultrasound measurements were performed to extract the mechanical properties of viscoelastic materials. The model was composed of the Kelvin-Voigt network to analogize the mechanical motion of ultrasound wave in a viscoelastic medium. The mechanical properties of the material could be derived from the estimated model parameters. The results show that the developed model structure could predict the measurements. The model could capture the dynamic ultrasound transmission through the mediums. Classification analysis by *K*-mean clustering and linear discriminant analysis showed that the estimated mechanical properties could be used to differentiate and classify the samples. Multi-variate classification based on the mechanical properties

could differentiate soft tissues to high degree of accuracy (> 90%). The model-based ultrasound measurement is thus potentially useful for viscoelasticity-based analysis of biological materials. This work was based on and limited to homogenous materials and transmitted waves. More complex material and measurement configurations require and warrant further research. Many more experiments are needed to establish the relationships between the true material property values and those obtained by the model-based ultrasound method.

CHAPTER 5

A TRANSFER FUNCTION METHOD TO COMPENSATE THE TRANSDUCER EFFECT ON ULTRASOUND TRANSMISSION WAVE MEASUREMENT

To isolate the effect of the sample medium on ultrasound propagation, a method was developed to determine the transfer function of transducer pairs. The determined transfer function was further used as a filter to eliminate the effects of transducer pair on measured data. Experiments were carried out to illustrate the developed method.

5.1 Introduction

Basically, an ultrasound transducer consists of a piezoelectric material that can convert electrical pulses into mechanical energy in the form of acoustic wave and vice versa. Figure 5.1 illustrates an ultrasound transmission measurement system with two ultrasonic transducers, one is used for ultrasound generation and the other as receiver. An electrical signal from a function generator is sent to the transmitter transducer and the transducer generates pressure waves at the transducer surface. The generated pressure waves then propagate through a medium ahead of the transducer. At the other end of the medium, the receiver transducer senses the acoustic waves and converts them into an electrical signal. The signals generated by transmitter and sensed by receiver can be displayed or recorded with an oscilloscope.

Biological materials generally behave as a low-pass filter with a certain bandwidth and affect ultrasound propagation. This is the rationale of using ultrasound to probe

mechanical properties of materials. For such an application, ultrasound transducers should be used. The frequency response of ultrasound transducers is, however, not a flat line. Because of the dynamic characteristics of either the emitter or receiver transducer, the spectrum of pressure wave from the emitter may not be the same as that from the function generator; and the output of the receiver transducer may not be the same as the response at the end of the medium (Figure 3.8c). As a result the measured system responses in Figure 5.1 contain the dynamics of both the medium and the transducers. The model parameter values reported in Chapters 3 and 4 were estimated from measurements without excluding the transducer effects. As a consequence, the derived values of material properties might be influenced by the transducer dynamics. In order to get more accurate results from the ultrasound measurement, there is a need to eliminate the effect of the transducer pair on the measured data.

Several methods have been developed to study the effects of ultrasound transducers on experimental measurements. Peirlinckx *et al*. (1993a,b) adopted linear viscoelastic theory to derive a transfer function model for compensating the transducer effects from ultrasound measurement in the presence of absorption and dispersion. The developed method was based on a reference waveform from a standard material with well-known acoustic properties. Fujisawa and Takei (2009) made an effort to derive the transducer effect theoretically, but the calculation relied on some estimated material properties for the transducers. Literature review suggests that there is a need for a simple and practical method for eliminating transducer effects. In this chapter, we described a method to determine the transfer function of transducer pairs and used it to suppress transducer effects in ultrasound measurements.

5.2 Determination of Transducer Pair Transfer Function

In Figure 5.1, *t* refers to time, *D* is the diameter of the two transducers, which are set up in pitch-catch mode with spacing *L*. If the medium can be treated as linear viscoelastic material (Findley *et al*., 1989) and the ultrasound transmission can be considered one-dimensional, the entire measurement system can be modeled as a linear system with electrical input and output (voltages). Based on these two assumptions, the transfer function of the measurement system in Figure 5.1 can be expressed three blocks shown in Figure 5.2.

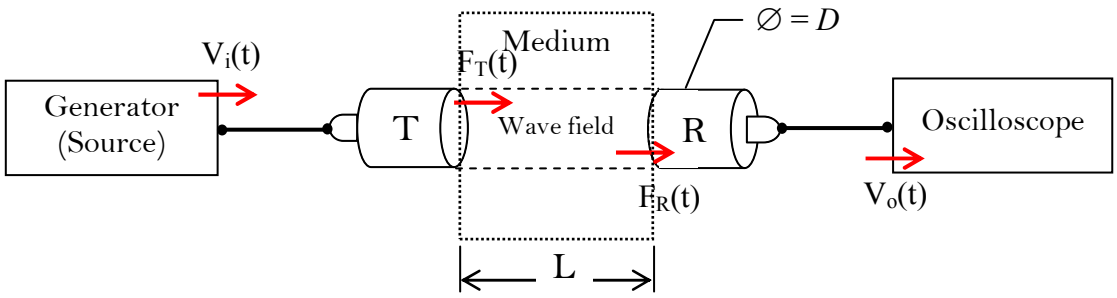

Figure 5.1. Illustration of ultrasound transmission measurement system

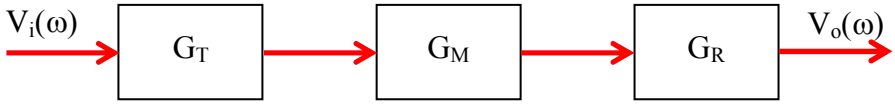

Figure 5.2. Input-output transfer function model of the ultrasound transmission measurement system

In Figure 5.2, ω refers to angular frequency, G_T is transfer function of the transmitter transducer, which relates the input voltage (V_i) to pressure (F_T) at transmitter transducer surface. G_M is the transfer function of the medium, which relates the wave pressures between the surfaces of the transducers. G_R is the transfer function of the receiver transducer, which relates the wave pressure at the receiver transducer surface and the output voltage. The losses associated with impedance mismatch between medium and transducer materials are included in G_T and G_R. The overall transfer function (G_{tot}) of the three blocks can thus be written as:

$$G_{tot}(\omega) = \frac{V_o(\omega)}{V_i(\omega)} = G_T(\omega)G_M(\omega)G_R(\omega) = G_T(\omega)G_R(\omega)G_M(\omega) \qquad (5.1)$$

or,

$$G_{tot}(\omega) = \quad G_{TR}(\omega)G_M(\omega) \qquad (5.2)$$

where $G_{TR}(\omega) = G_T(\omega)\,G_R(\omega)$.

If the two transducers are identical, $G_T(\omega) = K/G_R(\omega)$, $G_{TR}(\omega) = K$, and $G_{tot}(\omega) = KG_M(\omega)$, where $K < 1$ is a gain factor representing the losses resulting from impedance mismatches between materials. In reality, the two transducers are not perfectly identical, the transducer effects do not exactly reduce to a constant gain *K*. When the length of the medium is increased from *L* to *nL* (*n* is an integer), the transfer function of the media will be $G_M^n(\omega)$. If *nL* is still not long and the system can be considered linear, the overall transfer function ($G_{tot}^n(\omega)$) of the system with medium length *nL* is:

$$G_{tot}^{n}(\omega) = \quad G_{TR}(\omega) G_{M}^{n}(\omega) \tag{5.3}$$

Since $G_{tot}(\omega)$ and $G_{tot}^{nL}(\omega)$ can be determined from experiments, $G_M(\omega)$ and $G_{TR}(\omega)$ can thus be determined as:

$$G_M(\omega) = \sqrt[n]{\frac{G_{tot}^{n}(\omega)}{G_{tot}(\omega)}} \tag{5.4}$$

$$G_{TR}(\omega) = \frac{G_{tot}(\omega)}{\sqrt[n]{\frac{G_{tot}^{n}(\omega)}{G_{tot}(\omega)}}} \tag{5.5}$$

From the analysis above, the transfer function of a given transducer pair can be determined from Eqn. (5.5) by performing the measurement twice. If more measurements with different lengths of medium are performed (*e.g.* n = 1, 2, 3, 4….), a least-squares solution of $G_{TR}(\omega)$ can be determined. Once $G_{TR}(\omega)$ is determined, the transducer effects can be eliminated in the frequency domain from an application. If the measured response of a medium-transducer system is $y(t)$, the response of the medium is:

$$\hat{y}(t) = Z^{-1}\left(\frac{Y(\omega)}{G_{TR}(\omega)}\right) \tag{5.6}$$

where Z^{-1} is inverse Fourier Transform and $Y(\omega)$ is the spectrum of $y(t)$.

For determining $G_{TR}(\omega)$, water can be used as the medium because its mechanical properties are well known and it can transmit ultrasound in a broadband. Its attenuation and impedance are small (Laux *et al*., 2009). Water is also commonly used as a reference medium (Kourtiche *et al*., 2010) and most agricultural product characteristics are close to its behaviors.

5.3 Experiment

A pair of immersion ultrasonic transducers with a center frequency of 0.5 MHz (Panametrics, A301S) and identical element diameter of 2.54 cm were tested. Water was used as the medium to determine $G_{TR}(\omega)$. According to the characteristics of the ultrasound transducer pair provided by the manufacturer, they have far field at around 35 mm. Measurements were performed with medium lengths of 0, 5, 10, 15, 20, and 25 mm. For each length, the measurement was done five times as replications and their average was used for analysis.

All measurements were conducted at room temperature. The experiment was performed by applying either a broadband excitation (Pseudo-random binary sequences, PRBS) or sinusoidal signals to the system. The perturbation signals were generated with a function generator (Stanford Research Systems, DS340). Both the input and output voltage waveforms were digitized and recorded with an oscilloscope (GW Instek, GDS-2062). The schematic diagram of the experimental setup is shown in Figure 3.6 in Chapter 3.

5.4 Results and Discussion

Preliminary experiments showed that the spectrum of potato and most food/biological products such as beef tissues and apples are typically like a low band-pass filter. The bandwidth of water is very broad. In designing the PRBS signal, both the transducer and the medium were considered. According to the information from the transducer manufacturer, the center frequency of the transducer is 0.5 MHz with a bandwidth about 0.4 MHz (between 0.3 and 0.7 MHz). The bandwidth of the medium

was experimentally determined. The spectrum of the excitation signal was designed to accommodate the characteristics of the medium and the transducers. An example PRBS designed, its spectrum and the measurement spectrum through water are shown in Figure 3.8 in Section 3.4.4 of Chapter 3. Basically, the maximum frequency of the measured transmission wave through the medium is limited by the transducer bandwidth used.

Figure 5.3 shows the measured total frequency responses ($G_{tot}(\omega)$) through water of two lengths and the transducer pair transfer function ($G_{TR}(\omega)$) determined by Eqns. 5.4 and 5.5. The total frequency rsponses for 5 mm and 10 mm do not appear very different at frequencies away from the transducer center frequency but they are different close to the center. The measurement for other lengths were similar. The results indicate that additional length in water added little extra attenuation as expected. The measured responses, however, were strongly affected by the characteristics of transducers.

Figure 5.4 is a comparison between the frequency response of the transducer pair determined by the developed method and that provided by the manufacturer. The results show that the method produced correct frequency response of the transducer. Use of a sequence of sinusoidal waves as excitation gave similar results.

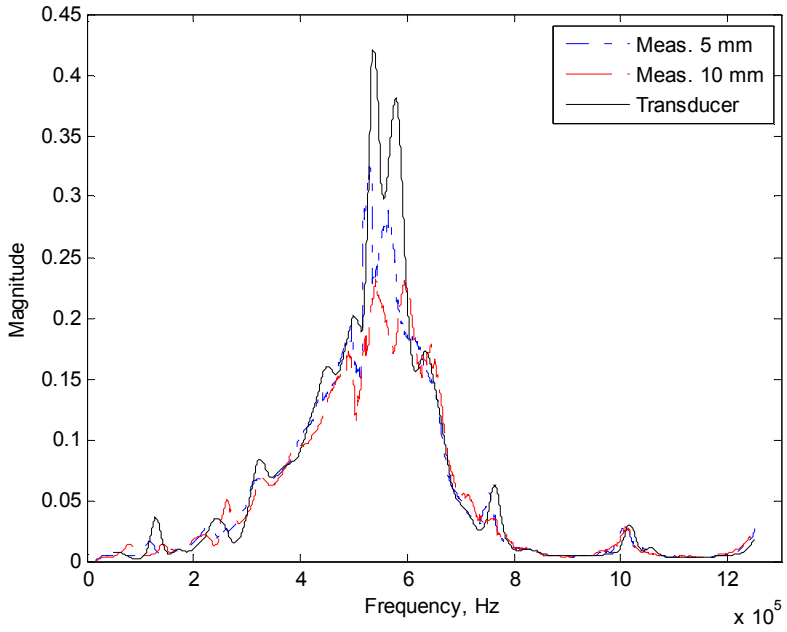

Figure 5.3. Frequency responses of the measurement system and transducer pair.

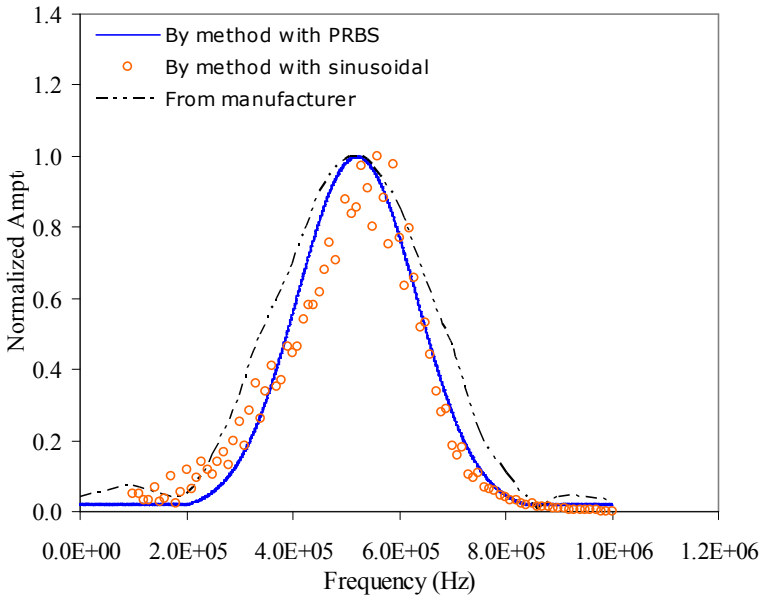

Figure 5.4. Comparison of transducer pair frequency responses obtained by the proposed method with PRBS excitation (solid line), with sinusoidal excitation (dot), and provided by manufacturer (dashed line).

5.5 Conclusion

A simple and practical method to compensate for the transducer pair effect in ultrasound wave transmission measurement based on transfer function technique was presented. Single harmonic and broadband excitation signals were used to perturb the medium. It was shown that the technique gave frequency responses of transducer pairs similar to that supplied by the manufacturer.

CHAPTER 6

MEASUREMENT OF MECHANICAL PROPERTIES OF BIOLOGICAL MATERIALS BY A MODEL-BASED ULTRASOUND APPROACH

This chapter discusses calibration of estimated material properties from the model parameters against values measured by conventional methods. Cyclic compression tests and shear dynamic tests were performed to yield property values in normal and shear directions, respectively. Regression equations of the material properties obtained from the model-based ultrasound and conventional tests are shown and the results discussed.

6.1 Introduction

Elasticity and viscosity are the two most important mechanical properties that define the fundamental characteristics of viscoelastic behavior of materials. These parameters have been used for quality evaluation of biological materials (Kuroki *et al*., 2006; Collins *et al*., 2008; Oke *et al*., 2008; Chang *et al*., 2009). Since the parameters are of great interest to material quality analysis, many attempts have been made to develop methods or techniques to study the behavior of viscoelastic materials and to determine the mechanical properties. The methods include stress-relaxation, quasi-static, and dynamic tests (Rao & Steffe, 1992; Fung, 1993). A method that has been popular in measuring mechanical properties is the dynamic oscillation test. In this measurement, a series of sinusoidal strains or stresses in a wide range of frequency is applied to the materials and the response is measured at each frequency. From this measurement the

mechanical properties can be determined in term of a storage modulus and a loss modulus. The properties at a particular frequency are usually considered independent to those at other frequencies. Zhang (2005) and Mahata & Söderström (2007), however, reported that the complex moduli depend on frequency.

Ultrasound measurement is another technique that reveals the mechanical properties of viscoelastic materials. Prior work typically used complex or a combination of ultrasound properties such as sound velocity and wave attenuation, each of which depends on multiple simple properties. For example, sound velocity and wave attenuation have been used to evaluate physical property changes of dough (Elmehdi *et al*., 2003), quality of wine (Jan *et al*., 2008) and yeast (Schöck & Becker, 2010) during fermentation. In general, food handling and processing involves heat. Since ultrasound velocity is dependent on temperature (e.g., Mulet *et al*., 1999), ultrasound measurement becomes of great interest to the food industry for monitoring the changes of physical properties during processing (Toubal *el al*., 2003; Koc & Vatandas, 2006). Even though ultrasound parameters correlated well with physical properties, the developed empirical relationships may be nonlinear and difficult to generalize (Zhao *et al*., 2005; Williams *et al*., 2006). The accuracy of ultrasound velocity and attenuation measurements is influenced by characteristics of medium and frequency of excitation (Leroy *et al*., 2008). Typically, a single-frequency excitation may not be enough to characterize a medium with ultrasound parameters (Jan *et al*., 2008).

In this work, we represented ultrasound transmission with a simple mechanical model that involves fundamental mechanical properties. A model-based ultrasound method was developed to yield property values, which were found useful for classifying

biological materials. The proposed model decomposed a biological sample into a network of viscoelastic elements represented by the Kelvin-Voigt model. An inverse method based on least-squares was used to estimate the model coefficients. Four model coefficients can be extracted from experimental data. The model coefficients are related to physical properties of the samples. The results showed that the model could capture the major dynamics of ultrasound transmission wave through viscoelastic materials. The model coefficients followed known trends and could be used to classify materials of different physical properties. Although the model can give major properties from acoustic measurements, the property values may not be equal to conventionally measured mechanical properties. The model coefficients thus need to be calibrated with standard measurements. The purpose of this study was to calibrate the mechanical properties from the developed model with conventional instrumental measurements. Cyclic compression and shear dynamic measurements were performed as conventional measurements and the results were compared with properties from the model-based ultrasound method.

6.2 Materials and Methods

6.2.1 Materials

Potatoes were used to test the ability of the developed method to extract viscoelastic properties. The mechanical properties of raw potatoes may or may not be of interest for real application, but they are a natural biological material and their mechanical properties could be easily varied. Baking potatoes were used for testing. The potato samples were purchased from a local store. The samples selected were at least 8

cm in diameter and had no defects or damage. For ultrasound measurement, each sample was cut into 3-cm thick slices.

6.2.2 Ultrasound Measurement

Two ultrasound transducers with a center of frequency of 0.5 MHz were used. They were set up in transmission mode as described in Section 3.3.1. One of the transducers was mounted on the measurement chamber and the position of the other one was adjustable along the center axis so that the transducers could have full contact with the sample. To keep the sample stationary during experiment a plate (8-cm square with thickness of 0.6 cm) was fastened on the casing of each transducer.

Pseudo-random binary sequences (PRBS) signal was used as perturbation. The PRBS was implemented with a function generator (Stanford Research Systems, Model DS340). The responses were acquired with a digital oscilloscope (GW Instek, Model GS-2062). The experimental trigger was controlled by a personal computer. For each sample the measurement was performed five times and the average was used for analysis. The applied perturbation signal and the measured response before and after transducer effect compensation were then used for model parameter identification. The filter for transducer effect compensation was described as in Chapter 5. Ten elements were used to discretize the medium. The procedures for model parameter estimation are described in Section 3.2.4.

6.2.3. Physical Property Measurement

In order to study the relationship between the material properties measured with the model-based ultrasound (MBUS) method and conventionally measured material properties, mechanical tests were performed on the samples. After ultrasound measurement, the samples were cored into cylindrical specimen with a diameter of 2.0 cm and length of 3.0 cm for dynamic mechanical measurements.

The relationship between material properties measured with the model-based ultrasound method and those measured with conventional methods was then determined by linear regression.

6.2.3.1. Density

After ultrasound measurement, the density of each sample was determined by measuring the weight and volume of a specimen. The weight was measured by using a balance (Denver Instrument XL-6100) while the volume was computed from diameter (~ 20 mm) and length of the specimen. Measurement of diameter and length was done with a caliper (Mitutoyo Corp., Japan). The averages of diameter and length from three different positions were used to compute the volume of the sample.

6.2.3.2. Compression properties

Cyclic compression tests were performed by using a Texture Analyzer (TA-HDi Texture Technologies Corp., NY). A cylindrical specimen, 20 mm in diameter and 30 mm in length, was put on the base and a cylindrical flat-ended aluminum punch was used for compression. A load cell of 50 kg was used in this test. Before testing, the distance

from the punch to the measurement base was determined as the initial position (x=0). The exerted force was applied in the axial direction to the specimen. The displacement was varied sinusoidally at a frequency of 1 Hz and amplitude of 0.2 mm, and the data were acquired at a sampling rate of 400 Hz. The force and displacement oscillations as functions of time were recorded through a control console and transferred to a PC for analysis. Figure 6.1 shows the measurement parameter setup for the cyclic compression test.

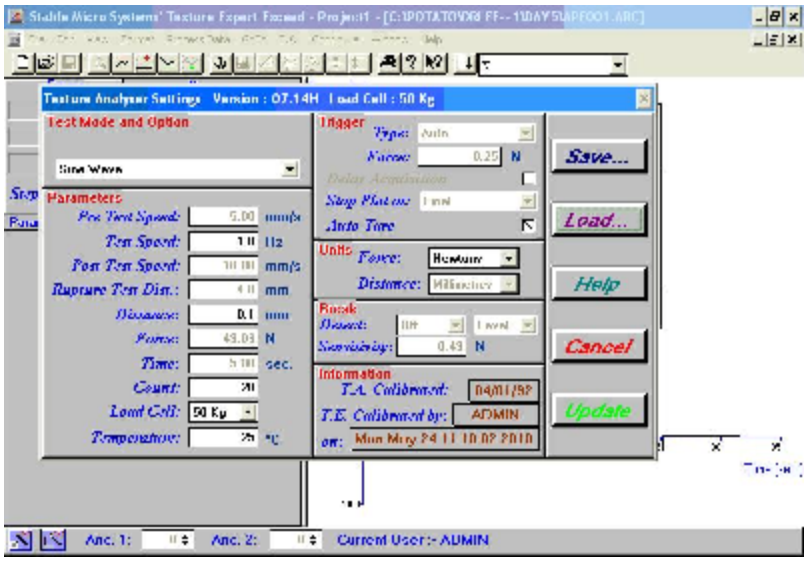

Figure 6.1. Measurement parameter setup for cyclic compression test

Figure 6.2 illustrates the spring-damper model for the cyclic compression test and the force and displacement oscillations. The cyclic compression test was done to derive the properties in the normal direction (k_σ and b_σ). Assuming that for a thin sample and at

low frequencies, inertia is negligible, the dynamic measurement can be expressed by the damper-spring model in Figure 6.2(a). The stiffness and damping coefficients of the system can be determined from the model representation based on Newton's equation of motion. The equation of motion can be expressed as

$$b\,\dot{x}(t) + k\,x(t) = u(t) \tag{6.14}$$

where t is time, x is the displacement from the equilibrium position, b and k are damping and stiffness coefficients, respectively, and u is driving force exerted to the medium. Dot denotes derivative with respect to time. The displacement was a sinusoidal function

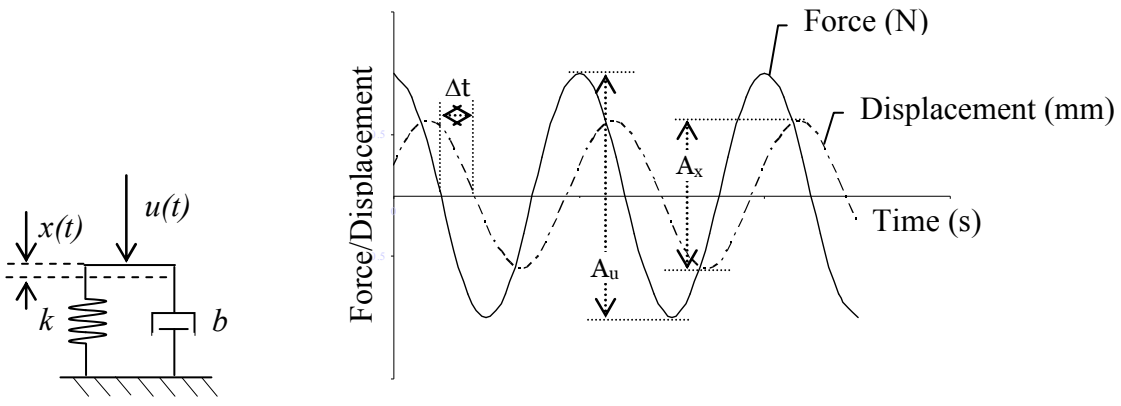

Figure 6.2. (a) Damper-spring representation for cyclic compression test. u is driving force exerted to the medium, x is the displacement from equilibrium position, k is stiffness coefficient, and b is damping coefficient. (b) Illustration of cyclic compression test. A_u is amplitude (N) of applied force, A_x is amplitude (mm) of displacement and Δt (in second) is phase delay between displacement and force.

$$x(t) = A_x \cos(\omega t) \tag{6.15}$$

where A_x is the amplitude of the displacement and ω is the angular frequency of the compression oscillation. Substituting the equation into Eqn. (6.14) and applying a trigonometry identity, we get

$$u(t) = A_u \cos(\omega t + \varphi) \tag{6.16}$$

where A_u is the steady state amplitude of exerted force and φ is the phase shift at steady state, both of which are functions of frequency, stiffness and damping coefficients. The amplitude of displacement (A_x) and frequency of cyclic compression (ω) can be specified on the measurement set up. The gain and phase of the system can be determined, respectively, as

$$G = \frac{A_x}{A_u} \tag{6.17}$$

$$\varphi = \frac{\Delta t}{T} 2\pi \tag{6.18}$$

where Δt is time shift and T is period as depicted in Figure 6.2(b). The unit of gain is m/N.

In general, the behavior of viscoelastic materials is frequency dependent as described earlier (Mahomed *et al*., 2008). To study the viscoelastic material behavior under different frequencies, the model representation of Eqn. (6.14) can be solved in the frequency domain. Taking the Laplace transform of the equation and assuming zero initial conditions, the transfer function of the system is defined as the ratio of output to input as

$$G(s) = \frac{x(s)}{u(s)} = \frac{1}{sb + k} \tag{6.19}$$

where $x(s)$ and $u(s)$ denote the Laplace transform of $x(t)$ and $u(t)$ in Eqn. (6.14), respectively. Setting $s = j\omega$ in Eqn. (6.19) yields

$$\left|G(j\omega)\right| = \frac{1}{\sqrt{\omega^2 b^2 + k^2}} \tag{6.20}$$

where $\left|G(j\omega)\right|$ is the gain or magnitude of the complex frequency response function, and

$$\varphi = \tan^{-1}\left[\frac{\omega\, b}{k}\right] \tag{6.21}$$

is the phase function. The gain and phase can be determined with, respectively, Eqns. (6.17) and (6.18) from measurement data. Then the damping coefficient and stiffness coefficient can be determined by solving Eqns. (6.20) and (6.21). Further, based on the geometry the model coefficients and mechanical properties are related by

$$E = \frac{l}{A}k \tag{6.22}$$

$$\eta = \frac{l}{A}b \tag{6.23}$$

where E is the elastic modulus, η is the viscosity, A is compression area of sample, and l is the length of sample. Eqns. (6.22) and (6.23) can then be used to calculate the elastic modulus and viscosity of the sample that correspond to the model parameters in the normal direction.

6.2.3.3. Shear properties

The specimen for the dynamic shear test had a 20-mm diameter and 3-mm thickness. The shear oscillatory measurement was performed with a RheoStress RS100 (Haake, Karlsruhe, Germany) equipped with a pair of plates (PP20, 20-mm diameter). Measurement was carried out at room temperature. The measurement was conducted with a frequency sweep from 0.1 to 100 rad/s and a constant stress of 100 Pa. The shear storage modulus (E') and the shear dynamic viscosity (η') as functions of shear deformation and shear stress are given by the measurement system. Three specimens were measured for replication and the average values were used for analysis. E' and η' respectively represent the elastic modulus and viscosity as shown below.

If a viscoelastic medium is treated as a pure Hookian elastic material, the stiffness coefficient (k^*) is the ratio of force input (u) over displacement (x), which should be equal to the inverse transfer function of the system in Eqn. (6.19).

$$k^* = \frac{u(s)}{x(s)} = k + bs \tag{6.24}$$

Similarly, if a viscoelastic medium is treated as a Newtonian viscous fluid, the Newton's coefficient of viscosity can be derived from Eqn. (6.14) as

$$b^* = \frac{u(s)}{\dot{x}(s)} = b + \frac{1}{s}k \tag{6.25}$$

In Eqns. (6.24) and (6.25), k and b can be expressed by the elastic modulus, E and dynamic viscosity, η, respectively. By setting $s = j\omega$, the equations can thus be expressed, respectively, as

$$E^* = E' + jE'' \tag{6.26}$$

$$\eta^* = \eta' + j\eta'' \tag{6.27}$$

where $j = \sqrt{-1}$, E^* is complex elastic modulus, E' is real elastic modulus, E'' is imaginary elastic modulus, η^* is complex shear viscosity, η' is real shear viscosity, and η'' is imaginary shear viscosity.

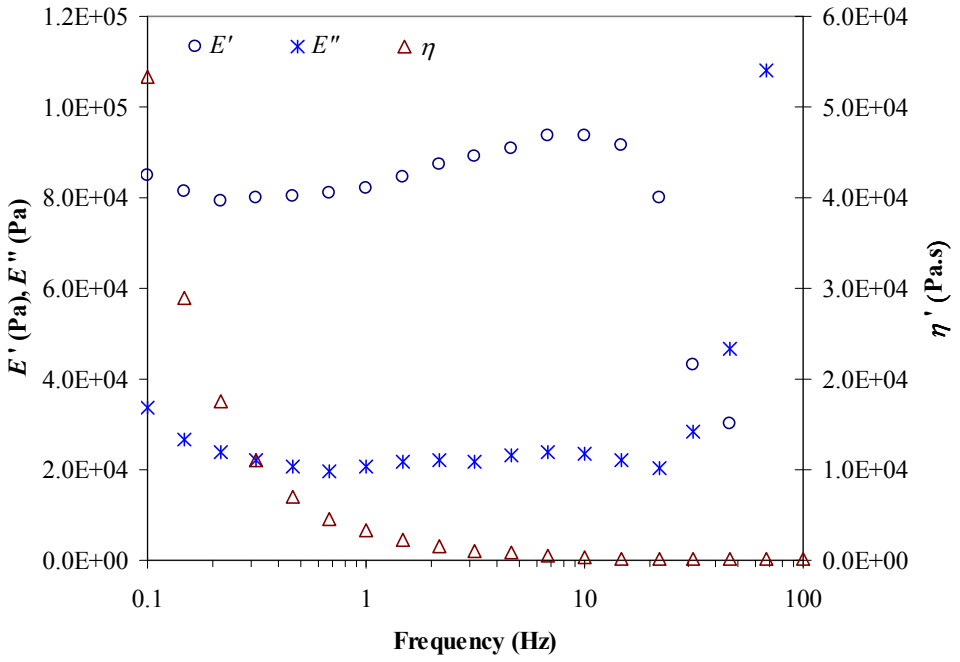

Figure 6.3. Frequency dependence of storage moduli (E' and E'') and real shear viscosity (η') of potatoes

Figure 6.3 is an example plot that shows the frequency dependence of dynamic viscoelastic properties of potatoes. From the figure, the storage modulus (E') is more

dominant than the viscous modulus (η'). The storage (E') and loss (E'') moduli in the shear dynamic measurement depend on the frequency of deformation. At frequencies between 2 Hz and 10 Hz, the elastic moduli (E' and E'') and real viscosity (η') values are nearly independent of frequency. The curve of the storage modulus rapidly decreased at frequencies around 12 Hz and increased at about 15 Hz. The rapid decreases and increases in the elastic moduli in the dynamic measurement are considered as a result of non-linear behaviors. For small displacement, the viscoelastic behavior of the sample may be considered as linear. For this, the behavior of viscoelastic properties is dependent on time only and not on the applied stress or strain and stress rate or strain rate (Rao and Steffe, 1992). The shear mechanical parameters around 10 Hz are relatively independent of stress rate or strain rate and were selected for analysis.

6.2.4 Statistical Analysis

The relationships between the model-based ultrasound (MBUS) parameters before and after transducer effect compensation and the conventionally measured properties were analyzed by linear regression. The regression coefficients were analyzed by *t*-test. The statistical analysis was done by using SPSS (SPSS 14.0 for Windows, SPSS Inc., Chicago, IL, USA).

6.3 Results and Discussion

In the model structure, four model coefficients must be identified: stiffness and damping coefficients in normal and shear directions. Parameters determined from compression tests would correspond to the model coefficients in the normal direction,

and parameters E' and η' would be compared with the model coefficients in the shear direction. The coefficients relate to the mechanical properties by Eqns. (6.10)-(6.13), (6.22), (6.23), (6.26), or (6.27).

The instruments used in this work, like other instruments available for mechanical measurements, typically work at low frequencies up to 100 Hz. The ultrasound frequencies, however, are usually much higher. In this work, the ultrasound frequencies used ranged from 0.3 MHz to 0.7 MHz. Because the viscoelastic properties are frequency-dependent, the elastic modulus and viscosity obtained from the two techniques are unlikely to be equal, although correlations may be expected.

Figures 6.4 – 6.7 compare elastic modulus and viscosity between the model-based ultrasound method (MBUS, before and after transducer effect compensation) and the conventional measurements. The slop and intercept of the calibration equations are presented in Table 6.1. The results show that the two methods for all the mechanical properties have linear positive correlations. The mechanical properties derived from the model-based ultrasound method, both before and after transducer effect compensation, increased with the conventionally measured mechanical properties.

The correlation coefficients in the normal direction are slightly higher than those in the shear direction. This was expected since the transducer used in this work generated longitudinal waves. The model representation of the ultrasound measurement should be close to the compression test. The low correlation coefficients in the shear direction are probably caused by the assumption of the shear transition zone for model development which may not represent the real situation. The cylindrical column assumption of pressure field may be satisfied only in a short traveling distance of sound wave and the

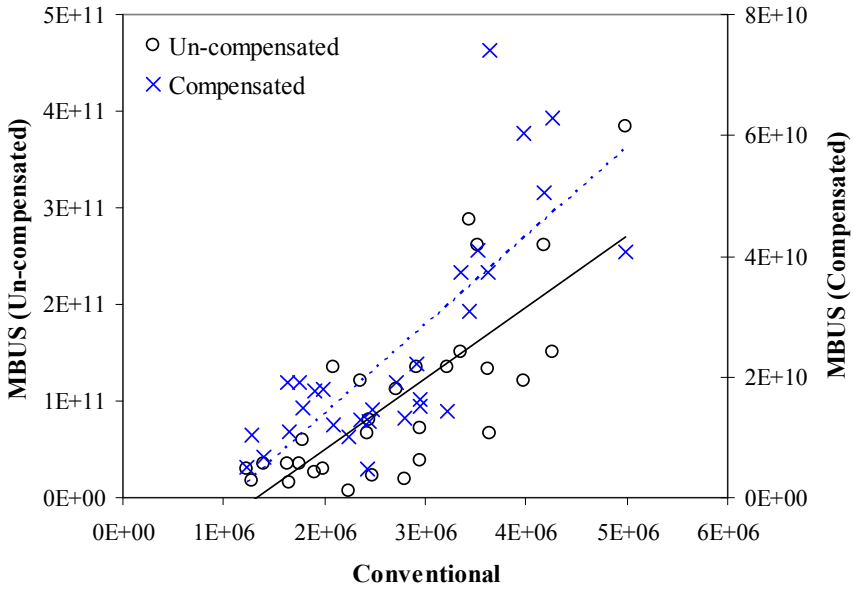

Figure 6.4. Correlation of normal elastic modulus obtained from model-based ultrasound measurement before and after transducer effect compensation with conventional measurements. Solid line is best fit line for uncompensated data and dashed line is best fit line for compensated data.

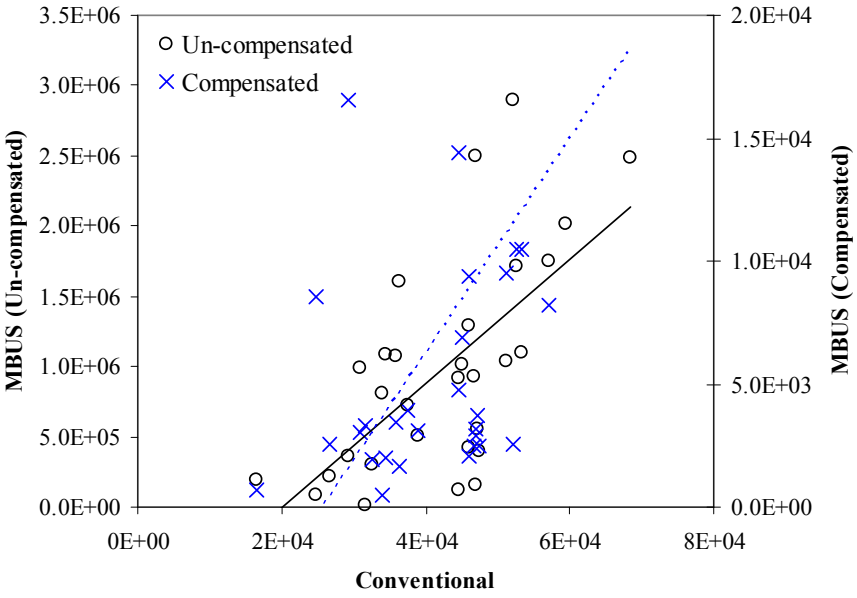

Figure 6.5. Correlation of normal viscosity obtained from model-based ultrasound measurement before and after transducer effect compensation with conventional measurements. Solid line is best fit line for uncompensated data and dashed line is best fit line for compensated data.

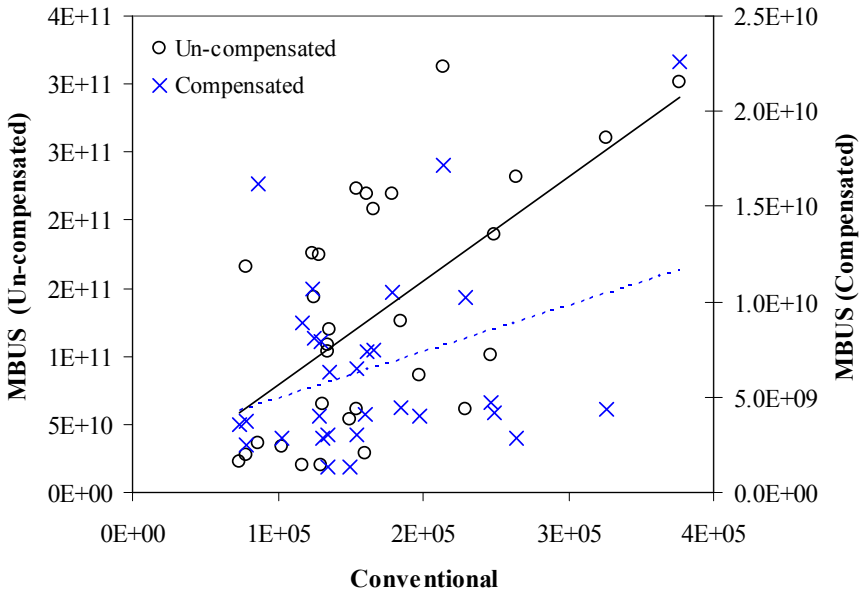

Figure 6.6. Correlation of shear elastic modulus obtained from model-based ultrasound measurement before and after transducer effect compensation with conventional measurements. Solid line is best fit line for uncompensated data and dashed line is best fit line for compensated data.

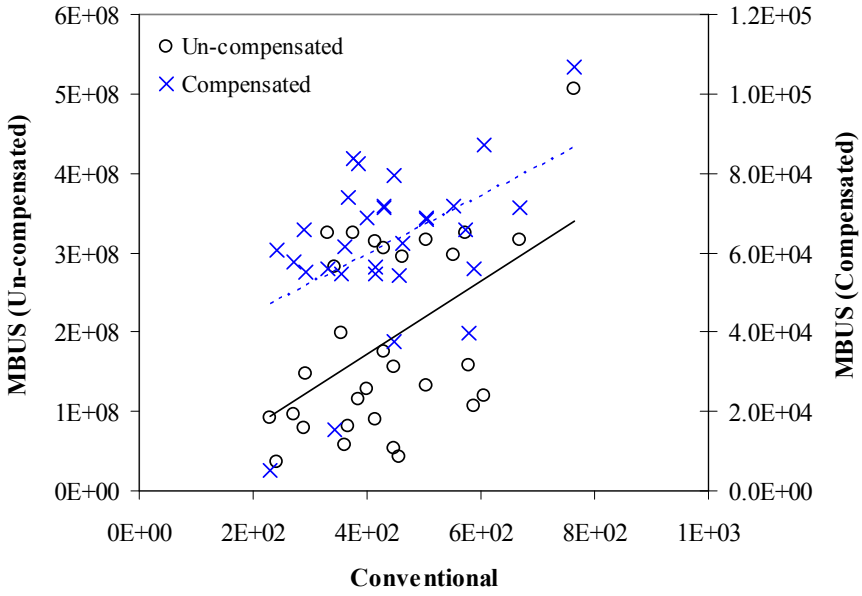

Figure 6.7. Correlation of shear viscosity obtained from model-based ultrasound measurement before and after transducer effect compensation with conventional measurements. Solid line is best fit line for uncompensated data and dashed line is best fit line for compensated data.

boundary of medium is far enough from the source transducer (Oshida *et al*., 1980; Michaels & Michaels, 2006). Further, for natural biological materials it is difficult to compensate for local variations in the sound field along the beam propagation direction (i.e., diffraction effects). The wave is not moving straight forward, but some are dispersed to random directions by the receiving transducer (Kauffman *et al*., 1995). Thus, the stress field around the pressure beam may be much more complex than the shear field assumption used.

Compared with the stiffness coefficient from which the elastic modulus is derived, the estimated damping coefficient from which viscosity is determined had lower correlation with the viscosity measured by standard tests. This may be due to the fact that damping is inherently nonlinear and dependent on frequency (Adhikari & Woodhouse, 2001). Damping is also more difficult to determine accurately from noisy data. Increasing the length of data can be a remedy for reducing the effect of noise (Chen *et al*., 1996).

Table 6.1 shows that the correlations between the conventionally measured material properties and those obtained by the MBUS method did not change much before and after transducer effect compensation. Although the compensation did not improve the correlations but it decreased the elastic modulus and viscosity values. This was expected as the transducer materials should add to the elasticity and damping of the system. As shown in Figures 6.5 and 6.7, the viscosity values decreased around 300 and 4,000 times on average after transducer effect compensation for normal and shear directions, respectively. The ranges of normal and shear viscosities of uncompensated measurement were 160 kPa.s – 2.9 MPa.s and 360 MPa.s – 0.51 GPa.s, respectively. After transducer effect compensation the property values decreased to 0.49 kPa.s – 380 kPa.s and 5.1

kPa.s – 0.11 MPa.s, respectively for normal and shear directions. This indicates that the transducers had major contributions to the estimated damping coefficients from the uncompensated data. Detailed value ranges of the mechanical properties are presented in Table 6.2.

Table 6.1. Slope and intercept of calibration equations for viscoelastic properties of potato

Mechanical Property	Un-compensated			Compensated		
	Slope	Intercept	r	Slope	Intercept	r
E_σ	7.387E+4	-9.824E+10	0.770*	1.469E+4	-1.560E+10	0.780*
η_σ	43.945	8.771E+5	0.645*	0.436	-1.121E+4	0.568*
E_τ	7.657E+5	2.441E+9	0.617*	2.437E+4	2.504E+9	0.352*
η_τ	4.566E+5	-1.030E+7	0.491*	73.817	2.994E+4	0.476*

* Significant at the 0.01 level (N = 30).

The conventionally measured mechanical properties differed in magnitude from those measured by the MBUS method. The mechanical properties measured with MBUS method are about 24, 200, and 0.4 times higher than the conventionally measured values for normal elastic modulus, shear elastic modulus, and shear viscosity, respectively. These results are consistent with Mason *et al*. (1949) who reported that increasing the frequency from below a hundred Hertz to mega Hertz led to a 200 times increase in the stiffness coefficient. The normal viscosity measured by the two methods is similar. The property values are dependent on frequency and thus differ between the two methods of measurement.

Table 6.2. Value ranges of the material properties of potato for different measurements

	E_σ, Pa	η_σ, Pa.s	E_τ, Pa	η_τ, Pa.s
		Conventionally measured		
Minimum	1.23E+06	1.65E+04	7.41E+04	2.30E+02
Maximum	4.99E+06	6.85E+04	3.77E+05	7.65E+02
Mean	2.71E+06	4.22E+04	1.66E+05	4.36E+02
Std. Deviation	9.68E+05	1.13E+04	7.14E+04	1.28E+02
		MBUS before compensation		
Minimum	7.39E+09	1.56E+04	1.94E+10	3.63E+07
Maximum	3.84E+11	2.90E+06	3.12E+11	5.06E+08
Mean	1.02E+11	9.76E+05	1.30E+11	1.89E+08
Std. Deviation	9.29E+10	7.72E+05	8.87E+10	1.19E+08
		MBUS after compensation		
Minimum	4.84E+09	4.87E+02	1.30E+09	5.14E+03
Maximum	7.41E+10	3.83E+04	2.26E+10	1.07E+05
Mean	2.42E+10	7.18E+03	6.56E+09	6.21E+04
Std. Deviation	1.82E+10	8.70E+03	4.94E+09	1.98E+04

It should be noted that in measuring natural materials difficulties arise from the high attenuation of ultrasound signal. Therefore, ultrasound transducers must be positioned very precisely. Even though plates are installed on the transducers to hold the sample it was sound difficult to keep the surrounding medium perfectly stationary during measurement. Errors in measurement could occur if the sample is not cut properly to ensure perfect contact between transducer and sample. Inconsistent contact pressure may also be a source of error.

6.4 Conclusion

This chapter presents the comparison results of mechanical properties derived from model-based ultrasound measurement and those obtained from conventional mechanical tests. Dynamic compression and shear tests were used as conventional measurements. The mechanical properties determined from the MBUS method and conventional measurements have positive correlations. Compensation of transducer effects in the ultrasound measurement reduced the estimated property values but the correlations with the conventional measurements did not significantly change.

CHAPTER 7

CRISPNESS PREDICTION FROM MODEL-BASED ULTRASOUND MEASUREMENTS

This section presents an application of the model-based ultrasound measurement for quality evaluation of food. The mechanical parameters estimated from the ultrasound measurement were used to predict the sensory crispness of apple.

7.1 Introduction

Several mechanical forces such as compression, bending, and shearing occur when a food is bitten and chewed in the mouth (Vincent, 1998). Stresses during power stroke of the chewing cycle may produce many sensations of the mouth that are delivered to the brain. This process may have significant influence on the acceptability of the food (Fillion and Kilcast, 2002). Interactions between teeth and foods, and the sensations generated, therefore, are of great interest in food quality evaluation.

Many attempts have been made to define the sensation of a food in the mouth. Texture, taste, flavor, and appearance are qualitative parameters commonly used to define consumer preference of food. Since the human sensation of food in the mouth is very complex and combines a wide range of perceptions (Luyten *et al*., 2004), food quality evaluation by human perception is naturally fuzzy and inconsistent (Tan *et al*., 1998; Tan, 2001).

Many studies have been done to develop instrumental techniques to correlate sensory attribute with mechanical parameters derived from uniaxial compression test,

resonance test, and dynamic test. For examples, Szczesniak (1988) associated sensory crispness with brittleness, crackling, snapping, crunchiness, and sound emission during eating. Vickers (1988) reported that sensory crispness correlates with fracturability and stiffness measured by using a snap test. Harker *et al*. (2002) studied the relationship between sensory attributes of apples and mechanical parameters determined by using puncture, tensile, twist, and Kramer shear tests. Mehinagic *et al*. (2003; 2006) studied the sensory crunchiness, chewiness and touch resistance of apple and correlated them to compression parameters such as flesh firmness and stiffness. In general, they found reasonable relationships between these sensory attributes and mechanical parameters.

Beside taste and appearance, crispness is one of the texture attributes of fruits and vegetables that have significant influence on consumer acceptance (Civille, 1991; Konopacka *et al*., 2007). Even though some relationships between instrumental parameters and sensory crispness have been found, the term crispness is still not well defined. Currently, there is no agreement on a single definition for crispness. It combines a wide range of perceptions (Luyten *et al*., 2004) and multiple parameters. The relationship among them may not be linear. In some cases, crispness is synonymous with freshness and wholesomeness and may correlate with water content of the product (Goerlitz *et al*., 2007; Primo-Martin *et al*., 2008).

Ultrasound characteristics have been correlated well with mechanical parameters representing firmness (Kim *et al*., 2009), but very few studied the correlation of ultrasound with sensory parameters. We developed a mechanical model to estimate mechanical properties of biological samples from acoustic wave transmission measurements. We have validated the model's ability to capture the major dynamics of

the ultrasound transmission through viscoelastic mediums. In this study, the model-based ultrasound method would be tested for its usefulness in food quality evaluation.

7.2 Materials and Methods

7.2.1 Test Materials

Forty-six fresh apples purchased from local stores were used for testing. Several cultivars of apple such as 'Golden Delicious', 'Red Delicious', 'Granny Smith', and 'Fuji' were selected to provide a wide range of mechanical properties. The cultivars selected were considered having different mechanical properties in fresh conditions (McCracken *et al*., 1994). Since a series of measurements must be conducted for each sample, each apple selected and used should have a diameter at least 9 cm. One apple was cut into two halves, one piece for ultrasound test and the other for sensory crispness test. All testing was done in the same day, the first was the ultrasound test and the sensory crispness test afterwards. Prior to the sensory test (about 1 to 4 hours after ultrasound measurement), the samples were wrapped with plastic and stored in a refrigerator in order to maintain the freshness and avoid unwanted contaminants. The procedures for sample preparation were in compliance with procedures issued by the University of Missouri Campus Institutional Review Board.

7.2.2 Ultrasound Measurement and Model Parameter Estimation

The ultrasound transmission measurement setup and the procedure were described in Section 3.4.3. Two ultrasonic transducers with a center frequency of 0.5 MHz were used. The samples were cut into 6 mm thickness. To keep sample stationary during

measurement, a plate (8 cm square) was installed on each transducer. The pseudo-random binary sequence was used as perturbation signal. For each sample, the measurement was performed three times and the average was used for model parameter estimation.

The procedures for model parameter estimation followed the steps as described in Section 3.2.3 and is summarized in Figure 3.4.

7.2.3 Density of Samples

After ultrasound measurement the sample was cored with 2-cm diameter (thickness of 1.5 cm) to determine the density. The density of each specimen was determined by measuring weight and volume of the specimen. The weight was measured with a digital balance (Denver Instrument XL-6100), while the volume was computed from diameter and length of the specimen. Measurement of diameter and length was done with a caliper (Mitutoyo Corp., Japan). The averages of diameter and length from three different positions were used to compute the density of the sample.

7.2.4 Sensory Assessment of Crispness

After ultrasound measurement, the samples were peeled. Each sample was cut into eight slices and each slice was put in a plastic bag labeled with a sample code. The slices were arranged into eight groups, and each group must have slices representing all the samples tested.

Eight assessors were asked to judge the crispness of the samples and each of them evaluated one sample group. The assessors included of 4 females and 4 males between 23- and 46- years old. Before testing, the assessors were trained in evaluating the sensory

crispness of apple. Several samples considered having different mechanical properties were prepared and the assessors were asked to bite and feel them to get familiarized with the sample variances and to use them as reference in evaluating the sensory crispness. The scores and grading of the training samples were obtained by consensus among the assessors. Furthermore, in order for all assessors to have an understanding of sensory crispness, they were asked to discriminate the sensory crispness with the other sensory attributes such as hardness, juiciness, and sweetness. In the sensory test, the assessors were asked to bite the sample, mark on a graphical line on a provided sensory evaluation sheet, and sip some water to rinse their mouths before tasting the next sample. The scores ranged 0 to 9 with 0 meaning "Not Crispy" and 9 meaning "Very Crispy". The mean of sensory scores from eight assessors for each sample was used for data analysis. The sensory assessment procedures for this study were approved by the University of Missouri Campus Institutional Review Board.

7.2.5 Neural Network Modeling

A neural network model was developed and coded in Matlab (version 7.1, The MathWorks Inc., USA) to predict the sensory crispness of apples from the estimated model parameters of ultrasound transmission. The neural network consists of an input layer with neurons representing input variables (x_i), an output layer with a neuron representing the output variable (y_i), and one or more hidden layers containing neurons to capture the linearity or nonlinearity of the data. The network structure used in this work is a multilayer perceptron as shown in Figure 7.1. The network function is determined by the connections between neurons. During training, the weights and biases of the

connection among the neurons are adjusted. In this study the Levenberg-Marquardt back-propagation algorithm was used for network training. The objective is to adjust the network weights and biases so that the output of the model is closest to the target.

Four parameters yielded from the model based-ultrasound measurement were used as inputs in the neural network. Combinations of two or more parameters would be used to predict sensory crispness of apple. The samples were first split randomly into three data sets. One data set of 35 samples (~76%) was used to train the neural network, a second data set of 10 samples (~22%) was used for validation, and one sample left was used for testing. The samples were resegregated until each sample was used for testing. This technique is also called the 'leave-one-out' method. The input and output values were normalized to the range of 0 to 1 (Sofu and Ekinci, 2007).

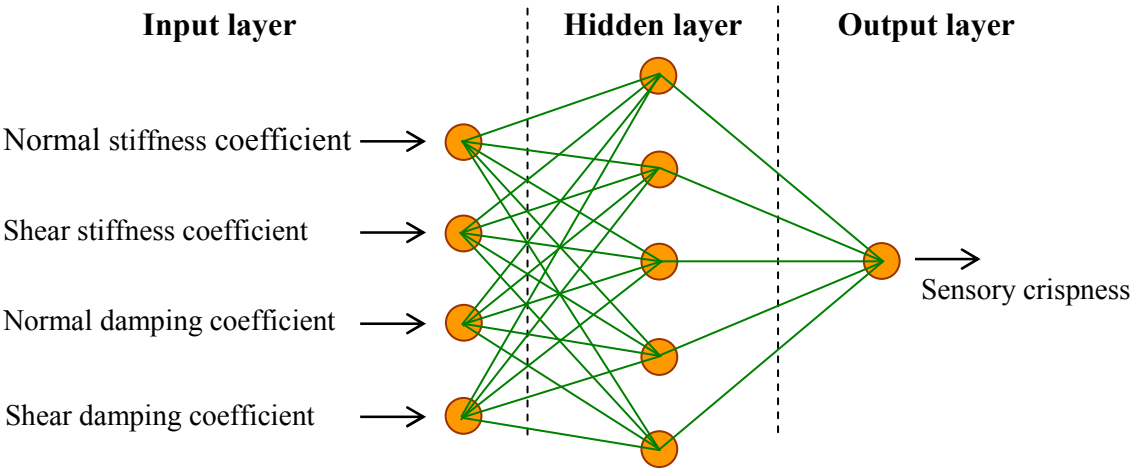

Figure 7.1. An example neural network structure for predicting sensory crispness of apple

7.2.6 Statistical Analysis

The sensitivity of assessors to the sensory crispness of apple was tested by analysis of variance (ANOVA). The test was used to determine how well the assessors agreed with one another on evaluating the crispness of apple. SPSS (version 14.0 for Windows, SPSS Inc.) was employed for the analysis. Significance level of differences was set $\alpha \leq 0.05$. The differences among assessors were compared with the least significant difference.

The neural network model was implemented to predict the sensory crispness from a set of the ultrasound model parameters. The measured and predicted sensory crispness values were then compared. The equality of two correlation coefficients (r) was tested through Fisher's Z transformation, and the parallelism of slope and the equality of intercept were tested by using the Student's t test (Kleinbaum *et al*., 2008). The tests were performed by using SPSS and a significance level α = 0.10. Sensitivity tests were performed by computing the change in predicted crispness score when an input was changed by 10%.

$$\delta_\theta = \frac{\Delta y}{\Delta \theta} \tag{7.2}$$

where y is predicted crispness score, and θ is a model parameter (k_σ, k_τ, b_σ, or b_τ).

7.3 Results and Discussion

7.3.1 Statistics of Sensory Crispness Scores

Table 7.1 shows the statistics for sensory crispness scores of apples. The results show that all the assessors had similar range of sensory crispness scores, or in other words, they had similar sensitivity to the sensory crispness of apples. The sensory crispness scores spread very widely from not crispy (close to 0) to very crispy (close to 9). This indicates that the assessors followed with the consensus reached in the training section.

Table 7.2 summarizes the range, mean and standard deviation of the sensory crispness grouped by cultivar. As expected the apple cultivars used for crispness testing differed from one to another. In general, by the mean of each group, 'Fuji' was scored as the crispest and 'Red Delicious' was the least crispy. Table 7.3 is the result of analysis of variance (ANOVA) for the data. The analysis indicates that the apple cultivars used in the experiment were significantly different in sensory crispness.

Table 7.1. Statistics of the sensory crispness grouped by assessor (n = 46)

Assessor	*min*	*max*	*mean*	*std*
Assessor 1	*0.50*	*8.20*	*4.72*	*1.65*
Assessor 2	*1.30*	*7.50*	*5.30*	*1.57*
Assessor 3	*1.50*	*8.90*	*6.27*	*1.50*
Assessor 4	*1.60*	*7.30*	*5.31*	*1.43*
Assessor 5	*1.80*	*8.80*	*7.02*	*1.57*
Assessor 6	*1.80*	*8.70*	*6.50*	*1.61*
Assessor 7	*0.30*	*8.30*	*4.44*	*2.18*
Assessor 8	*0.40*	*8.60*	*5.24*	*1.96*

Table 7.2. Statistics of the sensory crispness grouped by cultivar

Sample	*min*	*max*	*mean*	*std*
Fuji (8)	*3.00*	*8.30*	*6.12*	*1.35*
Red Delicious (12)	*0.30*	*8.80*	*4.93*	*2.31*
Golden Delicious (15)	*1.10*	*8.90*	*6.02*	*1.55*
Granny Smith (11)	*0.90*	*8.70*	*5.39*	*1.89*
Samples (46)	*0.30*	*8.90*	*5.60*	*1.68*

Table 7.3. Analysis of variance of sensory crispness by cultivar

Source of Variation	*SS*	*df*	*MS*	*F*	*P-value*	*F crit*
Apple cultivar	*62.6897*	*3*	*20.8966*	*9.1062*	*7.96E-06*	*2.6295*
Within Groups	*833.0014*	*363*	*2.2948*			
Total	*895.6911*	*366*				

Significance level $\alpha = 0.05$.

It is almost impossible to reach the ideal situation where all the assessors would give the same score for each sample used. Humans have broad definitions on sensory attributes (Roudaut *et al*., 2002) and the sensory system is commonly fuzzy, inconsistent, imprecise, and vague. Use of fuzzy set in sensory evaluation is described in Tan (2001). Interpreting the sensory data and their functional relationship may not always be simple since the sensory concept of crispness may not be clear-cut. It may be influenced by other sensory attributes, such as firmness, sweetness, and juiciness. Furthermore, some people may be sensitive to a particular attribute but they may not be able to completely separate

other attributes. Even though all the assessors scored apple crispness in a similar range, there is not guarantee that the assessors had reached a consensus on the meaning of crispness. The same value by two assessors does not necessarily mean that they define crispness in the same manner because of the complexity of human senses.

7.3.2 Sensory Crispness Prediction

Crispness is considered to be a combination of several physical and mechanical properties (Roudaut *et al*., 2002). The relationship between these properties and sensory crispness is generally very complex and almost impossible to be expressed with a simple relationship. Thus, very often the relationship between physical and mechanical parameters and sensory crispness is obtained by nonlinear analysis. In this study, a feed-forward neural network was developed to describe the relationship between the ultrasound model parameters and sensory crispness of apples. A set of parameters derived from the model-based ultrasound measurement was used as input for the network model. The ultrasound model parameters correspond to the mechanical properties, such as modulus elasticity and viscosity. They might be potentially used to predict the sensory crispness of apples.

Several neural network structures were tested to determine the best network based on the least squares error. In general, the more complex the network structure, the smaller the sum of the squared errors. But a complex network model can suffer from over-fitting. The errors for different network structures decrease with training in a similar trend (Figure 7.2). The mean squared errors (MSE) for 2 inner layers with 3 neurons in each layer were higher than those for 1 inner layer and 5 to 10 neurons in the layer (not all of

results are shown in the Figure). On the other hand, a network with insufficient complexity can fail to capture the overall pattern of a complicated data set. Practically, the optimum network structure is model with the smallest number of inner layers and neurons that still give small errors. Based on the analysis, a network with 1 inner layer and 6 neurons was selected as the final model.

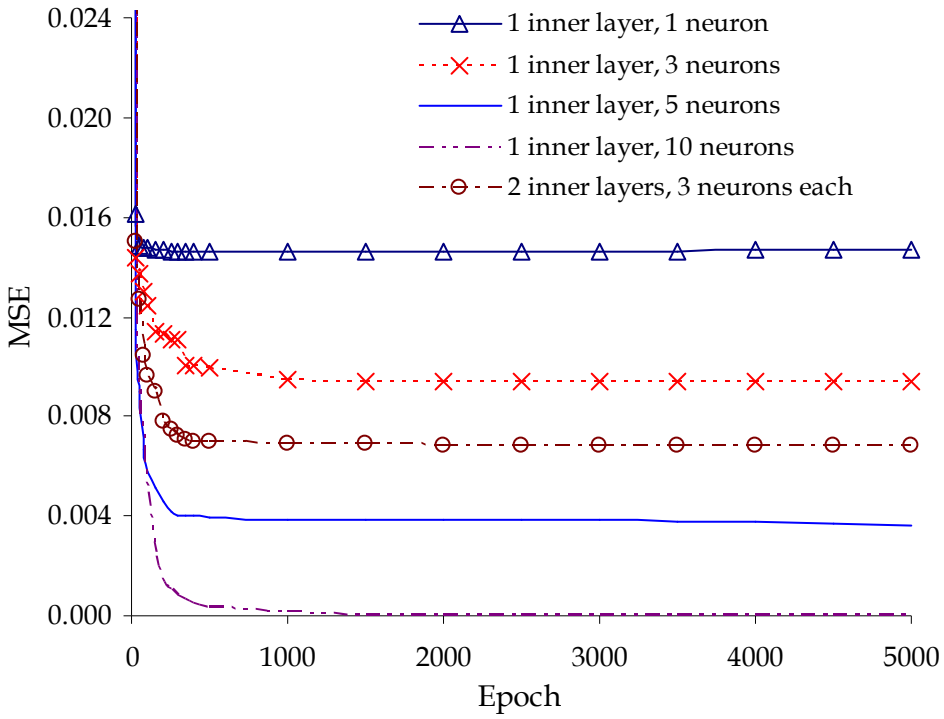

Figure 7.2. Comparison of MSE for different neural network structures

The neural network structure selected was used to predict the sensory crispness of apples. Combinations of the ultrasound model parameters were used as inputs to the network. Figures 7.3 and 7.4 are the plots of sensory crispness versus prediction with four

ultrasound model parameters (k_σ, k_τ, b_σ, and b_τ) and two ultrasound model parameters (k_σ and k_τ), respectively. The results show that the predicted scores had good agreement with the sensory scores of the samples. Correlation coefficients are 0.9197 for the network with four parameters as inputs and 0.9691 for the network with two parameters as inputs. The slopes of both regression equations are close to 45^o and the intercepts are relatively small. This means that the ultrasound model parameters could be used to predict the sensory crispness with acceptable precision.

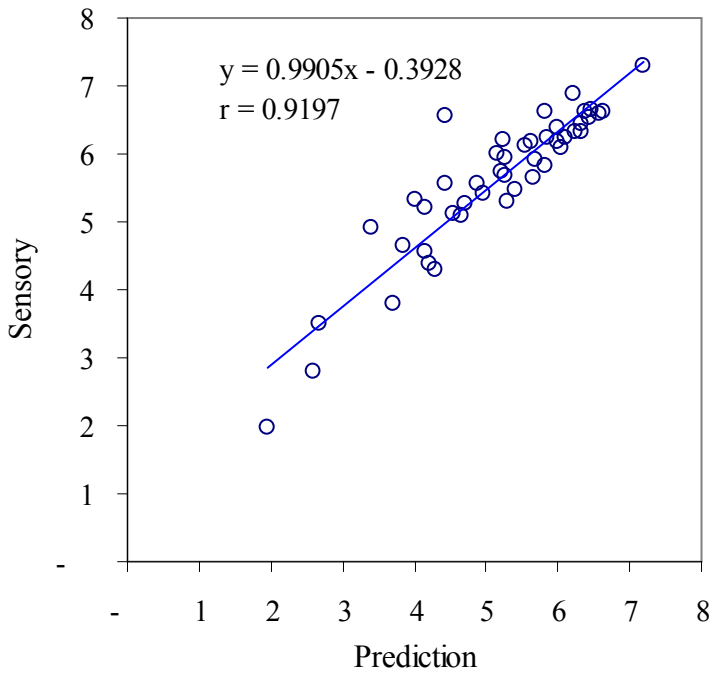

Figure 7.3. Comparison of sensory crispness of apples with neural network prediction with four ultrasound model parameters (k_σ,k_τ,b_σ, & b_τ) as inputs.

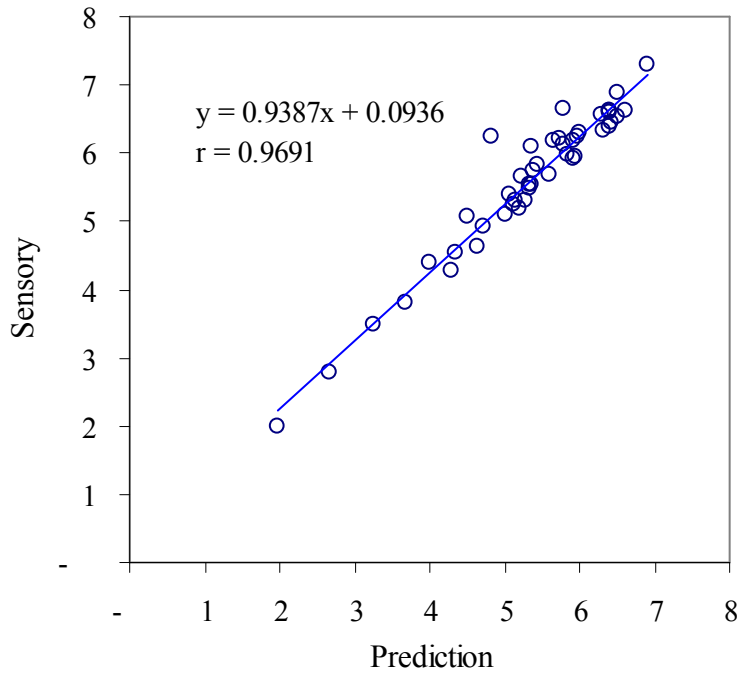

Figure 7.4. Comparison of sensory crispness of apples with neural network prediction with four ultrasound model parameters (k_σ & k_τ) as inputs.

The figures also indicate that more complex neural network structures do not always give better prediction. The relationship between input parameters and sensory crispness in a neural network is not simple. In the case where uncertainty in the model is high, it is more difficult for a more complex model to reach the target.

Table 7.4 shows that average and standard deviations of the absolute changes in the predicted crispness score when an input parameter was changed by 10%. For the model with four input parameters, changes of normal stiffness coefficient, shear stiffness coefficient, normal damping coefficient, and shear damping coefficient by 10% changed the sensory scores by 0.46; 0.46; 0.45; and 0.52, respectively. The results indicate that the model parameters had similar influence on crispness. Furthermore, analysis for the model

with two input parameters showed that sensory crispness is more sensitive to the normal stiffness coefficient (δ = 0.49) than to the shear stiffness coefficient (δ = 0.15). This agrees with the literature.

Table 7.4. Changes in predicted crispness resulting from 10% change in an input parameter

Parameter changed	Model with Four Input Parameters	Model with Two Input Parameters
Normal stiffness coefficient	0.46 (0.46)	0.49 (0.46)
Shear stiffness coefficient	0.46 (0.46)	0.15 (0.20)
Normal damping coefficient	0.45 (0.38)	-
Shear damping coefficient	0.52 (0.50)	-

Note: Numbers are average and standard deviation (number in parenthesis) of the absolute change in predicted crispness for 46 samples.

7.4 Conclusion

The dependence of sensory crispness on ultrasound model parameters is not a simple function and the relationship could be very complex. A feed-forward neural network model was developed to capture the complex pattern of sensory crispness predicted with the mechanical parameters. The neural network model showed good performance in predicting the sensory crispness of apple. This study showed that the normal stiffness coefficient was more useful in predicting apple crispness than the other

ultrasound model parameters. The results suggested that model parameters extracted from the model-based ultrasound method correlated to apple crispness and can be used to predict sensory crispness of apples. The technique applied can potentially be further developed and used as a method for sensory quality evaluation.

CHAPTER 8

SUMMARY

8.1 Major Results

A mechanical network based on the Kelvin-Voigt model was developed and used to discretize a viscoelastic medium and to represent wave propagation through the medium. Linear state-space equations were derived to provide a physically meaningful way for extracting viscoelasticity-dependent parameters from ultrasound measurements. To capture the frequency dependency of the mechanical parameters, a broad-band sound source named pseudo random binary sequences (PRBS) was designed and used to perturb the sample and the transmitted ultrasonic waves were measured. The Levenberg-Marquardt method was employed to adjust the model parameters and the least-squares algorithm was used to obtain optimal model parameters from which the mechanical properties: moduli of elasticity (E) and viscosity (η) were derived.

Model verification showed that the algorithm developed could converge to given true model parameters. The estimated model parameters reflected some known facts in the materials tested. The material properties derived from the model parameters showed consistency. The higher the viscosity of the sample is, the higher the estimated damping coefficients are. With a limited number of elements to discretize a medium, the proposed model could capture the major dynamics of transmitted ultrasonic waves and allowed repeatable estimation of model parameters.

The model parameters were used for biological tissue classification and differentiation. The results showed that the extracted viscoelastic properties could not only classify the materials tested but also follow expected trends of variation. The approach showed promise as a physically-based method for ultrasonic assessment of viscoelastic properties.

A practical transfer function based method was developed to estimate the frequency response of the transducer pair used as transmitter and receiver from experimental measurements. The frequency response obtained showed repeatability and consistency. It also agreed with data provided by the manufacturer. The frequency response was used to cancel the effects of transducer pair on the measurement.

Viscoelastic properties obtained from the model-based ultrasound method were compared with those measured with conventional methods. Cyclic compression and shear dynamic tests were done to determine the viscoelastic properties in the normal and shear directions, respectively. The results showed that the mechanical properties obtained from model-based ultrasound (MBUS) measurement had positive linear correlations with the conventionally measured values. The correlation coefficients between the MBUS method with data without transducer effect compensation and the conventional methods were 0.770, 0.645, 0.617, and 0.491 for $E_{\sigma,}$ η_{σ}, E_{δ}, and η_{δ}, respectively. With transducer effect compensation, the correlation coefficients were 0.783, 0.649, 0.433, and 0.314. The values of the viscoelastic properties from compensated data were closer to the conventionally measured. The differences in value are because the two methods use different excitation frequencies. The mechanical properties obtained by the MBUS measurement, however, were consistent with previous studies.

The model-based ultrasound measurement was used to evaluate the sensory crispness of apples. Neural network models were developed to predict the sensory crispness of apples from the model-based ultrasound measurements. The results show that the developed method could efficiently predict the sensory crispness. Correlation coefficient between predicted and sensory crispness values was 0.9197 for the model using four inputs and 0.9691 for the model using two inputs. The models show that crispness may be more strongly correlated to the elastic modulus rather than viscosity. This result is consistent with the previous studies.

8.2 Future Work

Based on this work, the MBUS measurement can potentially be developed as a means to study the behavior of food and biological materials. The true sound speed through a medium can be a crucial to the accuracy of the model parameter estimates. Although the least-squares method provides a good way to minimize errors between the measurement and the model response, the initial response corresponding to the onset of the input signal may not represent the true sound speed through the medium. Further research is needed to solve the problem.

The model showed ability to capture the major dynamics of ultrasound wave through homogeneous biological materials. In fact, most biological materials are not homogeneous. The model needs to be further developed without the assumption of homogeneity for application in a broad range of biological materials. This provides future research opportunities.

REFERENCES

Adhikari, S. & Woodhouse, J. 2001. Identification of damping: Part I, viscous damping. *Journal of Sound and Vibration*, 243(1): 43 – 61.

Akar, A., Baltaş, H., Çevik, U., Korkmaz F., & Okumuşoğlu, N.T. 2006. Measurement of attenuation for bone, muscle, fat and water at 140, 364 and 662 keV γ-ray energies. *Journal of Quantitative Spectroscopy & Radiative Transfer*, 102: 203 – 211.

American Society for Testing and Materials (ASTM). 2007. *Annual Book of ASTM Standards*, ASTM, West Conshohochen, Philadelphia, USA.

Ay, C. & Gunasekaran, S. 2003. Numerical method for determining ultrasound wave diffusivity through coagulation milk gel system. *Journal of Food Engineering*, 58: 103 – 110.

Blanc, R.H. 1993. Transient wave propagation methods for determining the viscoelastic properties of solids. *J. Appl. Mech.*, 60(3): 763 – 768.

Botros, N., Chu, W.K., & Cheung, J.Y. 1987. In-vivo ultrasound tissue differentiation through the acoustic attenuation coefficient. *IEEE Ultrasonics Symposium*: 927 – 930.

Bourne, M. 2002. *Food Texture and Viscosity: Concept and Measurement*. Academic Press, New York, USA,.

Brown, C. 2007. *Differential Equations: A Modeling Approach*. Sage Publications, Inc., New Delhi, India.

Castello, D.A., Rochinha, F.A., Roitman, N., & Magluta, C. 2008. Constitutive parameter estimation of a visocelastic model with internal variables. *Mechanical Systems and Signal Processing*, 22(8): 1840 – 1857.

Chang, S., Li, D., Lan, Y., Ozkan, N., Shi, J., Chen, X.D., & Mao, Z. 2009. Study on creep properties of Japonical cooked rice and its relationship with rice chemical compositions and sensory evaluation. *International Journal of Food Engineering*, 5(3), Article 10.

Chateline, S., Gennisson, J.L., Delon, G., Fink, M., Sinkus, R., Abouelkaram, S., & Culioli, J. 2004. Measurement of viscoelastic properties of homogeneous soft solid using transient elastography: An inverse problem approach. *J. Acoust. Soc. Am*. 1166: 3734 – 3741.

Cheeke, J.D.N. 2002. *Fundamentals and Applications of Ultrasonic Waves*. CRC Press LLC, Florida, USA.

Chen, E.J., Novakofski, J., Jenkins, K., & O'Brien Jr., W.D. 1994. Ultrasound elasticity measurements of beef muscle. In Proc. *IEEE Ultrasonics Symposium. IEEE UFFC*, 1994.

Chen, S., Fatemi, M., & Greenleaf, J.F. 2004. Quantifying elasticity and viscosity from measurement of shear wave dispersion. *Journal of Acoustical Society of America*, 115(6): 2781 – 2785.

Chen, S.Y., Ju, M.S., & Tsuei, Y.G. 1996. Estimation of mass, stiffness and damping matrices from frequency response function. *Transaction of the ASME*, 118: 78 – 82.

Civille, G.V. 1991. Food quality: Consumer acceptance and sensory attributes. *Journal of Food Quality*, 14(1): 1 – 8.

Collins, G.W., Patel, A., Dilley, A., & Sarker D.K. 2008. Molecular modeling directed by an interfacial test apparatus for the evaluation of protein and polymer ingredient function in situ. *Journal of Agric. Food Chem*., 56: 3846 – 3855.

Constantinides, A & Mostoufi, N. 1999. *Numerical Methods for Chemical Engineers with MATLAB Applications*. Prentice-Hall Inc., New Jersey, USA.

Coupland, J. & McClements, D.J. 2001. *Ultrasonics*. Marcel Dekker, Inc., New York, USA.

Deblock, Y., Lefebvre, F., Radziszewski, E., & Nongaillard, B. 1998. The determination of the viscoelastic properties of liquid materials at ultrasound frequencies by CW mode impedance measurements. *IEEE Trans. on Instrumentation and Measurement*, 473: 680 – 685.

Dukhin, A.S. & Goetz, P.J. 2002. Ultrasound for characterizing colloids, particle sizing, zeta potential, rheology. Elsevier Science Publishers Ltd., England.

Echeverría, G., Graell, J., Lara, I., López, M.L., & Puy, J. 2008. Panel consonance in the sensory evaluation of apple attributes: Influence of mealiness on sweetness perception. *Journal of Sensory Studies*, 23: 656 – 670.

Elmehdi, H.M., Page1, J.H., & Scanlon, M.G. 2003. Monitoring Dough Fermentation Using Acoustic Waves. *Trans IChemE*, 81(Part C): 217 – 223.

Farshad, M., Barbezat, M., Flueler, P., Schmidlin, F., Graber, P. & Niederer, P. 1999. Material characterization of the pig kidney in relation with the biomechanical analysis of renal trauma. *Journal of Biomechanics*, 32: 417 – 425.

Fillion, L. & Kilcast, D. 2002. Consumer perception of crispness and crunchiness in fruits and vegetables. *Food Quality and Preference*, 13: 23 – 29.

Findley, W.N., Lai, J.S., & Onaran, K. 1989. *Creep and Relaxation of Nonlinear Viscoelastic Materials*. Dover Publications, Inc. Mineola, New York, USA.

Forgacs, G., Foty, R.A., Shafrir, Y., & Steinberg, M.S. 1998. Viscoelastic properties of living embryonic tissues: A quantitative study. *Biophysical Journal*, 74 (5): 2227 – 2234.

Fujisawa, K. & Takei, Y. 2009. A new experimental method to estimate viscoelastic properties from ultrasound wave transmission measurements. *Journal of Sound and Vibration*, 323: 609 – 625.

Fukashiro, S., Noda, M., & Shibayama, A. 2001. In vivo determination of muscle viscoelasticity in the human leg. *Acta Physiol Scand*., 172: 241 – 248.

Fung, Y.C. 1993. *Biomechanics Mechanical Properties of Living Tissues*. Springer-Verlag, New York, USA.

Girnyk, S., Barannik, A., Barannik, E., Tovstiak, V., Marusenko, A., & Volokhov, V. 2006. The estimation of elasticity and viscosity of soft tissues *in vitro* using the data of remote acoustic palpation. *Ultrasound in Medicine & Biology*, 32(2): 211 – 219.

Godfrey, K. 1993. Introduction to perturbation signals for time-domain system identification. In *Perturbation Signals for System Identification*, K. Godfrey, Ed. Hertfordshire: Prentice Hall International Ltd., UK.

Goerlitz, C., Harper, W.J., & Delwiche, J.F. 2007. Relationship of water activity to cone crispness as assessed by positional relative rating. *Journal of Sensory Studies*, 22: 687 – 694.

Gómez, A.H., He, Y., & Pereira, A.G. 2006. Non-destructive measurement of acidity, soluble solids and firmness of Satsuma mandarin using Vis/NIR-spectroscopy techniques. *Journal of Food Engineering***,** 77(2): 313 – 319.

Haddad, Y.M. 1995. *Viscoelasticity of Engineering Materials*. Chapman & Hall, London, UK.

Harker, F.R., Maindonald, J., Murray, S.H., Gunson, F.A., Hallet, I.C., & Walker, S.B. 2002. Sensory interpretation of instrumental measurements 1: Texture of apple fruit. *Postharvest Technology & Biology*, 24: 225 – 239.

Hingorani, R.V., Provenzano, P.P., Lakes, R.S., Escarcega, A., & Vanderby Jr, R. 2004. Non-linear viscoelasticity in rabbit medial collateral ligament. *Annals of Biomedical Engineering*, 322: 306 – 312.

Hozumi, N., Kimura, A., Terauchi, S., Nagao, M., Yoshida, S., Kobayashi, K., & Saijo, Y. 2005. Acoustic impedance micro-imaging for biological tissue using a focused acoustic pulse with a frequency range up to 100 MHz. *IEEE Ultrasonics Symposium*: 170 – 173.

Jan, M.V.S., Guarini, M., Guesalaga, A., Pérez-Correa, J.R., & Vargas, Y. 2008. Ultrasound based measurements of sugar and ethanol concentrations in hydroalcoholic solutions. *Food Control*, 19(1): 31 – 35.

Kaufman, J.J., Xu, W., Chiabrera, A.E., & Siffert, R.S. 1995. Diffraction effect in insertion mode estimation of ultrasound group velocity. *IEEE Transaction on Ultrasonics, Ferroelectrics, and Frequency Controls*, 42(2): 232 – 242.

Khadeer, M.A., Mohiuddin, S., Krishna, G.G., & Ahmad, A. 2005. Muscle elasticity by ultrasound. J. Pure & Appl. Phys., 171: 35 – 36.

Kilcast, D. 2004. Measuring consumer perceptions of texture: an overview. Pages 1-28 in *Texture in Food*. Kilcast, D., (Ed.), Woodhead, Cambridge, UK.

Kim, K., Lee, S., Kim, M., & Cho, B. 2009. Determination of apple firmness by nondestructive ultrasonic measurement. *Postharvest Biology and Technology*, 52: 44 – 48.

Kleinbaum, D.G., Kupper, L.L., Nizam, A., & Muller, K.E. 2008. *Applied Regression Analysis and Other Multivariable Methods*. Fourth Edition. Thomson Higher Education, Belmont, California, USA.

Koc, A.B. & Vatandas, M. 2006. Ultrasonic velocity measurements on some liquids under thermal cycle: Ultrasonic velocity hysteresis. *Food Research International*, 39: 1076 – 1083.

Konopacka, D., Rutkowski, K.P., & Płocharski, W. 2007. Changes of acceptability of 'Jonagold' and 'Gala' apples during storage in normal atmosphere. *Vegetable Crops Research Bulletin*, 66: 177 – 186.

Kourtiche, D., Nadi, M., Rouane, A., & Chitnalah, A. 2010. Analysis of transducer effect sensitivity function in nonlinear ultrasound measurement system. *NDT & E International*, 43(2): 145 – 151.

Kubo, K., Kanehisa, H., Azuma, K., Ishizu, M., Kuno, S. Y., Okada, M., & Fukunaga, T. 2003. Muscle architectural characteristics in young and elderly men and women. *International Journal of Sports Medicine, 24,* 125-130.

Kuchařová, M., Ďoubal, S., Klemera, P., Rejchrt, P., & Navrátil, M. 2007. Viscoelasticity of biological materials – Measurement and practical impact on biomedicine. *Physiol. Res*., 56 Suppl. 1: S33 – S37.

Kuroki, S., Tohro, M., & Sakurai, N. 2006. Monitoring of the elasticity index of melon fruit in a greenhouse. *Journal Japan Soc. Hort. Sci.,* 75(5): 415 – 420.

Lakes, R.S. 2004. Viscoelastis measurement techniques. *Rev. Sci. Instrum.* 75: 797 – 811.

Lakes, R.S. & Vanderby, R. 1999. Interrelation of creep and relaxation: A modelling approach for ligaments. *ASME Journal of Biomechanical Engineering*, 1216: 612 – 615.

Laux, D., Lévêque, G., & Cereser Camara, V. 2009. Ultrasonic properties of water/sorbitol solutions. *Ultrasonics*, 49: 159 – 161.

Leroy, V., Strybulevych, A., & Page, J.H. 2008. Sound velocity and attenuation in bubble gels measured by transmission experiments. *J. Acoust. Soc. Am*. 123(4): 1931 – 1940.

Littrup, P.J., Nebojsa, D., Richard, L., Azevedo, S.G., Candy, J.V., Moore, T., Chambers, D.H., Mast, J.E., & Holsapple, E. 2002. Characterizing tissue with acoustic parameters derived from ultrasound data. In Medical Imaging 2002: Ultrasonic Imaging and Signal Processing, Insana, M.F. & Walker, W.F., (Eds.), *Proc. SPIE*, Vol. 4687: 354 – 361.

Liu, J.G. & Xu, M.Y. 2008. Study on the viscoelasticity of cancellous bone based on higher-order fractional models. *IEEE Ultrasonics Symposium*: 1733 – 1736.

Liu, J.G. & Xu, M.Y. 2006. Higher-order fractional constitutive equations of viscoelastic materials involving three different parameters and their relaxation and creep functions. *Mech Time-Depend Mater*, 10: 263 – 279.

Liu, Z. & Bilston, L. 2000. On the viscoelastic character of liver tissue: Experiments and modeling of the linear behavior. *Biorheology*, 37: 191 – 201.

Luyten, H., Plijter, J.J., & Van Vliet, T. 2004. Crispy/crunchy crust of cellular solid foods: A literature review with discussion. *Journal of Texture Studies*, 35: 445 – 492.

Mahata, K. & Söderström, T. 2007. Bayesian approaches for identification of the complex modulus of viscoelastic materials. *Automatica*, 43: 1369 – 1376.

Mahomed, A., Chidi, N.M., Hukin, D.W.L., Kukureka, S.N., & Shepherd, D.E.T. 2008. Frequency dependence of viscoelastic properties of medical grade silicones. *Journal of Biomedical Materials Research Part B: Applied Biomaterials*, 89B1: 210 – 216.

Mallikarjunan, P. 2004. Understanding and measuring consumer perception of crispness. Pages 82-103 in *Texture in Food*. Kilcast, D., (Ed.), Woodhead, Cambridge, UK.

Mamou, J., Oelze, ML., Zachary, J.F., & O'Brien Jr., W.D. 2003. Ultrasound scatterer size estimation technique based on a 3D acoustic impedance map from histological section. *IEEE Ultrasonics Symposium*: 1022 – 1025.

Mase, G.T. & Mase, G.E. 1999. *Continuum mechanics for engineers*. CRC Press, Florida, USA.

Mason, W.P., Baker, W.O., Mcskimin, H.J., & Heiss, J.H. 1949. Measurement of shear elasticity and viscosity of liquids at ultrasonic frequencies. *Phys. Rev*. 75(6): 936 - 946.

Masoudi, H., Tabatabaeefar, A., & Borghaee, A.M. 2007. Determination of storage effect on mechanical properties of apples using the uniaxial compression test. *Canadian Biosystems Engineering*, 49: 3.29 – 3.33.

McCracken, V.A., Maier, B., Boylston, T., & Worley, T. 1994. Development of a scheme to evaluate consumer apple variety preference. *Journal of Food Distribution Research*, 25(1): 56 – 63.

Mehinagic, E., Royer, G., Symoneaux, R., Bertrand, D., & Jourjon, F. 2003. Relationship between sensory analysis, penetrometry and visible – NIR spectroscopy of apples belonging to different cultivars. *Food Quality and Preference*, 14(5-6): 473 – 484.

Mehinagic, E., Royer, G., Symoneaux, R., Bertrand, D., & Jourjon, F. 2004. Prediction of the sensory quality of apples by physical measurements. *Postharvest Biology and Technology*, 34: 257 – 269.

Mehinagic, E., Royer, G., Symoneaux, R., & Jourjon, F. 2006. Relationship between apple sensory attributes and instrumental parameters of texture. *Journal of Fruit and Ornamental Plant Research*, 14(2): 25 – 37.

Meirovitch, L. 1997. *Principles and Techniques of Vibrations*. Prentice-Hall, Inc., New Jersey, USA.

Michaels, T.E. & Michaels, J.E. 2006. Application of acoustic wavefield imaging to non-contact ultrasonic inspection of bonded components. *Review of Quantitative Nondestructive Evaluation*, 25: 1484 – 1491.

Mittal, G.S., Zhang, M., & Barbut, S. 2007. Stress relaxation test conditions for meat products to measure viscoelasticity. *Journal of Muscle Foods*, 4(2): 91 – 107.

Mizrach, A. 2000. Determination of avocado and mango fruit properties by ultrasonic technique, *Ultrasonics*, 381-8: 717 – 722.

Mizrach, A. 2008. Ultrasound technology for quality evaluation of fresh fruit and vegetables in pre- and postharvest processes. *Postharvest Biology and Technology*, 48: 315 – 330.

Mizrach, A., Flitsanov, U., El-Batsri, R., & Degani, H. 1999. Determination of avocado maturity by ultrasonic attenuation measurements. *Scientia Horticulturae*, 80: 173 – 180.

Mohanty, S. 2009. Artificial neural network based system identification and model predictive control of a flotation column. *Journal of Process Control*, 19: 991 – 999.

Mulet, A. Benedito, J., Bon, J., & Rossello, C. 1999. Ultrasonic velocity in cheddar cheese as by temperature. *Journal of Food Science*, 64(6): 1038 – 1041.

Nakajima, K., Kudo, N., Yamamoto, K., Mikami, T., & Kitabatake, A. 1999. A study on frequency dependence of ultrasound attenuation of biological tissue in the frequency range of 2 – 40 MHz. *IEEE Ultrasonics Symposium*: 1381 – 1384.

Nitta, N. & Homma, K. 2005. Ultrasonic measurement of fluid viscosity for blood characterization. *Japanese Journal of Applied Physics*, 446B: 4602 – 4608.

Nitta, N. & Shiina, T. 2002. Estimation of nonlinear elasticity parameter of tissues by ultrasound. *Japanese Journal of Applied Physics*, 41: 3572 – 3578.

Oke, S.A., Oyetunji, E., Ogunwolu, L., & Omojuwa, E.O. 2008. Mathematical model on the effect of viscosity of oil palm on oil quality. *Agricultural Engineering International*: the CIGR Ejournal, Manuscript FP 07015, Vol. X, 1 – 13.

Ophir, J., Cespedes, I., Ponnekanti, H., Yazdi, Y., & Li, X. 1991. Elastography: a quantitative method for imaging the elasticity of biological tissues. *Ultrasonic Imaging*, 13 (2): 111 – 134.

Oshida, Y., Iwata, K., Nagata, R., & Ueda, M. 1980. Visualization of ultrasonic wave fronts using holographic interferometry. *Applied Optics*, 19(2): 222 – 227.

Özkaya, N., Margareta N., & Leger, D.L. 1998. *Fundamentals of Biomechanics: Equilibrium, Motion, and Deformation*. Birkhäuser.

Peirlinckx, L., Pintelon, R., & Van Biesen, L.P. 1993[a]. Identification of parametric models for ultrasound wave propagation in the presence of absorption and dispersion. *IEEE Transaction on Ultrasonics, Ferroelectrics, and Frequency Controls*, 40: 302 – 312.

Peirlinckx, L., Guillaume, P., Pintelon, R., & Van Biesen, L.P. 1993[b]. MIMO identification of parametric models for ultrasound reflection and transmission experiments. *IEEE Ultrasonics Symposium*, 723 – 728.

Primo-Martin, C., Castro-Prada, E.M., Meinders, M.B.J., Vereijken, P.F.G., & Van Vliet, T. 2008. Effect of structure in the sensory characterization of the crispness of toasted rusk roll. *Food Research International*, 41 (5): 480 – 486.

Purkayastha, S., Peleg, M., & Normand, M.D. 1984. Presentation of the creep curves of solid biological materials by a simplified mathematical version of the generalized Kelvin-Voigt model. *Rheologica Acta*, 23: 556 – 563.

Rao, M.A. & Steffe, J.F. 1992. *Viscoelastic Properties of Foods*. Elsevier Science Publishers Ltd., England.

Roudaut, G., Dacremont, C., Pamies, B.V., Colas, B., & Le Meste, M. 2002. Crispness: a critical review on sensory and material science approaches. *Trend in Food Science & Technology*, 13: 217 – 227.

Schöck, T. & Becker, T. 2010. Sensor array for the combined analysis of water-sugar-ethanol mixtures in yeast fermentations by ultrasound. *Food Control*, 21(4): 362 – 369.

Setsuo, H. & Jun'ichi, S. 1999. Nondestructive freshness and processing evaluation of fruits and vegetables by acoustic transmission velocity. A case study of cucumbers and kiwifruits. *Bulletin of Toyama Prefectural University*, 9: 87 – 92.

Seymour, S.K. & Hamann, D.D. 1988. Crispness and crunchiness of selected low moisture foods. *J. Texture Stud*. 19: 79 – 95.

Sharma, K.C. 1968. Ultrasonic attenuation in liquid metals. *Physical Review*, 1741: 309 – 313.

Shiina, T., Yoshida, M., Yamakawa, M., & Nitta, N. 2007. Basic investigation of three-dimensional ultrasound tissue viscoelasticity microscope. *Japanese Journal of Applied Physics*, 467B: 4851 – 4857.

Shull, P.J. & Tittmann, B.R. 2002. Ultrasound. In *Nondestructive Evaluation: Theory, Techniques, and Applications*. Shull, (Ed.), Marcel Dekker, Inc., New York, USA.

Singh, H., Rockall, A., Martin, C.R., Chung, O.K., & Lookhart, G.L. 2006. The analysis of stress relaxation data of some viscoelastic foods using a texture analyzer. *Journal of Texture Studies*, 37 (4): 383 – 392.

Sofu, A. & Ekinci, F.Y. 2007. Estimation of storage time of yogurt with artificial neural network modeling. *Journal of Dairy Science*, 90: 3118 – 3125.

Sung, S.W. & Lee, J.H. 2003. Pseudo-random binary sequence design for finite impulse response identification. *Control Engineering Practice*, 11: 935 – 947.

Sushilov, N.V. & Cobbold, R.S. 2004. Frequency – domain wave equation and its time – domain solutions in attenuating media. *J. Acoust Soc Am*., 115(4):1431 – 1436.

Szczesniak, A.S. 1988. The meaning of textural characteristics – crispness. *Journal of Texture Studies,* 19: 51 – 59.

Taha, M.M.R., Neidigk, S., & Noureldin, A. 2009. Variable stiffness rheological model for interrelating creep and stress relaxation in ligaments. *International Journal of Experimental and Computational Biomechanics*, 11: 96 – 113.

Tan, J. 2001. New techniques for food quality data analysis and control. In *Nondestructive Food Evaluation: Techniques to Analyze Properties and Quality*. Gunasekaran, (Ed.), Marcel Dekker, Inc., New York, USA.

Tan, J., Gao, X., & Gerrard, D.E. 1998. Application of fuzzy sets and neural networks in sensory analysis. *Journal of Sensory Studies*, 14: 119 – 138.

Tanaka, T., Kawai, M., Kuwahara, Y., Hirano, T., Hagihara, K., Ogata, A., Shima, Y., Kawase, I., Shirayania, D., & Arimitsu, J. 2008. Quantification of hardness, elasticity and viscosity of the skin of patients with systemic sclerosis. *Romanian Journal of Rheumatology*, XVII (2): 79 – 80.

Thornton, G.M., Oliynyk, A., Frank, C.B., & Shrive, N.G. 1997. Ligament creep cannot be predicted from stress relaxation at low stress: a biomechanical study of the rabbit medial collateral ligament. *Journal of Orthopaedic Research*, 15: 652 – 656.

Todo, I. & Tatsuzaki, I. 1974. Ultrasound velocity in $Ca_2PbC_2H_5CO_2$ near the phase-transition temperature. *Phys. Stat. Sol*. a, 23: 591 – 595.

Toubal, M., Nongaillard, B., Radziszewski, E., Boulenguer, P., & Langendorff, V., 2003. Ultrasonic monitoring of sol-gel transition of natural hydrocolloids. *Journal of Food Engineering*, 58: 1 – 3.

Vickers, Z.M. 1988. Instrumental measures of crispness and their correlation with sensory assessment. *Journal of Texture Studies,* 19: 1 – 14.

Vincent, J.F.V. 1998. The quantification of crispness. *Journal of Science Food & Agricultural*, 78: 162 – 168.

Wachinger, C., Shams, R., & Navab, N. 2008. Estimation of acoustic impedance from multiple ultrasound images with application to spatial compounding. *IEEE Computer Society Conference on Computer Vision and Pattern Recognition Workshops*. CVPRW '08.

Williams, R., Cherin, E., Lam, T.Y.J, Tavakkoli, J., Zemp, R.J., & Foster, F.S. 2006. Nonlinear ultrasound propagation through layered liquid and tissue-equivalent media: computational and experimental results at high frequency. *Phys. Med. Biol.*, 51: 5809 – 5824.

Wilson, S.S. 2005. Understanding the PRBS signal as an optimum input signal in the wavelet-correlation method of system identification using multi-resolution analysis. *IEEE Southeast Conference Proceedings*, 2005: 39 – 44.

Wismer, M.G. 2006. Finite element analysis of broadband acoustic pulses through inhomogenous media with power law attenuation. *J. Acoust. Soc. Am.*, 120(6): 3493 – 3502.

Yamakoshi, Y., Sato, J., & Sato, T. 1990. Ultrasonic imaging of internal vibration of soft tissue under forced vibration. IEEE Trans. on *Ultrasonic, Ferroelectrics, and Frequency Control*, 372: 45 – 53.

Yamamoto, H., Iwamato, M., & Haginuma, S. 1980. Acoustic impulse response method for measuring natural quality evaluation of apples and watermelons. *Journal of Texture Studies*, 11: 117 – 136.

Yang, X.H. & Zhu, W.L. 2007. Viscosity properties of sodium carboxymethyl-cellulose solutions. *Cellulose*, 14(5): 109 – 417.

Zhang, G. 2005. Evaluating the viscoelastic properties of biological tissues in a new way. *J. Musculoskelet Neuronal Interact*, 5(1): 85 – 90.

Zhang, M., Nigwekar, P., Castaneda, B., Hoyt, K., Joseph, J.V., di Sant'Agnese, A., Messing, E.M., Strang, J.G., Rubens, D.J., & Parker, K.J. 2008. Quantitative characterization of viscoelastic properties of human prostate correlated with histology. *Ultrasound in Medicine & Biology*, 34(7): 1033 – 1042.

Zhao, B., Basir, O.A., & Mittal, G.S. 2005. Estimation of ultrasound attenuation and dispersion using short time Fourier transform. *Ultrasonics*, 43: 375 – 381.

Zude, M., Herold, B., Roger, J., Bellon-Maurel, V., & Landahl, S. 2006. Non-destructive tests on the prediction of apple flesh firmness and soluble solids content on tree and in shelf life. *Journal of Food Engineering*, 77: 254 – 260.

Appendix: Approval Letter from the University of Missouri Campus Institutional Review Board

Campus IRB Exempt Approval Letter: IRB # 1159637

Campus IRB [umcresearchcirb@missouri.edu]
Sent: Tuesday, February 02, 2010 7:43 PM
To: [redacted]

Dear Investigator:

Your human subject research project entitled Sensory Evaluation of Apple Crispness meets the criteria for EXEMPT APPROVAL and will expire on February 02, 2011. Your approval will be contingent upon your agreement to annually submit the "Annual Exempt Research Certification" form to maintain current IRB approval. The Campus IRB is required to maintain a record of all human subject research activities conducted under its jurisdiction, and this includes exempt research.

You must submit the Annual Exempt Research Certification form before **December 19, 2010**. Failure to timely submit the certification form by the deadline will result in automatic expiration of IRB approval.

If you wish to revise your exempt activities, you must contact the Campus IRB office for a determination of whether the proposed changes will continue to qualify for exempt status. You may do this by email. You will be expected to provide a description of the proposed revisions and how it will impact the risks to subject participants. The Campus IRB will provide a written determination of the level of review required for the proposed revisions.

If the activities no longer qualify for exemption, an Expedited or Full Board IRB application must be submitted to the Campus IRB. The investigator may not proceed with the proposed revisions until IRB approval is granted.

Please be aware that all human subject research activities must receive prior approval by the IRB prior to initiation, regardless of the review level status. If you have any questions regarding the IRB process, do not hesitate to contact the Campus IRB office at (573) 882-9585.

Campus Institutional Review Board

BIOGRAPHICAL NOTE

Sri Waluyo was born in Klaten, Central Java, Indonesia on 11 March 1972. He received the B.S. in Agricultural Technology from Gadjah Mada University (UGM), in Jogjakarta, Indonesia in 1996. After graduation, he joined the University of Lampung as a faculty member. He pursued the master degree with Directorate General of Higher Education (DGHE) scholarship, government of Republic of Indonesia in Bogor Agriculture Institute (IPB) in Bogor, Indonesia and earned the M.S. in 2001. He entered the University of Missouri, Columbia, Missouri in 2006 for a Ph.D. program in Biological Engineering.